UNIVERSITY OF CALIFORNIA

Santa Barbara

Catalytic Depolymerization of Native and Technical Lignin into Phenolic Compounds Using Nickel Catalyst

A dissertation submitted in partial satisfaction of the

requirements for the degree Doctor of Philosophy

in Chemistry

by

Hao Luo

Committee in charge:

Professor Mahdi M. Abu-Omar, Chair

Professor Steven K. Buratto

Professor Peter C. Ford

Professor Susannah L. Scott

June 2018

The dissertation of Hao Luo is approved.

_____

Mahdi M. Abu – Omar, Committee Chair

_____

Steven K. Buratto

_____

Peter C. Ford

_____

Susannah L. Scott

May 2018

Catalytic Depolymerization of Native and Technical Lignin into Phenolic Compounds Using Nickel Catalyst

ACKNOWLEDGEMENTS

First of all, I would like to express the deepest appreciation to my family for all their support throughout my life, without whom this dissertation would not be possible.

I would also like to thank my research advisor Prof. Mahdi Abu-Omar for his guidance and persistent help throughout my graduate studies. His excellent mentorship and dedication towards excellence in science has made a tremendous impact on my life. His encouragement both academically and spiritually guaranteed the success of my graduate research.

In addition, I would like to thank all of the current and past group members of the Abu-Omar research group. Your help was one of the most important factors that allowed me to succeed as a researcher.

I am grateful for the Center for Catalytic Conversion of Biomass to Biofuels (C_3Bio) for all the interdisciplinary collaborations and technical support.

VITA OF HAO LUO

June 2018

EDUCATION

Bachelor of Science in Chemistry, Purdue University, May 2013

Doctor of Philosophy in Chemistry, University of California, Santa Barbara, June 2018

PROFESSIONAL EMPLOYMENT

2013-2016: Research Assistant, Department of Chemistry, Purdue University

2016-2018: Research Assistant, Department of Chemistry and Biochemistry, University of California, Santa Barbara

PUBLICATIONS

Hao Luo and Mahdi M. Abu-Omar. "Lignin Extract and Catalytic Upgrading from Genetically Modified Poplar". *Green Chem*. **2018**, 20, 745-753.

Hao Luo, Frederic A. Perras, Ximing Zhang, Nathan S. Mosier, Marek Pruski and Mahdi M. Abu-Omar. "Atomic-Level Structure Characterization of Biomass Pre- and Post-Lignin Treatment by Dynamic Nuclear Polarization-Enhanced Solid-State NMR". *J. Phys. Chem A.* **2017**, 121, 623-630.

Hao Luo and Mahdi M. Abu-Omar. (**2017**). Chemicals from Lignin. In M. Abraham (Ed.), *Encyclopedia of Sustainable Technologies* (pp. 573-585). Elsevier.

Fan Wang, Greg Michalski, Hao Luo and Marc Caffee. "Role of biological soil crusts in affecting soil evolution and salt geochemistry in hyper-arid Atacama Desert, Chile". *Geoderma*. **2017**, 307, 54-64

Hao Luo, Ian M. Klein, Yuan Jiang, Hanyu Zhu, Baoyuan Liu, Hilkka I. Kenttämaa and Mahdi M. Abu-Omar. "Total Utilization of Miscanthus Biomass, Lignin and Carbohydrates: Using Earth Abundant Ni/C Catalyst". *ACS Sustain. Chem. Eng*. **2016**, 4, 2316-2322.

Hanyu Zhu, Joann P. Max, Christopher L. Marcum, Hao Luo, Mahdi M. Abu-Omar and Hilkka I. Kenttämaa. "Identification of the Phenol Functionality in Deprotonated Monomeric and Dimeric Lignin Degradation Products via Tandem Mass Spectrometry Based on Ion-Molecule Reactions with Diethylmethoxyborane". *J. Am. Soc. Mass Spectrom.* **2016**, 27(11), 1813-1823.

Fan Wang, Wensheng Ge, Hao Luo, Ji-Hye Seo, Greg Michalski, "Oxygen-17 anomaly in soil nitrate: A new precipitation proxy for desert landscapes". *Earth. Planet. Sci. Lett.* **2016**, 438, 103-111.

FIELDS OF STUDY

Major Field: Inorganic Chemistry

Studies in Catalytic Conversion of Lignin with Professor Mahdi Abu-Omar

ABSTRACT

Catalytic Depolymerization of Native and Technical Lignin into Phenolic Compounds Using Nickel Catalyst

by

Hao Luo

Increasing greenhouse gas emissions as well as a series of environmental issues caused by fossil fuels combustion have motivated the development of renewable energy sources. Nonfood lignocellulosic biomass is a promising renewable source for making liquid fuels and valuable chemicals, due to its high energy content stored by the biosphere. However, the efficient utilization of biomass has been significantly hindered by its recalcitrant nature. Herein, we have investigated the use of Ni/C for the catalytic depolymerization of native lignin in Miscanthus, a grassy biomass. Under optimized conditions, over 69% yield of select aromatic products were obtained from lignin. Carbohydrates remaining after lignin removal were recovered as a solid residue, which upon treatment with iron chloride produced useful platform chemicals (furfurals and levulinic acid). Understanding bond connectivity in biomass (between lignin and carbohydrates) advances the development and commercialization of more efficient catalytic methods for biomass utilization. To achieve this goal, Dynamic Nuclear Polarization (DNP) Enhance Solid State NMR (ssNMR) was used to probe the atomic level structure of biomass pre- and post- lignin treatment. Our results revealed an increase in the relative ratio of crystalline cellulose upon the catalytic depolymerization of lignin (CDL) using Ni/C catalyst. In parallel with direct catalysis of native lignin in raw biomass, organosolv pretreatment was used to produce sulfur-free technical lignin in high

purity. Our study investigated the effect of biomass substrate and organosolv pretreatment methods on the isolated lignin towards further upgrading over a Ni/C catalyst. By comparing different solvents (acetic acid/formic acid, acetone and methanol) applied for lignin extraction, methanol was revealed to minimize the undesirable re-condensation of organosolv lignin.

TABLE OF CONTENTS

Chapter I. Introduction: Potential and Difficulties in Conversion of Lignin into Value-Added Compounds

A. Abstract

Increasing global energy consumption and environmental issues resulting from fossil fuel combustion motivated the development of renewable energy source. Nonfood lignocellulosic biomass serves as one of the most promising sources accounts for about 50% of total renewable energy, due to its relative abundance in the nature as well as the high energy content[1]. Lignin as a major component in biomass (25-30% by weight) is the only renewable feedstock composed of aromatic building block. It has the potential to produce high value chemicals which were traditionally derived from petroleum. However, the recalcitrant nature of lignin as well as less developed techniques largely limited its valorization into value-added products, and lead to its use in combustion for low value heat. This chapter reviews the current situations and difficulties of lignin utilization in different categories.

B. Lignin basics: Structure and isolation

1. Lignin structure: Building blocks and interlinkage

Utilization of non-food lignocellulosic biomass as the feedstock for second generation biofuels has received more attention these years. Unfortunately, lignocellulosic biomass has a rigid and compact structure, due to the cross-linking of carbohydrate with phenolic units of recalcitrant lignin[2]. The conversion of lignocellulose into valuable products is therefore highly challenging. Lignocellulosic biomass is composed of three major

components, cellulose, hemicellulose and lignin. Lignin is the second most abundant natural polymer after cellulose, and it's the only natural source of aromatics. Lignin represents about 30% of nonfossil carbon on earth, and it accounts for 40% of the energy in biomass, due to its high carbon content. Natural abundance of lignin in the biosphere is around 300 billion tons (3.0×10^{14} kg), with an annual increase of 20 billion tons (2.0×10^{13} kg)[3].

Lignin is a highly branched amorphous macromolecule with complex structure, which is largely dependent on the plant source. Lignin macromolecule is composed of three monomeric building blocks, namely p-hydroxyphenyl (H), guaiacyl (G) and syringyl (S), with the difference on the number of methoxy groups (**Figure 1.1**). Lignin monomers are connected to each other irregularly through interunit linkages. The type of linkages varyies from species to species, but in general, over two thirds are aryl ether linkage. β-O-4 linkage is by far the dominant one in all species (45%-60%), followed by some other linkages such as β-5 linkage (10%-12%) and 5-5 linkage (10%-20%) (**Figure 1.2**)[4].

Figure 1.1. Lignin monomeric building blocks.

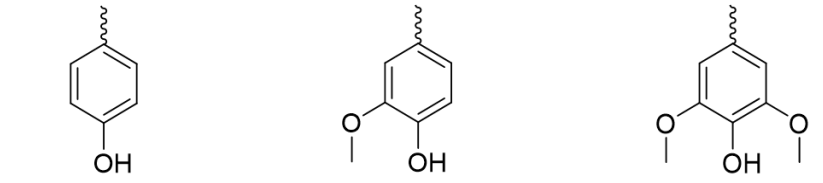

p-Hydroxyphenyl (**H**) Guaiacyl (**G**) Syringyl (**S**)

Figure 1.2. Illustration of (a) lignin macromolucule and (b) common lignin interunit linkages.

(a)

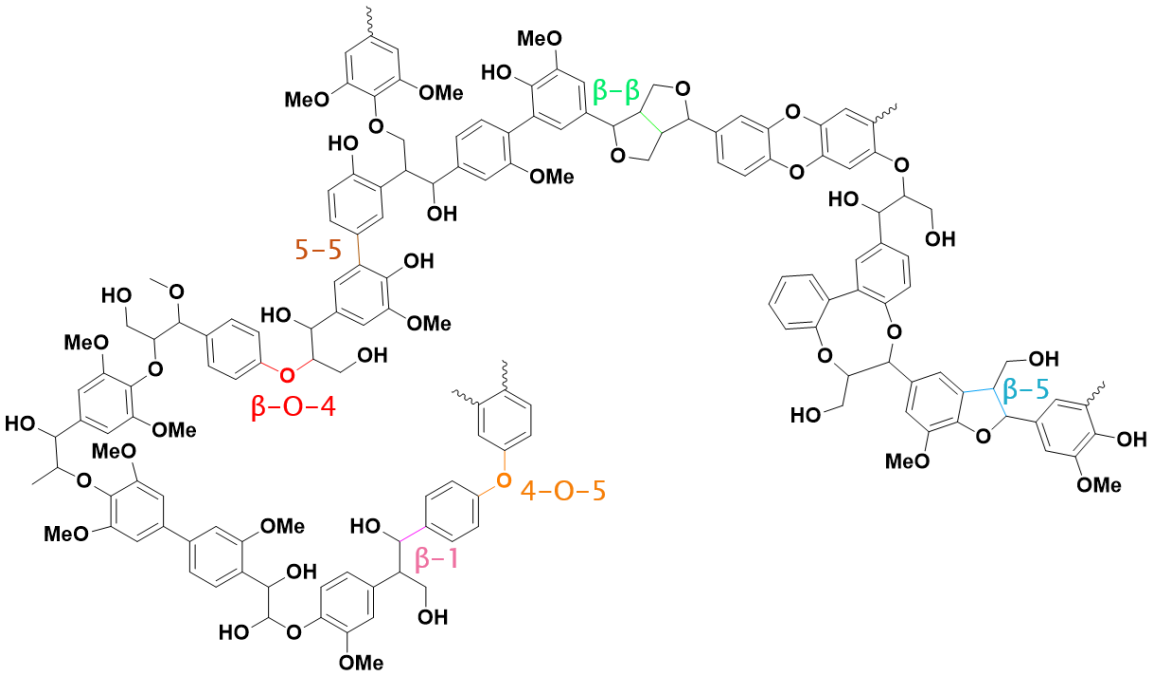

(b)

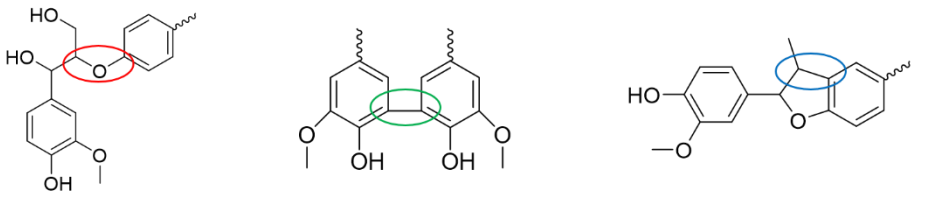

β-O-4 5-5 β-5

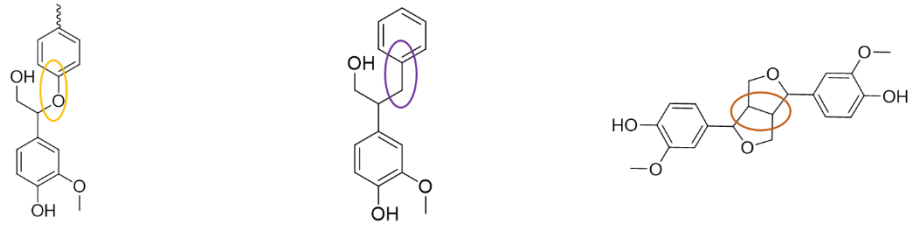

α-O-4 β-1 β-β

2. Lignin isolation technologies

A feasible pretreatment approach to separate different components of biomass from lignin is essential to make effective utilization of lignin. Currently, the isolation of lignin

from carbohydrate falls into two categories[4-5]. The first is to dissolve cellulose and hemicellulose, leaving lignin as an insoluble residue; while the second is to dissolve lignin, with cellulose and hemicellulose remained insoluble. Isolation techniques which derive high purity and high quality lignin are desirable. Different pretreatment processes resulted in the isolated lignin with main difference in its structure and property. In industry, there are four primary methods of isolating lignin from biomass with all of them using techniques to solubilize and extract lignin first: the Kraft, Sulfite, Soda, and Organosolv processes[6]. Different conditions applied for these treatment processes resulted in the isolated lignin with different molecular weight, solubility and purity, etc[7]. A brief summary of the four different technical lignin is provided in **Table 1.1**.

Table 1.1. Comparison of different technical lignin and their properties

	Kraft	Lignosulfonate	Soda	Organosolv
Lignin purity	High	Low-meidum	High	Very High
Sulfur content (%)	1-3	3-8	n/a	n/a
Molecular weight ($\times 10^3$ g mol^{-1})	1.5-5 (up to 25)	1 to 50 (up to 150)	0.8 to 3 (up to 15)	0.5 to 5
Solubility	Water, Alkali	Water	Alkali	Organosolvents
Separation techniques	Precipitation (pH change)	Ultrafiltration	Precipitation (pH change)	Precipitation (addition of non-solvent)

i. Kraft Process

Kraft process is currently the most common technique applied in the wood pulping industry. In this technique, wood chips are treated in an aqueous solution containing water, sodium hydroxide (NaOH), sodium sulfide (Na_2S) at the temperature of 150 ˚C -

180 ˚C for 2 hours[8]. Lignin generated in this process was precipitated by lowering the pH with CO_2, and recovered through filtration, drying and washing to give technical grade lignin. Due to the use of Na_2S, Kraft process introduces aliphatic thiol groups to the lignin side chain, resulted in the isolated lignin a sulfur content 1%-3%[7]. This caused the Kraft lignin unlikely to be largely used in commercial markets or being valorized to high-value chemicals. As a result, most of the lignin generated through Kraft process was directly applied as fuel to operate the relatively expensive chemical recovery boiler system. It is also possible to control the sulfur content in the isolated lignin by adjusting the temperature. In this case, the product properties can be tuned to be either different or similar from those of lignin isolated from the sulfite process, another widely employer treatment.

ii. Sulfite Process

Sulfite process is another widely used technique in paper and pulp industry for producing lignosulfonate. In this process, the pulping solution employed is sulfurous acid, either salts of sulfites (SO_3^{2-}), or bisulfites (HSO_3^{2-}). Several of the commonly used counter ions including single-valent sodium (Na^+), potassium (K^+), ammonium (NH_4^+), doubly-valent calcium (Ca^{2+}) and magnesium (Mg^{2+})[7]. Sulfite process is usually carried out at temperature of 130 ˚C - 160 ˚C for 4-14 h. In most cases, this process is performed under acidic conditions, using calcium or magnesium as counter ions. The recovered lignosulfonate from the cooking liquor steam is highly water soluble, with high sulfur content (3%-8%) and relatively high molecular weight. The purity of the isolated lignosulfonate is relatively low. This resulted in additional cost in the purification of lignosulfonate before further commercial and biorefinery utilization.

iii. Soda Process

Soda process is the main method for pulping nonwood biomass (straw, sugar cane bagasse, etc.)[5]. In this process, the biomass chips are treated with sodium hydroxide at approximately 160 ˚C to dissolve lignin[9]. Nonwood lignin recovered from this process is rich in p-hydroxyl units and lower in molecular weight, compared with the lignin from wood biomass[10]. Soda lignin is sulfur free, with high purity and is closer to the composition of native lignin. These properties of soda lignin make it suitable for direct utilization without need for further purification. Examples of applications of soda lignin include the production of phenolic resins, animal nutrition, and dispersants[11].

iv. Organosolv Process

Organosolv pretreatment is one of the techniques that has the advantage of producing separate streams of cellulose, hemicellulose and lignin. In the organosolv process, wood chips are treated by organic solvents, usually with the presence of mineral acid as catalyst[9]. The solvents being used for the organosolv treatment including acetic acid, formic acid, ethanol and organic peroxide, etc[12]. The organosolv lignin recovered from the cooking solvent is sulfur free and shows poor water solubility. Organosolv lignin typically has low molecular weight, and is of high purity and high quality[13]. These properties make it ideal for both direct use and upgrading into high value chemicals, such as low molecular weight phenols[5, 14]. Despite all the above-mentioned advantages, the limitation in the development of the organosolv technique lies in the high cost in handling and recovering the organic solvents[8].

C. Lignin valorization: Conversion into value-added materials

There has been a long-standing saying in industry that "One can make everything from lignin, except money"[15]. This embarrassing situation has driven significant amount of effort in the valorization of lignin. Numerous of research has focused on the techniques for the valorization of lignin into value-added materials during the past few decades. In 2007, a report from DOE reviewed the role of lignin as a renewable material source, and evaluated the technical barriers of lignin utilization based on the current development. Based on this report, the commercialization opportunities of lignin products were summarized as three categories: near-term (current uses and those within 3-10 years), medium-term (5 to perhaps 20 years), and long-term (more than 10 years and requiring significant new fundamental knowledge and technology development). The valorized products from lignin also fall into three categories: power/fuel, macromolecules and aromatics, based on the commercial value of these products (**Scheme 1.1**). This session mainly focused on a description of different categories of lignin valorized products.

Scheme 1.1. General illustration of lignin valorization process.

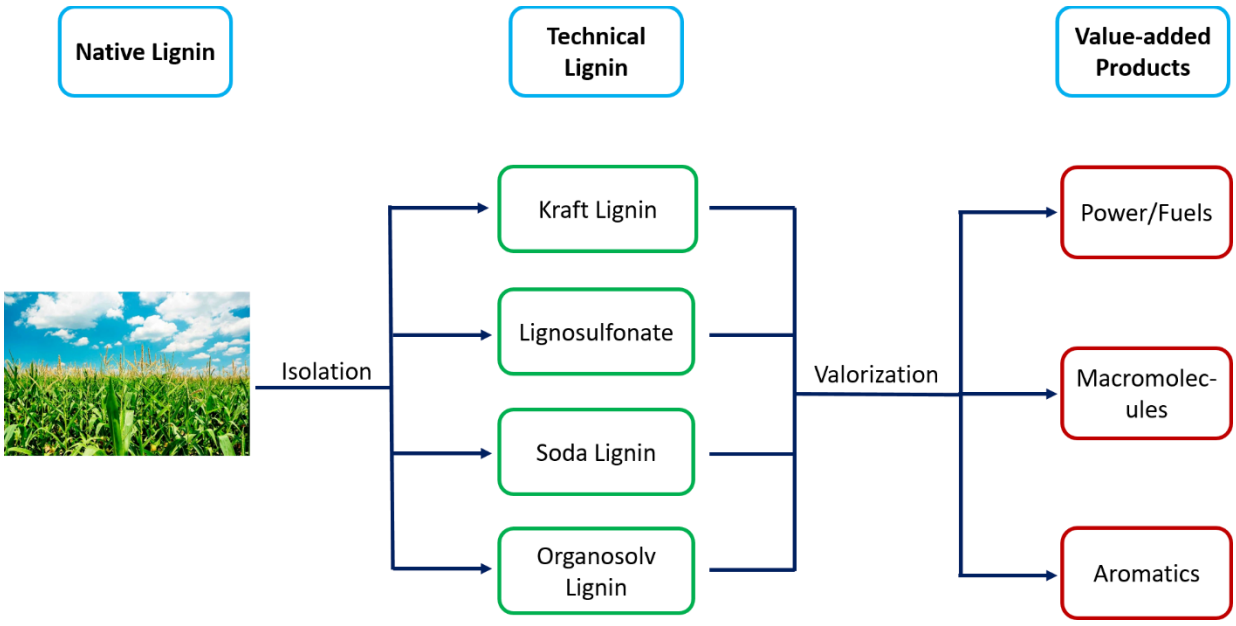

1. Lignin utilization as Power/Fuel

i. Combustion

Direct combustion of lignin is bar far the simplest technology for the utilization of isolated lignin, which derives the least value from lignin. The average heat value of dry lignin is around 25 MJ/kg, which is comparable to that of coal (24-30 MJ/kg). This makes lignin an ideal fuel for the combustion or cocombustion. The majority of lignin produced annually by the pulp and paper industry and by biorefineries (estimated at more than 70 billion kg) is burned for heat at a value of $80 per ton ($0.08 per kg)[16-18]. Lignin cofiring with coal was largely used in the operation of fired pulping boilers. Compared with the sole combustion using fossil fuels, cofiring with lignin was reported to increase the efficiency of combustion system by 38%, and decrease GHG (green-house gas) emission by as much as 60%[19-20]. Despite all these benefits, the combustion of lignin still remains as one of the lowest value applications of lignin.

ii. Gasification

Gasification is a thermochemical treatment of lignin in the presence of oxygen, air, and/or steam to produce syngas (when oxygen in use) or producer gas (when air in use). Here, syngas is a mixture of H_2, CO and a very small amount of CO_2; while producer gas has higher level of N_2 and lower level of H_2, CO and CO_2 compared with syngas[21].

Theoretically, 62 mol of hydrogen and 53 mol of carbon monoxide could be generated from gasification of 1kg of isolated lignin[22]. However, these numbers are never reached due to the decreased efficiency during the gasification process caused by the formation of tar and several other factors[23]. Tar is a black mixture of condensed hydrocarbons, including single ring to 5-ring aromatic compounds[24]. It is the side product

formed during the gasification process. Formation of tar is one of the most severe issues affecting the commercialization of lignin gasification processes, due to its blocking of pipes and valves, and the contamination of the gasification equipment[25]. The removal or reduction of tar is one of the greatest technical challenges; successfully handling tar would greatly increase commercial viability of the gasification process. Currently, several practical methods have been reported to efficiently reduce tar formation, which can be categorized as: modification of operation conditions; use of gasifier bed additives; and gasifier design modification[24].

Temperature and pressure are two of the main parameters that affect tar formation. Generally speaking, increasing the operation temperature to 1073 K and pressure to at least 2.0×10^6 Pa significantly decreases tar formation by 40%–74%[26-27]. Introducing catalysts into gasification systems has resulted in reducing tar formation[28]. The most widely studied catalysts include Ni-based catalysts, calcined dolomites and magnesites, zeolites, olivine and iron catalysts[24]. The efficiency of tar reduction varies with catalyst and loading amount. For example, a 3 wt% of calcined dolomite resulted in 40% reduction of tar; a comparable amount of olivine gave a reduction of tar as high as 90%[26, 29]. Design of the gasifier plays a crucial role in the formation of tar. Gasifiers with typical designs produce tar in the range of 1.0×10^3 mg m^{-3} to 1.0×10^5 mg m^{-3}.[30] A preferable tar concentration for the gasification engines was evaluated to be less than 10 mg m^{-3}, and all of the typical designs far exceed this evaluated limit[31]. Modification of the typical gasifiers includes introduction of a secondary air injection to the gasifier, making it a two-stage gasifier (**Figure 1.3.**)[32]. The gasification performed in a two-stage gasifier by

Asian Institute of Technology (AIT) resulted in a final tar content of only 50 mg m^{-3}, which is a significant improvement (**Table 1.2**)[31].

Figure 1.3. Simplified illustration of typical gasifier and secondary gasifier. (A). Typical gasifier. (B). Secondary gasifier.[23, 32]

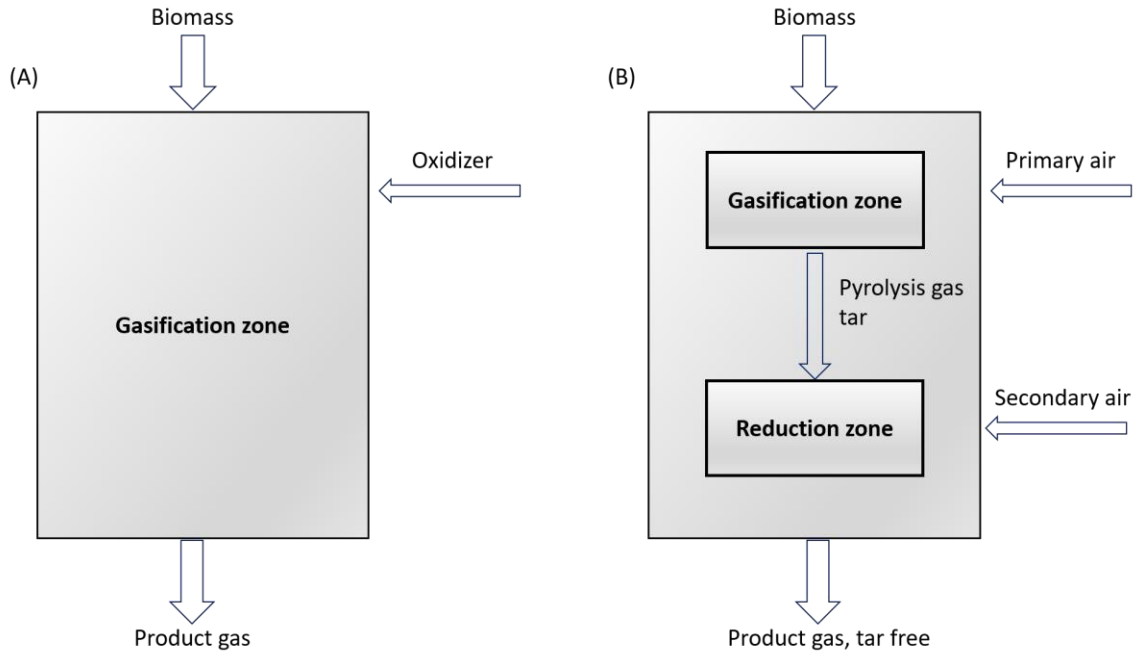

Table 1.2. Comparison of different tar removal methods and their efficiency.

	Operation condition modification	Gasifier bed additives	Gasifier design modification
Operation details	Temperature ≥ 1073K; Pressure ≥ 2.0×10^6 Pa.	Addition of catalysts: Ni based catalysts, calcined dolomites and magnesites, zeolites, olivine and iron catalysts.	Introduction of secondary air injection.

Tar removal efficiency	Tar reduction in range of 40-70%.	Tar reduction in range of 40-90%.	Final tar concentration as low as 50 mg m^{-3}.

iii. Pyrolysis

Pyrolysis of lignin is a thermal depolymerization process which occurred in a temperature range between 250 ˚C - 1000 ˚C, in the absence of oxygen.[33] The products from this process are generally noncondensable gases, liquid oil, and solids. A recent review by Patel et al. summarized the current development of pyrolysis technologies and subdivided into six categories: fast pyrolysis, slow pyrolysis, intermediate pyrolysis, flash pyrolysis, vacuum pyrolysis, and ablative pyrolysis[34]. Among them, fast pyrolysis is the most widely used technique in terms of lignin valorization into liquid bio-oils. It has the advantages of moderate operation temperature (400 - 550 ˚C) and low residence time[35-36].

Liquid bio-oil is the main product from lignin fast pyrolysis. It is a complex mixture of aromatic and nonaromatic compounds, with a wide molecular weight distribution. Addition of catalysts into the pyrolysis system is one way to significantly enhance the selectivity toward value-added hydrocarbon products. Zeolites (ZSM5, H-ZSM5, and H-USY) showed to be among the most efficient catalysts in shifting the products toward more deoxygenated compounds: about 75 wt% liquid products, which are aromatic hydrocarbons.[37] Raw liquid bio-oil from lignin pyrolysis is corrosive and highly oxygenated.[38] It is upgraded through technologies such as fluid catalytic cracking[39] and hydroprocessing. The refined bio-oil can be further used for generation of electricity[40], commodity chemicals[41], and renewable gasoline and diesel[42]. Commercial value of upgraded bio-oil is affected by several factors including labor, material transportation,

facility maintenance, and utility costs. One example using bio-oil as fuel is estimated to have a minimum fuel selling price of \$2.6 gal^{-1} (\$ 0.7 L^{-1})[38].

All of the approaches discussed so far fall within the near-term opportunities categorized by DOE, meaning that the technologies are currently available, but the value of the valorization products remain relatively low. One major competition in the fuels area is price competitiveness with fossil fuels.

2. Lignin utilization as macromolecules

Being a polymer, lignin has potential for commercialization in materials applications. Currently, around three quarters of the commercial products from lignin take advantage of this property[8]. The recalcitrant nature of lignin makes the depolymerization process energy intensive and economically costly. Thus, the direct use of lignin polymer as precursor for the production of value-added materials without additional depolymerization is promising[9]. Some of the well-studied lignin based macromolecular materials include carbon fiber and polyurethane[6].

i. Carbon fiber

Carbon fiber as of 2011 has an annual global market of 46,000 meteric tons valued at \$1.6 billion. This market is expected to increase to 140,000 meteric tons with a value of \$4.5 billion by the year 2020[3]. Currently, the main constraint on carbon fiber market growth is its high price, \$ 18 kg^{-1}. The reason for the high price is the high cost of its precursor polyacrylonitrile (PAN), which costs \$15 kg^{-1}.[3] Lignin as a natural low-cost carbon source with high carbon content (over 60% carbon by mass), has been proven to be an ideal low price precursor for carbon fiber synthesis[43].

The process to obtain carbon fiber from lignin includes several techniques: melting spin of isolated lignin; oxidative stabilization of lignin fiber; carbonization under N_2; surface treatment and sizing[15, 44]. Compared with PAN, two of the advantages for using lignin as a precursor are lower melting temperature and faster stabilization capability[44]. However, as the major source of lignin comes from Kraft lignin, the difficulty in recovering pure lignin leads to lignin-based carbon fiber with poor mechanical properties compared with traditional PAN-based carbon fiber[15]. Highly amorphous structure of lignin results in formation of disordered glassy carbon during pyrolysis[45]. Nowadays, the major technical challenge for using lignin as carbon fiber precursor comes from the difficulty in melt spinning. Several research techniques have been developed to address this problem include purification and chemical modification of lignin. Organic solvent purified lignin proved to have excellent spinnability characteristics as a precursor for producing carbon fiber compared with untreated lignin[44]. In addition, chemical modification of lignin using acid anhydrides (acetic, succinic, phthalic, and maleic) with tetrahydrofuran and methanol as a solvent showed similarly favorable results[46].

ii. Polyurethane

Polyurethane is one of the most versatile polymers with a wide variety of applications. Its global industry revenue was $52 billion in 2015, and the value is expected to increase to $77 billion by 2023. A typical polyurethane synthesis pathway includes the reaction of diisocyanates and polyols with terminal hydroxyl groups (**Scheme 1.2**)[47]. Polyurethane exists both in a rigid form and a flexible form. Rigid polyurethanes are commonly used as insulation and floating material, while the flexible variants are used more for cushioning and packaging material. Lignin as a polymer with

large numbers of hydroxyl groups has been shown to be able to replace polyols in synthesizing polyurethane.[48]

Scheme 1.2. Typical synthesis of polyurethanes by using diisocyanate and hydroxyl group terminated polyols.

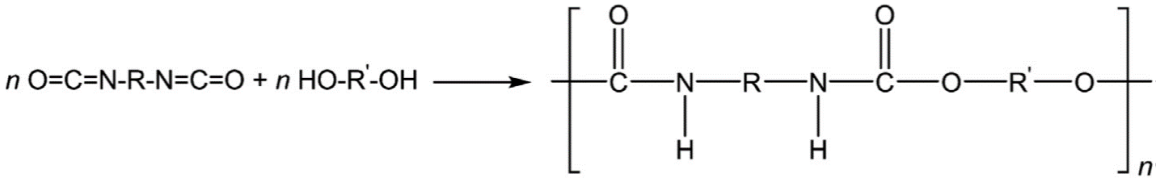

Lignin can be directly incorporated as a polyol in polyurethane synthesis; or chemically modified before the utilization[6, 49]. In order for lignin to incorporate successfully into polyurethanes with different properties, several factors have to be adjusted, such as reaction conditions, the employed diisocyanates, and chemical modification on lignin itself[50]. For example, using Kraft lignin and methylene diphenyldiisocyanate, generated a high molecular weight polyurethane (920,000 g mol^{-1}) by controlling the reaction temperature at 80˚C (353 K) and reaction time to 3 h[50]. Introducing amine groups into lignin improves its water solubility and reactivity with isocyanate. The resulting modified waterborne polyurethane proved to have improved mechanical and antiaging properties. Compared with traditional polyurethane, lignin incorporated polyurethanes show superior physical properties in some instances. One drawback of using lignin or modified lignin in producing polyurethane is that the resulting product exhibited more rigid and brittle characteristics compared to conventional polyurethane. Aniceto et al. indicated that a technique called oxypropylation could graft the poly (propylene oxide) on lignin, consequently converting it into liquid

polyols. In this scenario, the hydroxyl groups are optimized for polyurethane formulation.[51]

iii. Other macromolecules

Lignin can also be used for other macromolecular materials such as polymer modifiers, adhesives, and resins[5, 9, 15, 52]. In all these cases, lignin can be used directly as a macromonomer, or can be chemically modified before forming a final resin or thermoset. Since lignin from different biomass sources and isolation processes always has different properties, proper chemical and catalytic processes need to be developed for each specific case. Thermoset and resin macromolecules have a large commercial market, and the values of lignin valorized macromolecular materials are significantly higher than using lignin as a source for power and fuel. In general, this category falls in the DOE's medium-term opportunity[8].

3. Lignin utilization as monomer aromatics

Lignin is the only natural source for aromatics[33]. At first glance, it may seem to be straight forward to convert lignin into monomeric aromatic products, but the complex structure of lignin as well as the highly cross-linked biological matrix in lignocellulosic biomass severely hinders conversion efficiency and selectivity. Monomeric aromatic compounds are among the highest value lignin valorization products, and this area of research and development falls into DOE's long-term opportunities[8]. So far, the vast majority of aromatic products are produced from petroleum feedstock. New technological developments for efficient depolymerization of lignin and upgrading into aromatics should contribute to reducing our reliance on fossil resources[3].

Depolymerization technologies

A large amount of research has focused on different technologies to depolymerize lignin, which can generally be categorized as: pyrolysis, gasification, hydrogenolysis, chemical oxidation, or hydrolysis under supercritical conditions[33, 53-55]. In general, a depolymerization process breaks the interunit linkages within the lignin macromolecule, converting complex lignin polymers into oligomers or monomeric aromatic products to be upgraded to specialty fuels and chemicals. Among all the well-studied technologies, chemical treatment is considered as one of the most effective depolymerization pathways, aiming to recover aromatic monomers from lignin. Chemical depolymerization, especially using heterogeneous catalysts, has the advantages of high efficiency, product selectivity, moderate reaction conditions, and ease of reaction control[55]. A broad range of transition metals have proven to be successful in catalyzing lignin depolymerization to phenolic products. Examples are Pt, Ru, Rh supported on active carbon[56], Cu/Mg/Al[57], ZrO_2–Al_2O_3–FeOx[58]; 4.4 wt.% formic acid together with 0.15 wt.% Pd[59]; γ-Al_2O_3-supported Ru, Ni, NiMo, CoMo[60], Co–Mo–S supported by Al_2O_3[61]; bimetallic catalysts NiPt/C, NiCu/C, and Zn/Pd/C[62-63]; and Ni/C[64-65]. Under heterogeneous catalytic treatment, the depolymerized products are in the range C6–C9 aromatics, the product selectivity varies case by case, depending on the catalyst and specific reaction conditions. However, due to the expense of noble metal catalyst, difficulties in separations of multiphase reaction streams, and required high pressures, most of these treatments have been limited to research scale.

Aromatic products from lignin

Examples of some high-value aromatic products that can be derived from lignin depolymerization include benzene, toluene, xylene (BTX), phenol, and vanillin[8].

i. BTX

BTX represented a $120 billion market in 2010, and is projected to grow at the rate of ca. 4.4% per year from 2010 to 2020[3]. Currently, all of the BTX comes from petroleum. The global production of BTX was around 100 million metric tons (1.0×10^{11} kg) in 2010[3]. Lignin-based BTX production is currently in the R&D stage, and is expected to reach commercial markets in 10–20 years. The technology to convert lignin into BTX is a two-step process: the first step includes lignin depolymerization into oxygenated monomer aromatics through CeO bond cleavage; followed by a second step of hydrodeoxygenation (HDO) and demethoxylation[66]. However, with some of the most common noble metal catalysts (Pt, Rh, Pd, Ru), the above pathways always result in over hydrogenation of the aromatic products, leading to the formation of cyclic alkanes[67-68]. In 2013, Jongerius reported that by using a novel catalyst system (CoMo/ Al_2O_3 and Mo_2C/CNF), lignin after liquid phase reforming treatment could be effectively converted to BTX[61]. BTX are used as precursors for the production of a series of materials, such as resins, nylon fibers, polyurethane, and polyester. Efficient technologies to derive BTX from lignin have the potential to increase the value of traditionally wasted material.

ii. Phenol

Phenol is mostly made from cumene, which in turn is produced from alkylation of benzene. The global market for phenol is around 8 million metric tons (8×10^9 kg), valued at $12 billion in 2010[3]. Similar to BTX, the lignin to phenol depolymerization also needs 10–20 years to reach commercial markets. Lignin is rich in both aliphatic and phenolic hydroxyl groups, the HDO of lignin produces phenolic products with different methoxylation degrees. Methoxy groups can be removed through demethoxylation by

using catalysts such as Mo_2N and $CoMo/Al_2O_3$.[61, 69] Phenols are widely used in the formation of formaldehyde resins as well as polyurethane[3]. Today, the price of phenol is directly affected by oil, getting the technology of converting lignin into phenol commercialized could significantly expand the use of naturally derived phenols and expand their commercial market.

iii. Vanillin

Vanillin has been reported to be commercially produced from lignin since 1937. The global market for vanillin in 2011 was estimated to be 16,000 metric tons (1.6×10^{11} kg), with a value of $230 million. About 20% of the synthetic vanillin comes from valorization of lignin, and the remaining 80% comes from crude oil[3]. The difference between vanillin and BTX or phenol is that it is considered as an end product, rather than a platform chemical. Vanillin is well known for its use as the world's largest flavoring agent[6]. Another difference between vanillin and BTX or phenol is that production of vanillin from lignin is through oxidative catalytic pathway, instead of hydrogenolysis pathway[70]. Borregarrd is the industry leader in commercial production of vanillin from lignin, which utilizes oxidative depolymerization of lignosulfonate from sulfite pulping[3]. The increased demand for natural vanillin is driving industrial interest in efficient production of high-quality vanillin form lignin.

D. Environmental benefits from utilization of lignin

Our heavy reliance on fossil fuels has led to significant increase in GHG, which is the main cause of climate change. In the United States alone, GHG emission was estimated to be 5.1×10^{12} kg in 2012. Coal combustion as the single largest contributor is

responsible for the release of 1.6×10^{12} kg GHG. Moreover, fossil fuels are not renewable and will eventually reach unsustainable levels, which would become a threat to our global energy system. All of these factors point to the importance and urgency in developing renewable energy sources and sustainable technologies. Using nonedible lignocellulosic biomass to provide fuels and materials is part of the solution to sustainability. In the coming decades, society will see a shift from fossil feedstock-based chemical industry to one that relies on renewable feedstock for making fuels, chemicals, and materials. The US Departments of Agriculture and Energy have set up ambitious goals to derive 20% of the US transportation fuel and 25% of the US chemical commodities from biomass by 2030[54]. Lignin combustion or cocombustion with different fossil fuels presents the near-term opportunity to reduce a significant amount of gaseous pollutants such as CO, CO_2, NOx, and SO_2. As indicated by Farrell et al. and Scown et al., a general GHG emission by gasoline combustion is 95 g CO_2 eq MJ^{-1}, while using lignin as a substitute energy source, this emission is reduced by 60%[20, 71]. Lignin cofiring with coal in a general power plant can also result in a 40% reduction in life-cycle water consumption[20].

Lignin as a renewable precursor, utilized in producing macromolecules, can potentially replace fossil-based materials and toxic chemicals. Use of lignin-based carbon fiber in the automotive industry can significantly reduce vehicle weight and improve fuel economy[8]. Recent research has illustrated a novel pathway for producing polyurethanes with lignin and soybean oil, avoiding the use of environmentally hazardous isocyanates[72]. Lignin's aromaticity makes it a promising feedstock for producing aromatic products. However, due to current technological limitations, the vast majority of aromatic products being used are derived from petroleum. With the development of new technologies on the

lab scale for deriving monomeric aromatics from lignin, commercialization can be realized eventually and in the long-term lignin may play an important role in decreasing the demand for oil.

E. Conclusion

Lignin, traditionally a waste byproduct of paper and pulp and biorefining, is now attracting more attention than ever. The field of lignin valorization has seen significant growth and advances in the past decade. Lignin's aromatic properties has strong market potential. Lignin utilization is both environmentally and sustainably beneficial. However, with current technologies, lignin utilization is still largely limited to relatively low value fuel and power supply. Commercialization of lignin as precursor for high performance macromolecular materials and aromatic products requires further research and development. There are still barriers existing between the analysis of intrinsic lignin structure, processing of lignin depolymerization, and final product application. Each of these areas is being studied exhaustively, but there is serious lack in synergy and collaborations. The translation of new laboratory transformations and reactions to scalable commercial products requires a strong collaboration across different disciplines in science and engineering, and better understanding of the economics of the entire supply chain. There is also always the question of feedstock variability from location to location as well as from one growing season to another. Nevertheless, with these challenges comes an opportunity in which lignin can be a substitute to traditional fossil-based feedstock for many products. Furthermore, governments can play an important role in catalyzing commercialization by setting bold policies that push for fossil feedstock

replacements. Multidisciplinary and collaborative team research in lignin valorization is expected to continue to grow and thrive in the near future.

F. References:

1. Luo, H.; Abu-Omar, M. M., Chemicals from lignin. In *Encyclopedia of Sustainable Technologies*, Abraham, M. A., Ed. 2017; pp 573–585.

2. Zhao, C.; Lercher, J. A., Selective Hydrodeoxygenation of Lignin-Derived Phenolic Monomers and Dimers to Cycloalkanes on Pd/C and HZSM-5 Catalysts. *Chemcatchem* **2012,** *4* (1), 64-68.

3. Smolarski, N., High-value opportunities for lignin: unlocking its potential. *Frost & Sullivan, Paris* **2012,** *15*.

4. Pandey, M. P.; Kim, C. S., Lignin Depolymerization and Conversion: A Review of Thermochemical Methods. *Chem Eng Technol* **2011,** *34* (1), 29-41.

5. Lora, J. H.; Glasser, W. G., Recent industrial applications of lignin: A sustainable alternative to nonrenewable materials. *J Polym Environ* **2002,** *10* (1-2), 39-48.

6. Strassberger, Z.; Tanase, S.; Rothenberg, G., The pros and cons of lignin valorisation in an integrated biorefinery. *Rsc Adv* **2014,** *4* (48), 25310-25318.

7. Kai, D.; Tan, M. J.; Chee, P. L.; Chua, Y. K.; Yap, Y. L.; Loh, X. J., Towards lignin-based functional materials in a sustainable world. *Green Chem* **2016,** *18* (5), 1175-1200.

8. Holladay, J. E.; White, J. F.; Bozell, J. J.; Johnson, D. *Top Value Added Chemicals from Biomass-Volume II, Results of Screening for Potential Candidates from Biorefinery Lignin*; Pacific Northwest National Lab.(PNNL), Richland, WA (United

States); National Renewable Energy Laboratory (NREL), Golden, CO (United States): 2007.

9. Upton, B. M.; Kasko, A. M., Strategies for the Conversion of Lignin to High-Value Polymeric Materials: Review and Perspective. *Chem Rev* **2016,** *116* (4), 2275-2306.

10. Wormeyer, K.; Ingram, T.; Saake, B.; Brunner, G.; Smirnova, I., Comparison of different pretreatment methods for lignocellulosic materials. Part II: Influence of pretreatment on the properties of rye straw lignin. *Bioresource Technol* **2011,** *102* (5), 4157-4164.

11. Vishtal, A.; Kraslawski, A., Challenges in Industrial Applications of Technical Lignins. *Bioresources* **2011,** *6* (3), 3547-3568.

12. Barta, K.; Warner, G. R.; Beach, E. S.; Anastas, P. T., Depolymerization of organosolv lignin to aromatic compounds over Cu-doped porous metal oxides. *Green Chem* **2014,** *16* (1), 191-196.

13. Luterbacher, J. S.; Azarpira, A.; Motagamwala, A. H.; Lu, F. C.; Ralph, J.; Dumesic, J. A., Lignin monomer production integrated into the gamma-valerolactone sugar platform. *Energ Environ Sci* **2015,** *8* (9), 2657-2663.

14. Cai, Z. P.; Li, Y. W.; He, H. Y.; Zeng, Q.; Long, J. X.; Wang, L. F.; Li, X. H., Catalytic Depolymerization of Organosolv Lignin in a Novel Water/Oil Emulsion Reactor: Lignin as the Self-Surfactant. *Ind Eng Chem Res* **2015,** *54* (46), 11501-11510.

15. Ragauskas, A. J.; Beckham, G. T.; Biddy, M. J.; Chandra, R.; Chen, F.; Davis, M. F.; Davison, B. H.; Dixon, R. A.; Gilna, P.; Keller, M.; Langan, P.; Naskar, A. K.;

Saddler, J. N.; Tschaplinski, T. J.; Tuskan, G. A.; Wyman, C. E., Lignin Valorization: Improving Lignin Processing in the Biorefinery. *Science* **2014,** *344* (6185), 709-+.

16. Xing, R.; Qi, W.; Huber, G. W., Production of furfural and carboxylic acids from waste aqueous hemicellulose solutions from the pulp and paper and cellulosic ethanol industries. *Energ Environ Sci* **2011,** *4* (6), 2193-2205.

17. Rose, M.; Babi, M.; Moran-Mirabal, J., The study of cellulose structure and depolymerization through single-molecule methods. *Industrial Biotechnology* **2015,** *11* (1), 16-24.

18. Hu, L.; Zhao, G.; Hao, W.; Tang, X.; Sun, Y.; Lin, L.; Liu, S., Catalytic conversion of biomass-derived carbohydrates into fuels and chemicals via furanic aldehydes. *Rsc Adv* **2012,** *2* (30), 11184-11206.

19. Khitrin, K. S.; Fuks, S. L.; Khitrin, S. V.; Kazienkov, S. A.; Meteleva, D. S., Lignin utilization options and methods. *Russ J Gen Chem+* **2012,** *82* (5), 977-984.

20. Scown, C. D.; Gokhale, A. A.; Willems, P. A.; Horvath, A.; McKone, T. E., Role of Lignin in Reducing Life-Cycle Carbon Emissions, Water Use, and Cost for United States Cellulosic Biofuels. *Environ Sci Technol* **2014,** *48* (15), 8446-8455.

21. Sikarwar, V. S.; Zhao, M.; Clough, P.; Yao, J.; Zhong, X.; Memon, M. Z.; Shah, N.; Anthony, E. J.; Fennell, P. S., An overview of advances in biomass gasification. *Energ Environ Sci* **2016,** *9* (10), 2939-2977.

22. Azadi, P.; Inderwildi, O. R.; Farnood, R.; King, D. A., Liquid fuels, hydrogen and chemicals from lignin: A critical review. *Renew Sust Energ Rev* **2013,** *21*, 506-523.

23. Huber, G. W.; Iborra, S.; Corma, A., Synthesis of transportation fuels from biomass: Chemistry, catalysts, and engineering. *Chem Rev* **2006,** *106* (9), 4044-4098.

24. Devi, L.; Ptasinski, K. J.; Janssen, F. J. J. G., A review of the primary measures for tar elimination in biomass gasification processes. *Biomass Bioenerg* **2003,** *24* (2), 125-140.

25. Qin, Y. H.; Feng, J.; Li, W. Y., Formation of tar and its characterization during air-steam gasification of sawdust in a fluidized bed reactor. *Fuel* **2010,** *89* (7), 1344-1347.

26. Narvaez, I.; Orio, A.; Aznar, M. P.; Corella, J., Biomass gasification with air in an atmospheric bubbling fluidized bed. Effect of six operational variables on the quality of the produced raw gas. *Ind Eng Chem Res* **1996,** *35* (7), 2110-2120.

27. Knight, R. A., Experience with raw gas analysis from pressurized gasification of biomass. *Biomass Bioenerg* **2000,** *18* (1), 67-77.

28. Sutton, D.; Kelleher, B.; Ross, J. R. H., Review of literature on catalysts for biomass gasification. *Fuel Process Technol* **2001,** *73* (3), 155-173.

29. Rapagna, S.; Jand, N.; Kiennemann, A.; Foscolo, P. U., Steam-gasification of biomass in a fluidised-bed of olivine particles. *Biomass and bioenergy* **2000,** *19* (3), 187-197.

30. Milne, T. A.; Evans, R. J.; Abatzaglou, N. *Biomass Gasifier"Tars": Their Nature, Formation, and Conversion*; National Renewable Energy Laboratory, Golden, CO (US): 1998.

31. Bui, T.; Loof, R.; Bhattacharya, S. C., Multi-stage reactor for thermal gasification of wood. *Energy* **1994,** *19* (4), 397-404.

32. Devi, L.; Ptasinski, K. J.; Janssen, F. J. J. G., A review of the primary measures for tar elimination in biomass gasification processes. *Biomass and bioenergy* **2003,** *24* (2), 125-140.

33. Li, C.; Zhao, X.; Wang, A.; Huber, G. W.; Zhang, T., Catalytic transformation of lignin for the production of chemicals and fuels. *Chem. Rev* **2015,** *115* (21), 11559-11624.

34. Patel, M.; Zhang, X.; Kumar, A., Techno-economic and life cycle assessment on lignocellulosic biomass thermochemical conversion technologies: A review. *Renewable and Sustainable Energy Reviews* **2016,** *53*, 1486-1499.

35. Iribarren, D.; Peters, J. F.; Dufour, J., Life cycle assessment of transportation fuels from biomass pyrolysis. *Fuel* **2012,** *97*, 812-821.

36. Isahak, W. N. R. W.; Hisham, M. W. M.; Yarmo, M. A.; Hin, T.-y. Y., A review on bio-oil production from biomass by using pyrolysis method. *Renewable and sustainable energy reviews* **2012,** *16* (8), 5910-5923.

37. Ma, Z.; Troussard, E.; van Bokhoven, J. A., Controlling the selectivity to chemicals from lignin via catalytic fast pyrolysis. *Applied Catalysis A: General* **2012,** *423*, 130-136.

38. Brown, T. R.; Thilakaratne, R.; Brown, R. C.; Hu, G., Techno-economic analysis of biomass to transportation fuels and electricity via fast pyrolysis and hydroprocessing. *Fuel* **2013,** *106*, 463-469.

39. Corma, A.; Huber, G. W.; Sauvanaud, L.; O'Connor, P., Processing biomass-derived oxygenates in the oil refinery: Catalytic cracking (FCC) reaction pathways and role of catalyst. *J Catal* **2007,** *247* (2), 307-327.

40. Martone, P. T.; Estevez, J. M.; Lu, F. C.; Ruel, K.; Denny, M. W.; Somerville, C.; Ralph, J., Discovery of Lignin in Seaweed Reveals Convergent Evolution of Cell-Wall Architecture. *Curr Biol* **2009,** *19* (2), 169-175.

41. Nowakowski, D. J.; Bridgwater, A. V.; Elliott, D. C.; Meier, D.; de Wild, P., Lignin fast pyrolysis: Results from an international collaboration. *J Anal Appl Pyrol* **2010,** *88* (1), 53-72.

42. Ahmad, M. M.; Nordin, M. F. R.; Azizan, M. T., Upgrading of bio oil into high value hydrocarbons via hydrodeoxygenation. *American journal of applied sciences* **2010,** *7* (6), 746-755.

43. Mainka, H.; Tager, O.; Korner, E.; Hilfert, L.; Busse, S.; Edelmann, F. T.; Herrmann, A. S., Lignin - an alternative precursor for sustainable and cost-effective automotive carbon fiber. *J Mater Res Technol* **2015,** *4* (3), 283-296.

44. Baker, D. A.; Rials, T. G., Recent advances in low-cost carbon fiber manufacture from lignin. *J Appl Polym Sci* **2013,** *130* (2), 713-728.

45. Saha, D.; Payzant, E. A.; Kumbhar, A. S.; Naskar, A. K., Sustainable Mesoporous Carbons as Storage and Controlled-Delivery Media for Functional Molecules. *Acs Appl Mater Inter* **2013,** *5* (12), 5868-5874.

46. Chatterjee, S.; Jones, E. B.; Clingenpeel, A. C.; McKenna, A. M.; Rios, O.; McNutt, N. W.; Keffer, D. J.; Johs, A., Conversion of Lignin Precursors to Carbon Fibers with Nanoscale Graphitic Domains. *Acs Sustain Chem Eng* **2014,** *2* (8), 2002-2010.

47. Engels, H. W.; Pirkl, H. G.; Albers, R.; Albach, R. W.; Krause, J.; Hoffmann, A.; Casselmann, H.; Dormish, J., Polyurethanes: Versatile Materials and Sustainable Problem Solvers for Today's Challenges. *Angew Chem Int Edit* **2013,** *52* (36), 9422-9441.

48. Zhang, Q.; Zhang, G.; Xu, J.; Gao, C.; Wu, Y., RECENT ADVANCES ON LIGIN-DERIVED POLYURETHANE POLYMERS. *Reviews on Advanced Materials Science* **2015,** *40* (2).

49. Nadji, H.; Bruzzese, C.; Belgacem, M. N.; Benaboura, A.; Gandini, A., Oxypropylation of lignins and preparation of rigid polyurethane foams from the ensuing polyols. *Macromol Mater Eng* **2005,** *290* (10), 1009-1016.

50. Duong, L. D.; Nam, G. Y.; Oh, J. S.; Park, I. K.; Luong, N. D.; Yoon, H. K.; Lee, S. H.; Lee, Y.; Yun, J. H.; Lee, C. G.; Hwang, S. H.; Nam, J. D., High Molecular-Weight Thermoplastic Polymerization of Kraft Lignin Macromers with Diisocyanate. *Bioresources* **2014,** *9* (2), 2359-2371.

51. Aniceto, J. P. S.; Portugal, I.; Silva, C. M., Biomass-Based Polyols through Oxypropylation Reaction. *Chemsuschem* **2012,** *5* (8), 1358-1368.

52. Zhao, S.; Abu-Omar, M. M., Biobased Epoxy Nanocomposites Derived from Lignin-Based Monomers. *Biomacromolecules* **2015,** *16* (7), 2025-2031.

53. Nakamura, T.; Kawamoto, H.; Saka, S., Condensation reactions of some lignin related compounds at relatively low pyrolysis temperature. *J Wood Chem Technol* **2007,** *27* (2), 121-133.

54. Zakzeski, J.; Bruijnincx, P. C. A.; Jongerius, A. L.; Weckhuysen, B. M., The Catalytic Valorization of Lignin for the Production of Renewable Chemicals. *Chem Rev* **2010,** *110* (6), 3552-3599.

55. Wang, H.; Tucker, M.; Ji, Y., Recent development in chemical depolymerization of lignin: a review. *Journal of Applied Chemistry* **2013,** *2013*.

56. Yan, N.; Zhao, C.; Dyson, P. J.; Wang, C.; Liu, L. t.; Kou, Y., Selective Degradation of Wood Lignin over Noble‐Metal Catalysts in a Two‐Step Process. *Chemsuschem* **2008,** *1* (7), 626-629.

57. Matson, T. D.; Barta, K.; Iretskii, A. V.; Ford, P. C., One-pot catalytic conversion of cellulose and of woody biomass solids to liquid fuels. *J Am Chem Soc* **2011,** *133* (35), 14090-14097.

58. Yoshikawa, T.; Yagi, T.; Shinohara, S.; Fukunaga, T.; Nakasaka, Y.; Tago, T.; Masuda, T., Production of phenols from lignin via depolymerization and catalytic cracking. *Fuel Process Technol* **2013,** *108*, 69-75.

59. Liguori, L.; Barth, T., Palladium-Nafion SAC-13 catalysed depolymerisation of lignin to phenols in formic acid and water. *J Anal Appl Pyrol* **2011,** *92* (2), 477-484.

60. Patil, P. T.; Armbruster, U.; Richter, M.; Martin, A., Heterogeneously catalyzed hydroprocessing of organosolv lignin in sub-and supercritical solvents. *Energy & Fuels* **2011,** *25* (10), 4713-4722.

61. Jongerius, A. L.; Jastrzebski, R.; Bruijnincx, P. C. A.; Weckhuysen, B. M., CoMo sulfide-catalyzed hydrodeoxygenation of lignin model compounds: An extended reaction network for the conversion of monomeric and dimeric substrates. *J Catal* **2012,** *285* (1), 315-323.

62. Song, Q.; Wang, F.; Xu, J., Hydrogenolysis of lignosulfonate into phenols over heterogeneous nickel catalysts. *Chemical Communications* **2012,** *48* (56), 7019-7021.

63. Parsell, T.; Yohe, S.; Degenstein, J.; Jarrell, T.; Klein, I.; Gencer, E.; Hewetson, B.; Hurt, M.; Im Kim, J.; Choudhari, H., A synergistic biorefinery based on catalytic

conversion of lignin prior to cellulose starting from lignocellulosic biomass. *Green Chem* **2015,** *17* (3), 1492-1499.

64. Luo, H.; Klein, I. M.; Jiang, Y.; Zhu, H.; Liu, B.; Kenttämaa, H. I.; Abu-Omar, M. M., Total utilization of Miscanthus biomass, lignin and carbohydrates, using earth abundant nickel catalyst. *Acs Sustain Chem Eng* **2016,** *4* (4), 2316-2322.

65. Song, Q.; Wang, F.; Cai, J.; Wang, Y.; Zhang, J.; Yu, W.; Xu, J., Lignin depolymerization (LDP) in alcohol over nickel-based catalysts via a fragmentation–hydrogenolysis process. *Energ Environ Sci* **2013,** *6* (3), 994-1007.

66. Jongerius, A. L., Catalytic conversion of lignin for the production of aromatics. **2013**.

67. Lee, C. R.; Yoon, J. S.; Suh, Y.-W.; Choi, J.-W.; Ha, J.-M.; Suh, D. J.; Park, Y.-K., Catalytic roles of metals and supports on hydrodeoxygenation of lignin monomer guaiacol. *Catalysis Communications* **2012,** *17*, 54-58.

68. Zhao, C.; Lercher, J. A., Selective Hydrodeoxygenation of Lignin‐Derived Phenolic Monomers and Dimers to Cycloalkanes on Pd/C and HZSM‐5 Catalysts. *Chemcatchem* **2012,** *4* (1), 64-68.

69. Sepúlveda, C.; Leiva, K.; García, R.; Radovic, L. R.; Ghampson, I. T.; DeSisto, W. J.; Fierro, J. L. G.; Escalona, N., Hydrodeoxygenation of 2-methoxyphenol over Mo 2 N catalysts supported on activated carbons. *Catalysis Today* **2011,** *172* (1), 232-239.

70. Werhan, H.; Mir, J. M.; Voitl, T.; Rudolf von Rohr, P., Acidic oxidation of kraft lignin into aromatic monomers catalyzed by transition metal salts. *Holzforschung* **2011,** *65* (5), 703-709.

71. Farrell, A. E.; Plevin, R. J.; Turner, B. T.; Jones, A. D.; O'Hare, M.; Kammen, D. M., Ethanol can contribute to energy and environmental goals. *Science* **2006,** *311* (5760), 506-508.

72. Lee, A.; Deng, Y., Green polyurethane from lignin and soybean oil through non-isocyanate reactions. *European Polymer Journal* **2015,** *63*, 67-73.

Chapter II. Total Utilization of Miscanthus Biomass: by Using Earth Abundant Metal Catalyst

A. Introduction

Lignin depolymerization into fuels and chemicals is a significant challenge given the intrinsic heterogeneity of lignin. Also, the cross-linking between lignin and carbohydrate inhibits the accessibility of carbohydrate and results in a less effective conversion into useful chemicals (soluble sugars, furan derivatives, organic acids, etc.). The selective conversion of lignin does not only make use of a major component of the biomass, it also makes the carbohydrates more accessible.[1-3]

There have been several methods reported for the conversion of lignin in production of high value chemicals. Generally speaking, these methods can be summarized into five different categories: base catalyzed, acid catalyzed, metallic catalyzed, ionic liquids-assisted and supercritical fluids-assisted lignin depolymerization.[4] Among them, heterogeneous metal catalyzed lignin depolymerization was proved to be the most efficient one because of high lignin conversion, moderate reaction conditions, and intact carbohydrate recovery after lignin removal. A large amount of research has been carried out in this area focusing on the functionality of different metal catalysts in catalytic depolymerization of lignin (CDL), as well as different reaction conditions[5-8]. A previous work in Abu-Omar lab demonstrated an efficient lignin depolymerization strategy using a bimetallic combination of Pd/C together with Zn^{II} salts in methanol solvent. Under 225 $^{\circ}$C, over 50% lignin conversion was observed, as well as high selectivity for dihydroeugenol (DHE) and propylsyringol (PS).[5] Use of Pt, Ru and Rh supported on activated carbon have also been reported to give aromatic products in over 40% yield,

with Dioxane/H_2O as solvent at 250 ˚C[7]. The concept aqueous-phase reforming (APR) depolynmerization of lignin was reported by Zakzeski et al. In this case, Pt, Pd and Ru supported on Al_2O_3 and activated carbon as catalysts in 1:1 ratio of ethanol and water as solvent at 200-220 ˚C, with total yield of phenolic products of 17%.[8] Matson et al. reported a one-step catalytic conversion of biomass into liquid fuels under harsher conditions, 300-320 ˚C, 160-220 bar pressure, in supercritical methanol and Cu/Mg/Al catalyst[6]. The use of other metal catalysts (Co-Mo-S/Al_2O_3 and γ-Al_2O_3-supported Ru, Ni, NiNo, CoMo catalyst) to cleave C-O linkages in both lignocellulosic biomass and lignin model compound have also been reported[9-10]. However, the cost for most of the precious metal catalysts mentioned above as well as the harsh conditions limit scale up and broad applicability. Research based on earth-abundant and efficient catalysts under moderate conditions is needed to develop CDL reactions.

B. Catalytic depolymerization of lignin (CDL) in miscanthus biomass using Ni/C catalyst

One of the reasonable substituents for the precious metal catalysts in catalyzing hydrodeoxygenation reaction is nickel. Nickel as an earth abundant element has been shown to be effective in catalyzing a wide range of chemical transformations[11]. Supported nickel gave promising results for lignin depolymerization[12-15]. In our recent work in Abu-Omar lab, we demonstrate the utility of nickel supported on activated carbon (Ni/C) as a heterogeneous catalyst for the depolymerizatin of lignin in miscanthus under different conditions. Although woody biomass species have been investigated a lot, lignin depolymerization studies of grasses are rare[5-6, 12-16]. Furthermore, in comparison

with wood species, grasses contain ferulate/diferulate linkages in their cell walls[14, 17-18]. Under hydrodeoxygenation (HDO) reaction conditions, the ferulate/diferulate linkages can be selectively cleaved to release ferulic acid as the methyl ferulate ester in methanol medium. This notable selectivity makes grass biomass a suitable substrate for producing monomeric ferulic acid and related derivatives, which have wide applications in cosmetics as well as in the flavor and fragrance industry[19]. After removal of lignin, the carbohydrates remained as a solid residue, which was converted in a subsequent step to platform chemicals (hydroxymethylfurfural, levulinic acid, formic acid, etc.) using an earth abundant Lewis acid catalyst. Therefore, in a two-step process (CDL followed by carbohydrate upgrading) all three major components of biomass are converted to high value products with an overall yield of 55% of accessible biomass components with 98% mass balance closure.

C. Identification and quantification of aromatic products

The one step catalytic depolymerization of lignin (CDL) reaction into aromatic products and carbohydrate residue is illustrated in **Scheme 2.1**. Miscanthus was first milled to pass through a 40 mesh screen and then reacted with Ni/C catalyst in MeOH as solvent at 225 °C under H_2 pressure. The lignin content of miscanthus used in this study was determined according to standard NREL analysis procedures to be 13% by weight[1]. The starting biomass was fractionated by the CDL reaction into two phases, the liquid methanol phase containing aromatic products from lignin and a solid phase composed mainly of carbohydrates. A small amount of soluble sugars, mainly from the decomposition of hemicellulose, is extracted into the liquid phase; these can be separated from the aromatic products via liquid-liquid (H_2O and Et_2O) extraction. All aromatic

products were identified by LC/MS and quantified by HPLC/UV (against calibrations with authentic samples). By modifying the reaction conditions, we observed seven major high value phenolic products form the CDL reaction. These phenolic products can be further hydrogenated to produce various high value fuels and chemicals[20-21].

Scheme 2.1. One-step catalytic depolymerization of lignin (CDL) of intact biomass into phenolic products and carbohydrate residue.

(**1** = Dihydroeugenol**; 2** = Propylsyringol**; 3** = Dihydro *p*-Coumaric acid methyl ester; **4** = Dihydro Ferulic acid methyl ester; **5** = Isoeugenol; **6** = *p*-Coumaric acid methyl ester; **7** = Ferulic acid methyl ester)

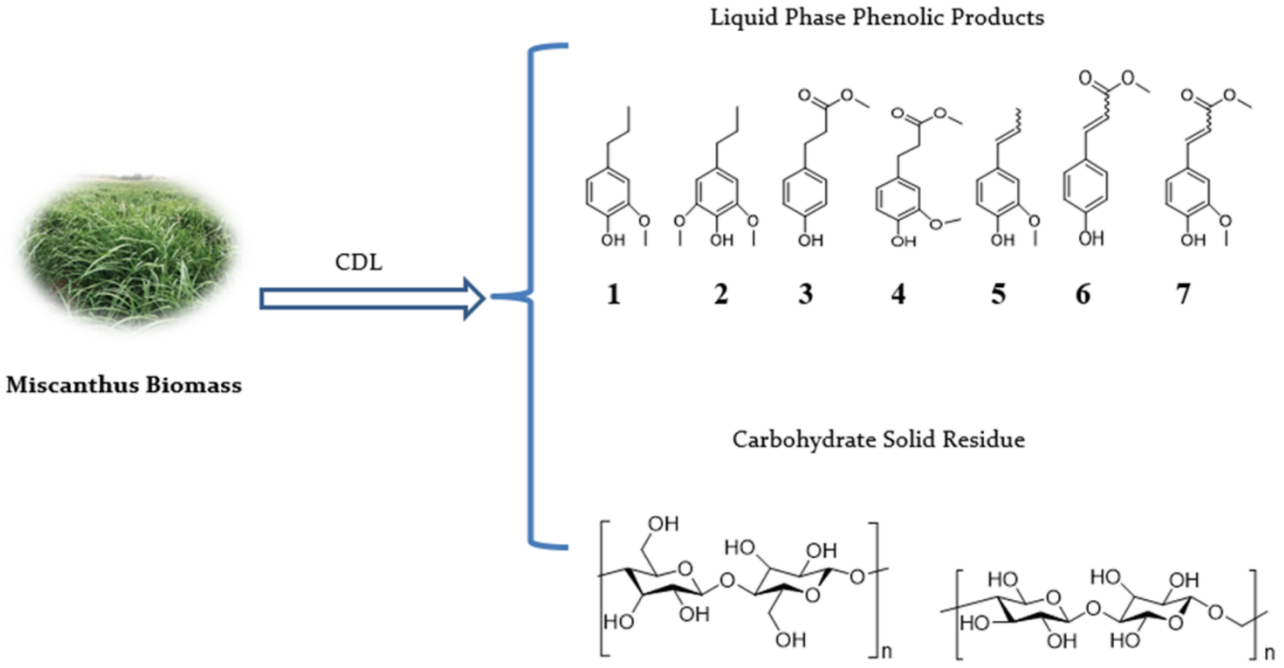

Under 35 bar of H_2 pressure, CDL reaction with Ni/C resulted in the formation of **1-4** as major products (**Table 2.1**). These four products account for 68% of the lignin in the starting miscanthus biomass (**Table 2.1**, entry 1). Compared with wood biomass species, miscanthus being a grass species contains ferulate linkages in its lingocellulose. These linkages, characteristic to grasses, accounts for products **3** and **4**, which are not observed in CDL reactions of wood species. These products account for the higher yields observed

for miscanthus (68% conversion) compared to those reported for wood species (50% conversion or so)[5, 22], as **3** and **4** represent ca. 25% of total lignin component of biomass. Despite the lower lignin content in miscanthus (13%) compared to that in hardwood (20-25%), the higher conversion of linin and ferulate linkages in miscanthus makes it a suitable biomass substrate for making valuable phenolic chemicals. Entries 1-3 are for CDL reactions in which the Ni/C catalyst was contained in a microporous cage. Entries 4-6 represent CDL reactions in which the Ni/C catalyst was added to the biomass without the use of a cage. In the latter cases, the biomass and catalyst come into direct solid-to-solid contact and the resulting biomass residues cannot be separated from the catalyst. The use of a microporous cage allows easy separation of the catalyst from the biomass residue post lignin depolymerization. It is interesting to note that CDL reactions without having the catalyst come into direct solid-to-solid contact with the biomass afforded comparable results to those in which both solids, catalyst and biomass, were mixed in the same chamber. This finding led to the hypothesis that lignin must be depolymerized into soluble oligomeric units in the hot methanol solution and the oligomeric fragments are upgraded further to monomeric tractable products by the Ni/C catalyst. Entry 7 supports our hypothesis in that some products even monomeric species are observed albeit at lower conversion in the absence of a catalyst. Variation in catalyst loading displayed little effect on yields and selectivity (**Table 2.1**).

Table 2.1. Catalytic depolymerization of lignin (CDL) reaction with Miscanthus under different conditions.[a]

Entry	% Yield of Major Phenolic Products[b]	Comments/

	1	**2**	**3**	**4**	**5-7**	Total Yield %	Conditions
1	21	19	12	16	-	68	15 wt% Ni/C in microporous cage
2	18	18	13	15	-	65	10 wt% Ni/C in microporous cage
3	16	14	11	14	1	56	5 wt% Ni/C in microporous cage
4	22	20	10	15	-	67	15 wt% Ni/C
5	19	18	12	16	-	65	10 wt% Ni/C
6	11	12	8	13	9	53	5 wt% Ni/C
7	-	-	-	-	22	22	No catalyst

[a.] Miscanthus biomass (1.0g), milled to 40 mesh, in 45 mL MeOH at 225˚C and 35 bar H_2 for 12 hours.

[b.] Yields are calculated based on theoretical lignin content in Miscanthus substrate (12.7% by weight).

In addition to producing nickel free cellulosic biomass residue, the use of a catalyst cage allows catalyst recyclability studies (**Table 2.2**). Although the Ni/C catalyst was reused in three consecutive reactions effectively, it did show overall reduction in lignin conversion as well as a shift in product selectivity toward products **5-7**. This suggested that the ability of the Ni catalyst to function as a hydrogenation catalyst decreased with each reuse.

Table 2.2. Catalyst recyclability test.[a]

Recycle Reaction	%Yield of Major Phenolic Products[b]					Total Yield%
	1	**2**	**3**	**4**	**5-7**	
1	21	20	12	17	-	70
2	10	11	8	15	7	51
3	7	7	7	14	12	47

[a.] Miscanthus biomass (1.0g), milled to 40 mesh, in 45 mL MeOH at 225˚C and 35 bar H_2 for 12 hours.

[b.] Yields are calculated based on theoretical lignin content in Miscanthus substrate (12.7% by weight).

The effect of hydrogen pressure on yields and distribution of products was investigated (**Table 2.3**). Comparison of **Table 2.1** and **Table 2.3** shows a general trend in decrease of phenolic product yield with the decrease of H_2 pressure. Even under N_2 pressure, some conversion was observed (Table 2.3, entry 3). However, conversions were significantly reduced from ca. 69% (**Table 2.1**) to less than 30% with compounds **6** and **7** accounting for the majority of the products yields. These compounds are the esters of ferulic and coumaric acids, which are responsible for linking lignin to hemicellulose[14], and can be obtained under our reaction conditions even in the absence of a catalyst (**Table 2.3**, entries 4 and 5). In all of these cases, lignin conversion was lower than the catalytic reactions listed in Table 2.1, suggesting that besides ferulic and coumaric acids, the lignin oligomers recondense in the absence of catalyst and high H_2 pressures. Therefore, the catalyst facilitates breaking up oligomeric lignin fragments and upgrading them via hydrodeoxygenation (HDO) to give products **1, 2** and **5**. The Ni/C catalyst interacts with aromatic groups in lignin fragments and form Ni-arene complexes, which further undergoes β-H elimination and C-O bond breakage to release monomeric phenolic products[22-25].

Table 2.3. Catalytic depolymerization of lignin (CDL) reaction of Miscanthus under different pressures of H_2 and N_2.[a]

Entry	% Yield of Major Phenolic Products[b]			Total Yield %	Comments/ Conditions
	5	**6**	**7**		
1	7	10	12	29	10 bar H_2
2	7	11	12	30	5 bar H_2
3	7	9	11	27	35 bar N_2

4	2	10	11	23	35 bar H_2, no catalyst
5	2	12	13	27	35 bar N_2, no catalyst

[a] 40 mesh Miscanthus (1.0 g), 10 wt% (0.10 g) Ni/C catalyst in mesoporous cage unless specified otherwise, in 45 mL MeOH at 225 °C for 12 h.

[b] Yields are calculated based on theoretical lignin content in Miscanthus (12.7% by weight).

D. Composition analysis of carbohydrate residue

After CDL, the solid biomass residue byproduct (solid stream in **Scheme 2.1**) was separated from the liquid phase by filtration and subjected to composition analysis as described above. In the acid hydrolysis process, the solid biomass residue degraded to give glucose, xylose, and arabinose as major products (**Table 2.4**).

Table 2.4. Quantitative compositional analysis of biomass solid residue post catalytic depolymerization of lignin (CDL) reaction.[a]

Entry	% Yield of carbohydrate				CDL reaction conditions
	Glucan	Xylan	Arabinan	Total	
1	56	21	9	86	15 wt% Ni/C, 35 bar H_2
2	59	17	10	86	10 wt% Ni/C, 35 bar H_2
3	52	19	11	82	10 wt% Ni/C, 10 bar H_2
4	52	19	10	81	10 wt% Ni/C, 35 bar N_2
5	55	21	7	83	no catalyst, 35 bar H_2
6	43	15	8	66	no catalyst, 35 bar N_2

[a] For all CDL reactions, 1.0g miscanthus was used as substrate with MeOH as solvent, under 225°C for 12 hours.

[b] Yields are calculated based on theoretical carbohydrate content in Miscanthus prior to CDL.

Glucose accounted for most of the mass, as would be expected given that cellulose is the major component of miscanthus lignocellulose (ca. 46% by weight). Interestingly, the carbohydrate composition of the solid residue was not sensitive to CDL conditions, except when no catalyst was used under N_2 atmosphere (**Table 2.4**, entry 6). This result suggests that our CDL conditions are selective for lignin degradation and the carbohydrates in miscanthus remain intact. Solid residue composition analysis gives high carbohydrate yield when the CDL reactions were performed under H_2 pressure with Ni/C catalyst (**Table 2.4**, entries 1−5). However, in the case of no catalysts and under inert N_2 atmosphere, lignin degradation was ineffective leaving significant lignin content in the resulting biomass residue. A comprehensive mass balance was carried out for all tractable aromatic products, sugars (extracted in the liquid MeOH phase as well as solid residue), ash and other unknowns as shown in **Figure 2.1**. The whole mass balance ends up to be 98%, within which phenolic products together with sugars (glucan, xylan and arabinan) account for 70% (625 mg), and other unidentified species accounting for 30% (267 mg).

Figure 2.1. Mass balance calculation of catalytic lignin depolymerization (CDL) reaction.

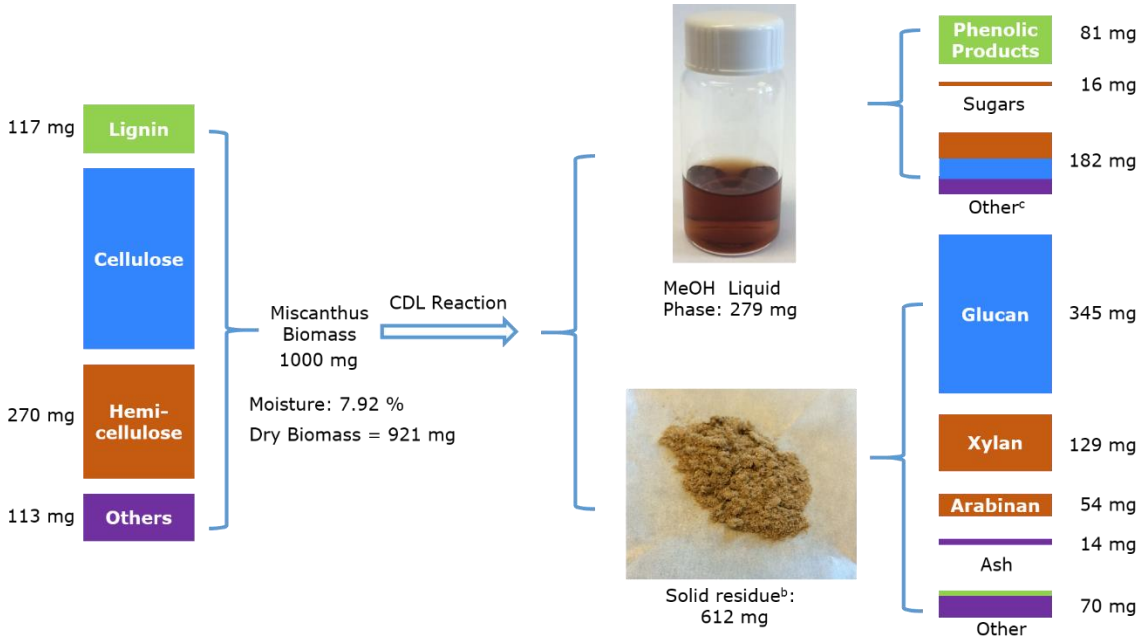

(a) CDL reaction condition: 15 wt % Ni/C, 35 bar H2, 225 °C, 12 h. Mass of phenolic products includes loss of O into H_2O during CDL reaction.

(b) Does not include Ni/C catalyst as it remained in microporous cage.

(c) Other components in the liquid phase are made of hemicellulose (71 mg), cellulose (76 mg) and others (35 mg), in the ratio hemicellulose: cellulose: other = 2:2:1.

E. Upgrading of carbohydrate residue into platform chemicals using $FeCl_3$

In addition to making phenolic products from CDL, the carbohydrate solid residue retains its value as shown by the composition analyses in **Table 2.4** and it can be used to produce platform chemicals[26-27]. Herein we report on the conversion of the carbohydrate solid residue after CDL reaction into furfural (FF) and levulinic acid (LA) using earth-abundant iron salts (**Table 2.5**). Reaction conditions were first optimized for Avicel conversion to LA: $FeCl_3$, 200 °C microwave heating for 90 min, biphasic medium H_2O/MeTHF. These conditions proved suitable for the conversion of the resulting biomass carbohydrate residue. Products were quantified by GC versus calibration with

authentic pure samples. The percent yields of FF (from xylan and arabinan) and LA (from glucan) are based on content in the carbohydrate residue post CDL reaction (**Table 2.4**). Our results showed that by using the carbohydrate residue from CDL as substrate, significantly higher yields can be obtained than with raw biomass or Avicel (**Table 2.5**).

These results demonstrate that after lignin removal pretreatment (CDL), the carbohydrates can be converted to chemicals selectively. Additionally, cellulose might be more amorphous after CDL. As discussed above, CDL reaction conditions of 15 wt % Ni/C, under 35 bar H_2 and 225 °C for 12 h gives the best phenolic products yield (**Table 2.1**, entry 1). Thus, lignin is thoroughly removed under this reaction condition and as a result, the carbohydrate solid residue is primed for conversion. Indeed, residue 1 was among the highest yielding (**Table 2.5**, entry 3).

Table 2.5. Conversion of carbohydrate solid residue to platform chemicals and comparison with raw miscanthus and crystalline cellulose.[a]

Entry	Substrate	% Yield		CDL Reaction Conditions
		LA	FF	
1	Avicel	61	11	
2	Miscanthus	52	41	
3	Residue 1	76	55	15 wt% Ni/C, 35 bar H_2
4	Residue 2	66	62	10 wt% Ni/C, 35 bar H_2
5	Residue 3	70	54	10 wt% Ni/C, 10 bar H_2
6	Residue 4	69	53	10 wt% Ni/C, 35 bar N_2
7	Residue 5	63	62	no catalyst, 35 bar H_2
8	Residue 6	76	71	no catalyst, 35 bar N_2

[a] Reaction conditions: 0.10 M $FeCl_3$ in H_2O/MeTHF (4 mL) at 200 °C for 90 min.
[b] Residues 1-6 are in accordance with the carbohydrate solid residues discussed in Table 2.4.

[c] All CDL reactions were performed using 1.0 g 40 mesh Miscanthus, Ni/C in microporous cage, 225 °C, 12 h.

Figure 2.2. Two-step transformation of whole biomass (CDL reaction conditions: 15 wt% Ni/C, 35 bar H_2, 225 °C, 12 h. Mass of phenolic products includes loss of O into H_2O during CDL reaction). Yield of platform chemicals is based on 1.0 g of starting miscanthus biomass.

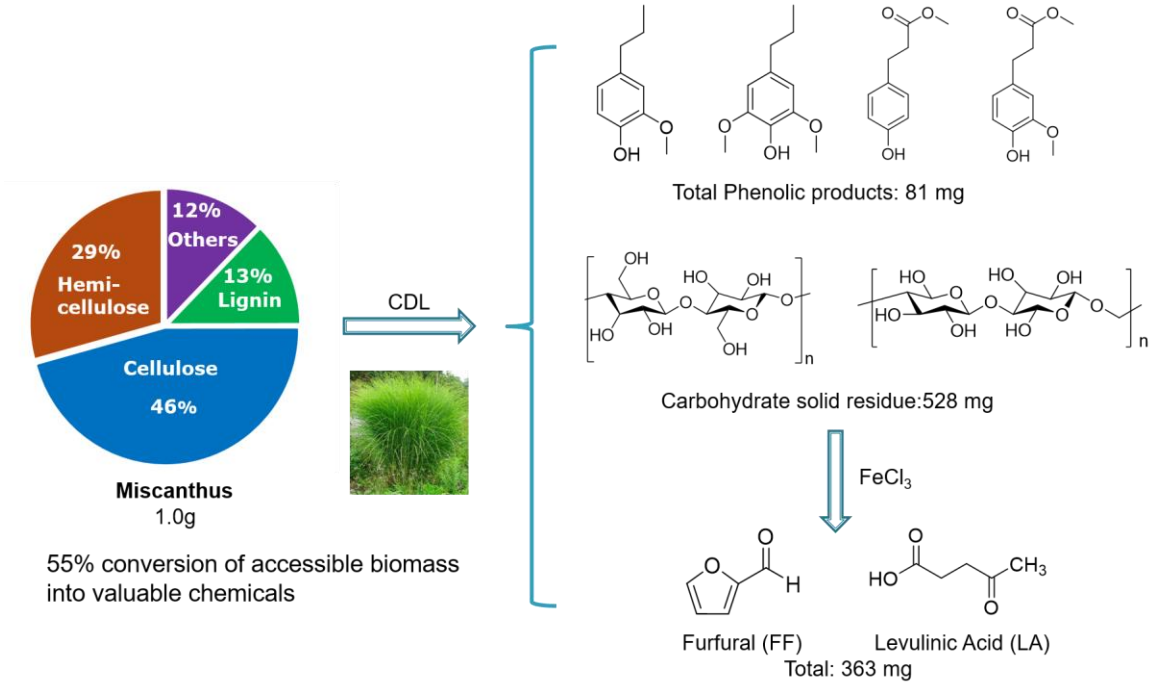

F. Conclusion

Ni/C is an efficient catalyst for catalytic depolymerization of lignin (CDL) reactions, giving 68% conversion of lignin in miscanthus into four phenolic products (**1**−**4**). The coproduced carbohydrate solid residue was found to be rich in glucan and xylan, demonstrating that the CDL reaction leaves the cellulose intact and renders it accessible for further transformations. Earth abundant iron chloride was used to convert the carbohydrate solid residue post CDL to the platform chemicals furfural and levulinic acid in yields of 55 and 76%, respectively. The outcome of the reported two step

transformations (CDL to make phenols followed by iron chloride catalysis of the carbohydrates) are six high value chemicals accounting for 55% of the accessible miscanthus biomass (Figure 2.2). The highlight of this study is that all three major components of biomass (lignin, cellulose and hemicellulose) are efficiently utilized to make high value chemicals. This result is important in demonstrating the feasibility of using a sustainable feedstock in its entirety to make chemicals via minimal (two reaction steps) number of processes.

G. Supporting information

1. Materials and methods

Materials.

Miscanthus was obtained from Repreve Renewables and milled to pass through a 40 mesh screen using a Mini Wiley Mill (Thomas Scientific, Swedesboro, NJ). Ni/C catalyst, containing 11 wt % Ni dispersed on activated carbon support, was synthesized and characterized based on reported literature methods. Methanol was purchased from Macron fine chemicals. Hydrochloric acid (37 wt %), sulfuric acid (98 wt %), 2-methyltetrahydrofuran (MeTHF), $FeCl_3 \cdot 6H_2O$, $FeCl_2$, $Fe_2(SO_4)_3 \cdot xH2O$, $FeSO_4 \cdot 7H_2O$ were purchased from Sigma-Aldrich. All chemicals were used as received without further purification.

General Heterogeneous Catalytic Reaction.

Miscanthus substrate was used without washing. In a general reaction, 1.0 g of 40 mesh miscanthus, 5−15 wt % Ni/C catalyst, and 45 mL of methanol were added to a stainless steel Parr reactor. To facilitate good separation of catalyst and substrate, Ni/C catalyst was first loaded into a microporous cage (325 mesh) before loading into the Parr reactor. The catalyst cage allows solvent as well as solute to pass through and access the

catalyst, while keeping the carbohydrate residue separate from the catalyst. The reactor was sealed, and then purged with UHP grade H_2 for 5 times while stirring. Then the whole reaction system was pressurized with 10−35 bar H_2 or N_2, heated to 225 °C at a stirring speed of 600 rpm, and the temperature maintained for 12 h. The reaction was terminated by cooling the reactor to room temperature. The reaction mixture was filtered to separate the liquid phase containing aromatic products from the solid biomass residue, which was washed with additional methanol to remove any remaining phenolic products on the solid surface, and the liquid wash was combined with the filtrate. The combined liquid phase was concentrated by rotary evaporation, diluted in a volumetric flask (10 mL), and analyzed by HPLC/UV as well as by HPLC/MS. The biomass solid residue was subjected to acid hydrolysis for composition analysis.

Acid hydrolysis and compositional analysis of biomass solid residue.

The biomass solid residue was separated from the liquid phase by filtration and subjected to composition analysis using NREL standard acid hydrolysis procedure. In specific, 0.5g of residue was first analyzed for moisture content using a moisture balance. Another 0.6g of residue was split into two portions, 0.3g each. For each portion, 3 mL of 72% H_2SO_4 was added, and mixed with the solid residue thoroughly. The residues sulfuric acid suspensions were placed in a water shaker and stirred at 30 ˚C for 1h. 84 mL of deionized H_2O was added, and the samples sealed and transferred to an autoclave for heating at 121 ˚C for 60 min. 1 mL of the final aqueous mixture containing solubilized carbohydrates was diluted using DI H_2O to a final volume of 10 mL, filtered through a 13 mm in diameter syringe filter with 0.2 μm PTFE and subjected to HPLC analysis to quantify soluble sugars resulting from the biomass residue.

Conversion of the biomass solid residue into furfural (FF) and levulinic acid (LA).

Dehydration of carbohydrates were performed with a CEM Discover SP/S-class microwave reactor. A 1 mL aqueous solution (made with Millipore filtered water) of 0.1 M iron salt and 0.25 M substrate (Avicel, raw biomass or biomass solid residue from our CDL reaction) was added to a 10 mL glass microwave reaction vessel. 3 mL of 2-methyltetrahydrofuran (MeTHF) was added to the vessel along with a small Teflon coated stir bar. Using the fixed power control method, reactions were heated to 200 °C at 200W of microwave power for up to 90 min. Reaction times began once the temperature was reached as indicated by the instrument's IR temperature sensor. Reactions were quenched by a nitrogen gas flow that cooled the system to 60 °C. The organic MeTHF phase was separated from the aqueous phase and subjected to GC (gas chromatography) analysis. The aqueous phase was analyzed by HPLC.

Carbohydrate determination in methanol phase.

In order to determine the sugar content in the methanol phase after CDL reaction, 20 mL H_2O was first added into 10 mL methanol solution. The resulting solution was then extracted with 20 mL diethyl ether three times to remove aromatic products. The methanol-H_2O layer was collected, and methanol was removed from H_2O under reduced pressure. The H_2O layer which contains carbohydrate was subjected to acid hydrolysis by following standard NREL procedures, and the solution was analyzed by HPLC.

2. Instrumentation and and chromatographic conditions

HPLC-MS analysis

All HPLC separations for mass spectrometry analysis were performed on a Surveyor Plus HPLC system from Thermo Scientific consisting of a quaternary pump, an autosampler, a photodiode array (PDA) detector, and a Zorbax SB-C18 column. A non-linear gradient of water (A) and acetonitrile (B) was used as follows: 0.00 min, 95% A and 5% B; 10.00 min, 95% A and 5% B; 30.00 min, 40% A and 60% B; 35.00 min, 5% A and 95 %; 38.00min, 5% A and 95% B; 38.50 min, 95% A and 5% B; 45.00 min, 95% A and 5% B. Flowrate of the mobile phase was kept at 500 μL/min. PDA detector was set at the wavelength of 254 nm.

Mass spectrometric analysis (MS, MS^2 and MS^3) of HPLC eluent was performed using a Thermo Scientific linear quadrupole ion trap (LQIT) mass spectrometer equipped with an electrospray ionization (ESI) source. All mass spectrometry experiments were performed under negative ion mode. HPLC eluents were mixed via a T-connector with 1% sodium hydroxide water solution at a flow rate of 0.1 μL/min before entering the ESI source. Addition of sodium hydroxide facilitates deprotonation of the analytes. ESI source conditions were set as: 3.5 kV spray voltage; 50 (arbitrary units) sheath gas (N_2) flow and 20 (arbitrary units) auxillary gas (N_2) flow. MS^3 analysis was performed using the data dependent scan function of the Thermo Xcalibur software. The most abundant ion formed upon ESI was isolated and subjected to collision-activated dissociation (CAD). The most abundant fragment ion was further selected for isolation and fragmentation. For all MS^3 experiments, an isolation window of 2 m/z units was used along with a normalized collision energy of 30 (arbitrary units). All mass spectrometry experiments were performed under negative ion mode.

HPLC/GC analysis

The liquid phase from lignin depolymerization reactions with methanol as solvent was analyzed with Agilent 1260 Infinity Quaternary High-Performance Liquid Chromatography (HPLC) system, using Zorbax Eclipse XDB-C18 Column (250 x 74.6mm) set at 30 ˚C. The chromatography apparatus is equipped with G1315D Diode Array Detector (DAD). A mixture of H2O (A) and acetonitrile (B) were used as the mobile phase at a flow rate of 0.5 mL/min. Nonlinear gradient was used (80% A and 20% B from beginning to 5% A and 95 % B at 55.0 min). A fixed amount (400μL) of internal standard 3-methoxy phenol (10 mM) was added into each sample for the quantification purposes. Standard curves for all the aromatic products were made by comparison of the products to internal standard. All results were analyzed and quantified according to standard curves. Before analyzing by HPLC, the liquid samples were filtered through a 0.22μm cutoff syringe filter (2 5mm diameter).

All sugar samples as well as aqueous phase after solid carbohydrate dehydration reaction were analyzed with Agilent 1260 Infinity Quaternary High-Performance Liquid Chromatography (HPLC) system, using Aminex HPX-87H column (300 x 7.8 mm) set at 70 ˚C. The chromatography apparatus is equipped with G1362A Refractive Index Detector (RID) calibrated with external standards. A 0.005 M sulfuric acid solution was employed as the mobile phase with flow of 0.6 mL/min. A fixed amount (400 μL) of internal standard tert-butyl alcohol (10 mM) was added into each sample for quantification purposes. Standard curves (glucose, xylose, and arabinose) were made by comparison of the products with internal standard. All results were analyzed and quantified according to standard curves. Before analyzing by HPLC, the aqueous solutions were filtered through a 0.22μm cutoff syringe filter (25 mm diameter).

The organic phase after solid carbohydrate dehydration reaction was analyzed by Agilent Technologies 6890N Network Gas Chromatography (GC) System, equipped with a J&W Scientific DB-5 capillary column. Oven temperature was ramped from 50 °C to 250 °C at 15 °C min^{-1}, and from 250 °C to 300 °C at 25 °C min^{-1} by using constant flow mode at 1.0 mL min^{-1}. Products (furfural and levulinic acid) were identified by retention time and compared to standards. Products were quantified by using a standard calibration curve. Before analyzing by GC, the organic solutions were filtered through a 0.22μm cutoff syringe filter (25 mm diameter).

H. References:

1. Luo, H.; Klein, I. M.; Jiang, Y.; Zhu, H.; Liu, B.; Kenttämaa, H. I.; Abu-Omar, M. M., Total utilization of Miscanthus biomass, lignin and carbohydrates, using earth abundant nickel catalyst. *Acs Sustain Chem Eng* **2016,** *4* (4), 2316-2322.
2. Luo, H.; Abu-Omar, M. M., Chemicals from lignin. In *Encyclopedia of Sustainable Technologies*, Abraham, M. A., Ed. 2017; pp 573–585.
3. Mosier, N.; Wyman, C.; Dale, B.; Elander, R.; Lee, Y. Y.; Holtzapple, M.; Ladisch, M., Features of promising technologies for pretreatment of lignocellulosic biomass. *Bioresource Technol* **2005,** *96* (6), 673-686.
4. Wang, H.; Tucker, M.; Ji, Y., Recent development in chemical depolymerization of lignin: a review. *Journal of Applied Chemistry* **2013,** *2013*.
5. Parsell, T.; Yohe, S.; Degenstein, J.; Jarrell, T.; Klein, I.; Gencer, E.; Hewetson, B.; Hurt, M.; Im Kim, J.; Choudhari, H., A synergistic biorefinery based on catalytic

conversion of lignin prior to cellulose starting from lignocellulosic biomass. *Green Chem* **2015,** *17* (3), 1492-1499.

6. Matson, T. D.; Barta, K.; Iretskii, A. V.; Ford, P. C., One-pot catalytic conversion of cellulose and of woody biomass solids to liquid fuels. *J Am Chem Soc* **2011,** *133* (35), 14090-14097.

7. Yan, N.; Zhao, C.; Dyson, P. J.; Wang, C.; Liu, L. t.; Kou, Y., Selective Degradation of Wood Lignin over Noble‐Metal Catalysts in a Two‐Step Process. *Chemsuschem* **2008,** *1* (7), 626-629.

8. Zakzeski, J.; Jongerius, A. L.; Bruijnincx, P. C. A.; Weckhuysen, B. M., Catalytic lignin valorization process for the production of aromatic chemicals and hydrogen. *Chemsuschem* **2012,** *5* (8), 1602-1609.

9. Jongerius, A. L.; Jastrzebski, R.; Bruijnincx, P. C. A.; Weckhuysen, B. M., CoMo sulfide-catalyzed hydrodeoxygenation of lignin model compounds: An extended reaction network for the conversion of monomeric and dimeric substrates. *J Catal* **2012,** *285* (1), 315-323.

10. Patil, P. T.; Armbruster, U.; Richter, M.; Martin, A., Heterogeneously catalyzed hydroprocessing of organosolv lignin in sub-and supercritical solvents. *Energy & Fuels* **2011,** *25* (10), 4713-4722.

11. Ananikov, V. P., Nickel: the “spirited horse” of transition metal catalysis. ACS Publications: 2015.

12. Li, C.; Zheng, M.; Wang, A.; Zhang, T., One-pot catalytic hydrocracking of raw woody biomass into chemicals over supported carbide catalysts: simultaneous conversion of cellulose, hemicellulose and lignin. *Energ Environ Sci* **2012,** *5* (4), 6383-6390.

13. Klein, I.; Saha, B.; Abu-Omar, M. M., Lignin depolymerization over Ni/C catalyst in methanol, a continuation: effect of substrate and catalyst loading. *Catalysis Science & Technology* **2015,** *5* (6), 3242-3245.

14. Morvan, D.; Rauchfuss, T. B.; Wilson, S. R., π-Complexes of Lignols with Manganese (I) and Ruthenium (II). *Organometallics* **2009,** *28* (11), 3161-3166.

15. Song, Q.; Wang, F.; Xu, J., Hydrogenolysis of lignosulfonate into phenols over heterogeneous nickel catalysts. *Chemical Communications* **2012,** *48* (56), 7019-7021.

16. Yang, H.; Yan, R.; Chen, H.; Zheng, C.; Lee, D. H.; Liang, D. T., In-depth investigation of biomass pyrolysis based on three major components: hemicellulose, cellulose and lignin. *Energy & Fuels* **2006,** *20* (1), 388-393.

17. Hatfield, R. D.; Ralph, J.; Grabber, J. H., Cell wall cross-linking by ferulates and diferulates in grasses¹. *Journal of the Science of Food and Agriculture* **1999,** *79*, 403-407.

18. Rouau, X.; Cheynier, V.; Surget, A.; Gloux, D.; Barron, C.; Meudec, E.; Louis-Montero, J.; Criton, M., A dehydrotrimer of ferulic acid from maize bran. *Phytochemistry* **2003,** *63* (8), 899-903.

19. Kumar, N.; Pruthi, V., Potential applications of ferulic acid from natural sources. *Biotechnology Reports* **2014,** *4*, 86-93.

20. Hama, S.; Li, X.; Yukawa, K.; Saito, Y., Dehydrogenation of cycloalkanes by suspended platinum catalysts. *Chemistry letters* **1992,** *21* (12), 2463-2466.

21. Russell, C. L.; Klein, M. T.; Quann, R. J.; Trewella, J., Catalytic hydrocracking reaction pathways, kinetics, and mechanisms of n-alkylbenzenes. *Energy & fuels* **1994,** *8* (6), 1394-1400.

22. Song, Q.; Wang, F.; Cai, J.; Wang, Y.; Zhang, J.; Yu, W.; Xu, J., Lignin depolymerization (LDP) in alcohol over nickel-based catalysts via a fragmentation–hydrogenolysis process. *Energ Environ Sci* **2013,** *6* (3), 994-1007.

23. Kelley, P.; Lin, S.; Edouard, G.; Day, M. W.; Agapie, T., Nickel-mediated hydrogenolysis of C–O bonds of aryl ethers: what is the source of the hydrogen? *J Am Chem Soc* **2012,** *134* (12), 5480-5483.

24. Sergeev, A. G.; Hartwig, J. F., Selective, nickel-catalyzed hydrogenolysis of aryl ethers. *Science* **2011,** *332* (6028), 439-443.

25. Huber, G. W.; Shabaker, J. W.; Dumesic, J. A., Raney Ni-Sn catalyst for H2 production from biomass-derived hydrocarbons. *Science* **2003,** *300* (5628), 2075-2077.

26. Zhao, C.; Lercher, J. A., Selective Hydrodeoxygenation of Lignin‐Derived Phenolic Monomers and Dimers to Cycloalkanes on Pd/C and HZSM‐5 Catalysts. *Chemcatchem* **2012,** *4* (1), 64-68.

27. Mohan, D.; Pittman, C. U.; Steele, P. H., Pyrolysis of wood/biomass for bio-oil: a critical review. *Energy & fuels* **2006,** *20* (3), 848-889.

CHAPTER III. Atomic Level Structure Characterization of Biomass Pre- and Post- Lignin Treatment by Dynamic Nuclear Polarization-Enhanced Solid State NMR.

A. Introduction

With an increased awareness of global climate change, the case for use of bio-renewable resources in production of biofuels, biomaterials and biospecialty chemicals is compelling. Lignocellulosic biomass is a promising sustainable feedstock for this purpose. It is mainly composed of carbohydrate polymers (cellulose, hemicellulose) and lignin. The latter is a heavily cross-linked polymer consisting of three principal building blocks, p-hydroxyphenyl (H), guaiacyl (G), and syringyl (S), (**Chapter 1, Figure 1.1**). Cellulose has great potential to be used as a renewable fuel source as it constitutes up to 40 − 50% of the dry plant mass, and its conversion into bioethanol and other platform chemicals has seen significant advances in recent years[1]. On the other hand, the recalcitrant structure of lignin and its cross-linking with carbohydrate resulted in the lignocellulosic biomass a rigid and compact structure, which renders it particularly resilient to biodegradation[2]. The conversion of lignocellulose into valuable products is therefore highly challenging and is an active field of research[3-4]. A number of studies have investigated the effects of crystallinity and the degree of polymerization on the enzymatic hydrolysis of cellulose[5-8], highlighting the need for pretreatment to expand the accessibility of cellulose[9]. The widely accepted model states that pretreatment both increases the surface area of cellulose and converts its crystalline phase into more reactive amorphous cellulose[10-11].

Our previous work in Abu-Omar group has demonstrated that catalytic depoymerization using metal catalyst is one of the most promising pathways for biomass utilization. Lignin in grass biomass can be efficiently depolymerized into monomeric phenolic compounds using Ni/C catalyst, while carbohydrate residue remain intact. However, till now, a detailed understanding of biomass structure is still lacking, due to the lack of appropriate noninvasive physical tools with sufficiently high resolution. Structure elucidation is very necessary in understanding the development and commercialization of the catalytic methods. To date, some structural data have been obtained by cross-polarization magic angle spinning solid-state NMR (CPMAS ssNMR), X-ray diffraction (XRD), infrared spectroscopy, and electron microscopy[12-15], but the elucidation of definite high resolution structures has been unattainable.

SSNMR is perhaps the only technique capable of providing atomic-level structural information on raw biomass, yet structural complexity leads to severe spectral crowding that limits the usefulness of SSNMR data. For this reason, the structure of lignin remains largely unexplored by SSNMR[16]. The advent of high-field dynamic nuclear polarization (DNP) combined with magic angle spinning (MAS), an effective hyperpolarization technique used to sensitize SSNMR spectroscopy, may very well provide a solution to this dilemma[17-19]. DNP utilizes the much larger Boltzmann polarization of the electrons in order to enhance nuclear polarization. Low concentrations of biradical dopants are impregnated into the sample as a source of unpaired electrons, and their electron paramagnetic resonance (EPR) transitions are irradiated by high-power microwaves to transfer polarization via the so-called cross-effect to the nuclei[18]. The theoretical maximum gain in sensitivity corresponds to the ratio of the magnetogyric ratios of the

electron and the nucleus, that is, to ~660 for ^{1}H and ~2600 for ^{13}C. Although the application of DNP does not reduce the line widths, the vast improvement in sensitivity offered by this technique can enable the measurement of two-dimensional (2D) ^{13}C–^{13}C homonuclear correlation spectra at natural isotopic abundance[20-23]. By spreading the broad resonances of biomass along a second dimension, many overlapping components can then be separated, and identified, without destroying the sample. Here, we used this new technology to study the atomic-level structure of intact and catalytically-treated genetic variants of poplar.

B. Catalytic depolymerization of lignin (CDL) in gene mutant poplar species using Ni/C catalyst

We previously reported a unique process for selective CDL of wild-type (WT) poplar as well as two genetic variants having an increased, or decreased, S lignin content (high-S and low-S). This process involves the treatment of intact lignocellulosic biomass with a Pd/C + $Zn(OAc)_2 \cdot 2H_2O$ bimetallic catalyst in methanol under 35 bar of hydrogen at 225 °C. During this process, lignin was removed from the intact biomass and upgraded into monomeric phenolic products. The solid carbohydrate byproduct residue (cellulose and hemicellulose) was first separated and analyzed for the composition, followed by further converted into glucose by cellulose enzyme digestion. In our study, CDL reaction for poplar yields high selectivity for two phenolic products, 2-methoxy-4-propylphenol (1) and 2,6-dimethoxy-4-propylphenol (2) (**Scheme 3.1**), which originate from G and S lignin, respectively. Moreover, variations in the lignin monomer compositions in different genetic variants allow the selectivity between the two products to be tuned (**Table 3.1**).

Scheme 3.1. CDL from Lignocellulosic Biomass

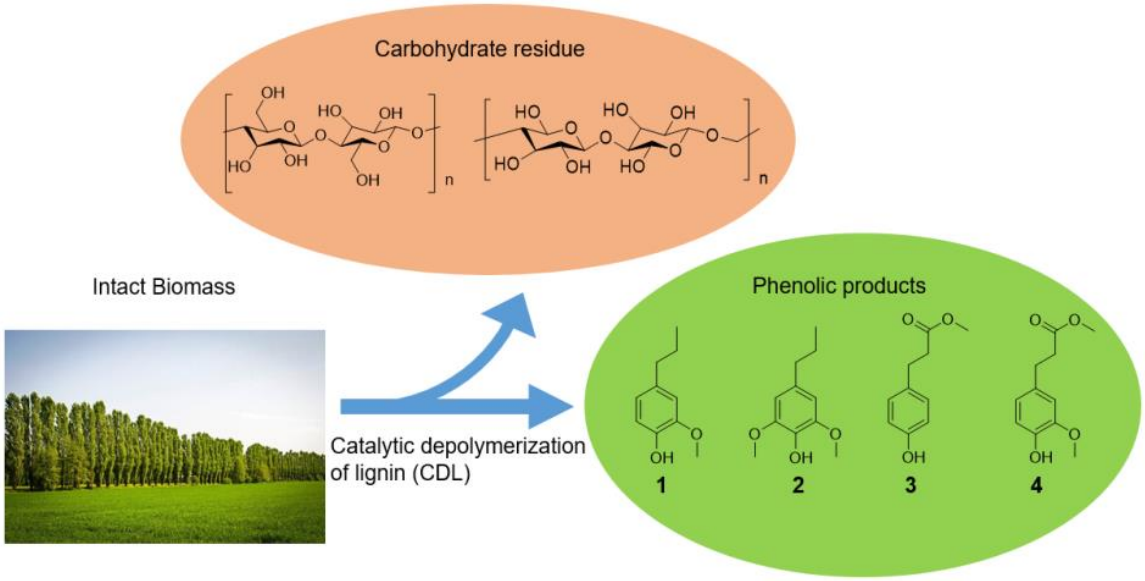

Subsequently, we have demonstrated the total utilization of a grass biomass species, miscanthus, by using an earth-abundant metal catalyst (Ni/C)[24]. Due to differences in the grass and hardwood cell wall compositions and structures, the lignin component in grass is more easily accessed, thus giving a higher yield[25]. Additionally, when compared with wood biomass, grass species contain abundant ferulate and diferulate linkages, which connect hemicellulose with lignin[26-28]. Under hydrodeoxygenation (HDO) reaction conditions, these linkages can be selectively cleaved to release ferulic acid methyl ester (**4**) and dihydro p-coumaric acid methyl ester (**3**) as products (**Scheme 3.1** and **Table 3.1**).

Table 3.1. Product Yields from CDL Reactions of Lignocellulosic Biomass Samples[a]

% Yield of major phenolic products[b]

Substrate	Catalyst	1	2	3	4	Total Yield%
WT poplar	Pd/C+$Zn(OAc)_2$	9	23			32
High-S poplar	Pd/C+$Zn(OAc)_2$	5	35			40
Low-S poplar	Pd/C+$Zn(OAc)_2$	13	13			26
Miscanthus[c]	Ni/C	21	19	12	16	68

[a] Reaction conditions: Substrates (1.0g) milled to 40 mesh, in 45 mL of methanol at 225 °C under 35 bar of H_2 for 12h.

[b] Yields are calculated based on theoretical lignin content in different biomass substrates.

[c] Reference 33.

The CDL reactions are highly selective for the removal of lignin, and thus the remaining cellulose residues become more accessible for further transformations. Conversion of carbohydrate residue into platform chemicals resulted in higher yield of products compared with intact biomass. We further performed enzymatic hydrolysis of raw and CDL-treated biomass samples (**Figure 3.1**). Prior to CDL treatment, the saccharification of intact biomass resulted in low yields for monomer sugar (ca. 10%). No significant differences in the saccharification kinetics and yields were observed of the three poplar variants, despite the differences in the monomeric constituents of lignin. As comparison, microcrystalline cellulose (Avicel) is hydrolyzed to 59% within 72 h, and wood pulp (Solka Floc) is hydrolyzed to a yield of 89%. These results are consistent with previous reports and indicate that carbohydrate is largely inaccessible in raw lignocellulosic biomass because of the cross-linking with lignin[29]. After CDL treatment, we observed significant enhancement in the enzyme hydrolysis yield of monomer sugar

among all three genetic variants, and all exceeded the yield achieved with Avicel. The CDL-treated high-S poplar was the best-performing material, with a quantitative conversion after 72 h. Carbohydrate residue of WT poplar performed similar to commercial wood pulp (Solka Floc), and the los-S poplar residue gave the lowest conversion among the three. Ciesielski and co-workers noticed a similar trend in lignin-modified *Arabidopsis Thaliana*, which they performed maleic acid pretreatment prior to enzymatic hydrolysis[30]. Their results, as well as ours, indicated that genetic modification of the lignin in the raw biomass has a clear impact on the enzyme digestibility of plant cell walls following treatment to remove lignin[29].

Figure 3.1. Enzymatic hydrolysis of different cellulose sources plotted as a function of time.

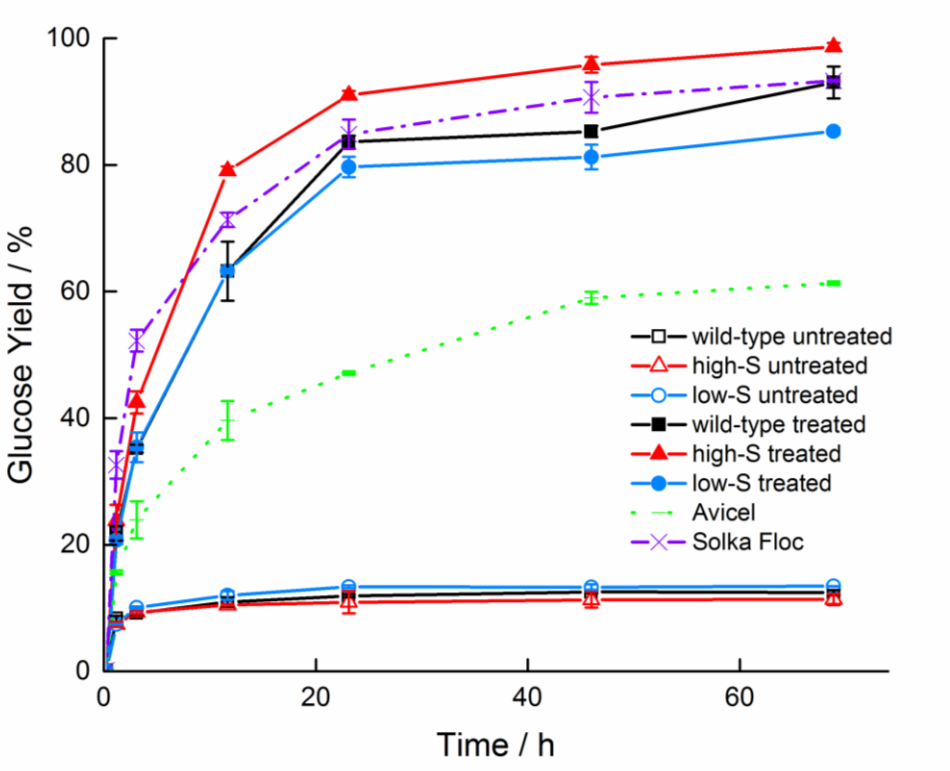

XRD analysis were performed on three gene modified poplar species before and after CDL treatment. We found that the relative crystalline index (RCI) of the three poplar variants increased from 46−50% to 67−69% following CDL treatment (**Figure 3.2**). Because lignin has a highly amorphous structure, its removal may increase the apparent crystallinity of the remaining cellulose[31]. The XRD data also indicate that there is no correlation between the relative crystallinity of the cellulose and the corresponding enzymatic hydrolysis yields. These findings seem to contradict the general belief that only amorphous cellulose is accessible for hydrolysis[9-10] and show that crystallinity is not the sole factor determining the rate of hydrolysis. Other factors, such as surface area and accessibility of cellulose, also affect the enzymatic hydrolysis rate[11, 32].

Figure 3.2. Normalized XRD diffractograms of raw and CDL treated poplar species are shown for (a) wild type poplar, (b) high S poplar, and (c) low S poplar.

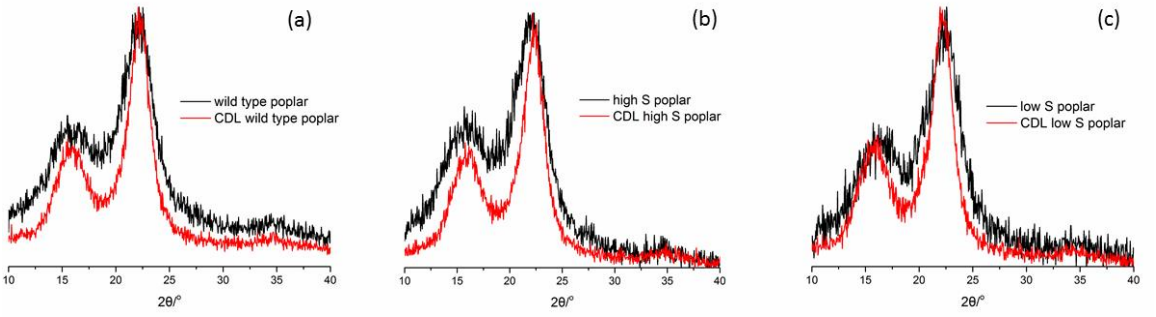

Table 3.2. Relative Crystalline index (RCI) for three poplar species before and after CDL treatment.

sample	RCI (untreated) / %	RCI (CDL-treated) / %
wild type	49.8%	69.1%
high S	46.3%	68.1%

low S	46.2%	67.1%

C. DNP enhanced ssNMR analysis on biomass

1. Comparison of cellulose region pre- and post- CDL treatment

The proportion of different interunit linkages connecting the lignin monomers as well as its cross-linking with carbohydrate may be the leading cause of the different catalytic efficacies in poplar variants. As mentioned earlier, information concerning the connectivities between the building blocks of plant cell walls in biomass can only be accessed by 2D $^{13}C–^{13}C$ homonuclear correlation SSNMR spectroscopy. One such experiment, namely, the 2D ^{13}C refocused Incredible Natural Abundance DoublE QUAntum Transfer Experiment (INADEQUATE)[33-34], is particularly useful because it provides simple to interpret spectra featuring exclusive resonances from pairs of directly bound ^{13}C nuclei. Performing such a measurement is unrealistic using conventional SSNMR without isotopic enrichment as only 1 of ∼10 000 carbon−carbon pairs can elicit an NMR response under natural abundance. Recently, Takahashi and co-workers demonstrated its feasibility under DNP conditions using microcrystalline cellulose[34]. It is, however, not immediately clear whether DNP-enhanced SSNMR is applicable to lignocellulosic biomass samples. The large grain sizes can act as barriers for the penetration of the biradical molecules, limiting the efficiency of the hyperpolarization[20, 35]. (On the other hand, this physical separation between the radicals and the studied biomass assures that its structure remains intact; note also that even the surface and subsurface regions of the sample must be separated from the nearest radical by at least 1 nm to be observed.) Nevertheless, DNP has been successfully applied to studying the

carbohydrate and protein structures of plant cell walls[36]. Here, we also observed that biomass samples absorbed meaningful quantities of an AMUPol[37] solution and yielded large signal-to-noise enhancement factors of 65−74, as demonstrated by the ^{1}D ^{13}C CPMAS spectra in **Figure 3.3**. Importantly, the enhancement is identical for both cellulose and lignin, a testament to their interconnected structures. DNP experiment with CDL treated carbohydrate samples has a reduction in DNP efficiency (enhancement factors of 26−33, depending on the sample), likely due to either the presence of trace amount of paramagnetic metal residues or a reduction in porosity.

Figure 3.3. DNP enhanced 1D ^{13}C CPMAS NMR spectra for raw (a,i), as well as CDL-treated (a,ii) high-S poplar.[a]

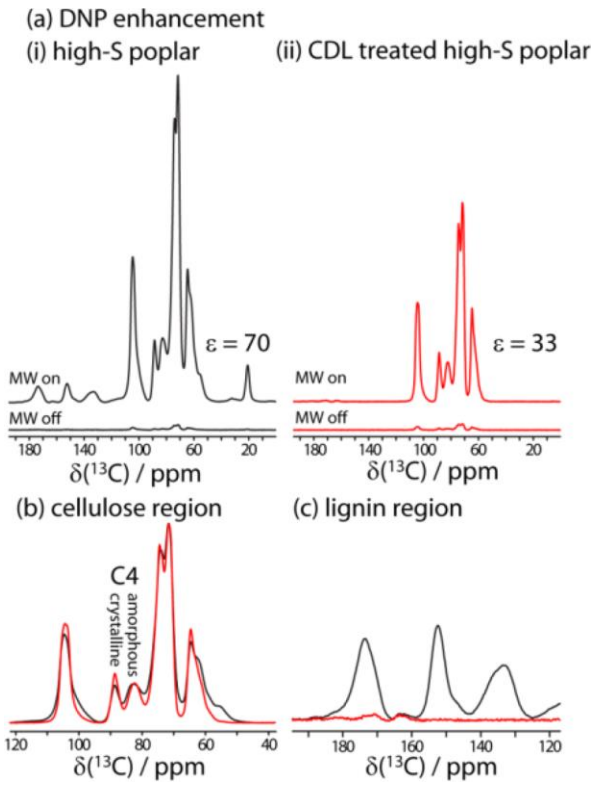

[a] The spectra acquired with and without the application of microwaves are shown in (a) along with the enhancement factor. Comparisons of the cellulose (b) and lignin (c) regions of the DNP-enhanced CPMAS spectra of the raw (black trace) and CDL-treated (red trace) high-S poplar samples are also shown. Note

that the C4 peak of crystalline cellulose (marked in the figure) has a higher relative intensity in the CDL-treated sample. The complete removal of lignin can be observed in the comparison shown in (c).

Figure 3.4. DNP enhanced 1D ^{13}C CPMAS NMR spectra for wild type, high-S and low-S poplar.[a]

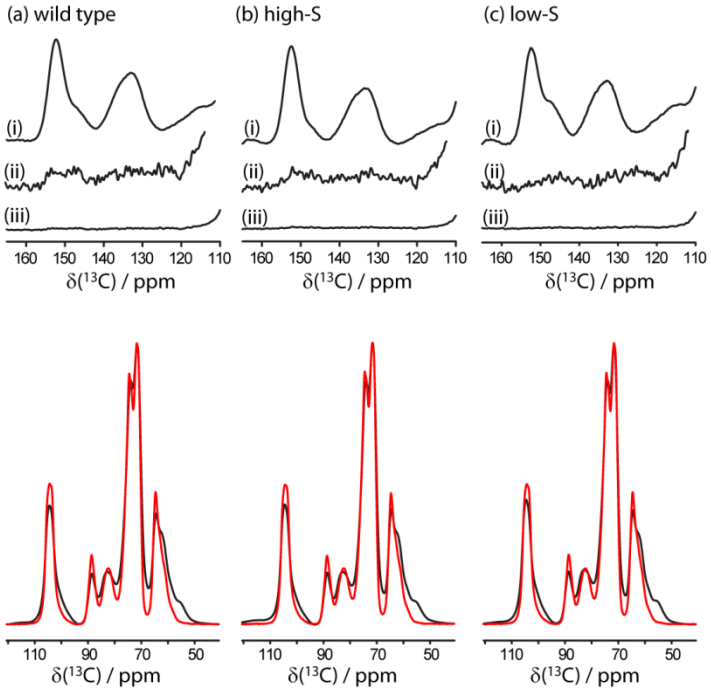

[a] Superpositions of the lignin (top) and cellulose (bottom) regions of the DNP enhanced ^{13}C CPMAS spectra of wild-type (a), high-S (b) and low-S (c) poplar are shown. The spectra in (i) correspond to the untreated biomass samples whereas those in (iii) are the treated samples (shown on the same scale). The spectra in (ii) are identical to those in (iii) but have been scaled up by a factor of 10. The red traces on the bottom correspond to the CDL-treated samples whereas the black traces correspond to the raw biomass.

We first noticed very similar 1D ^{13}C CPMAS spectra for all three poplar substrates (WT, high-S, low-S) pre- and post- CDL treatment (**Figure 3.4.**). All of these spectra are dominated by the resonances attributable to cellulose. C4 resonances from crystalline (88 ppm) and amorphous (82 ppm) cellulose can be well resolved, even though there is a considerable overlap[38-39]. Notably, it can be observed (**Figure 3.3b**) that

the relative crystalline cellulose content in the CDL-treated samples is higher than that in the raw biomass, in agreement with the XRD results. Lignin is represented by only three, very broad, resonances in the 1D spectra of untreated samples, which is due to the similar chemical shifts of the carbon nuclei in the three phenolic monomers of lignin. These peaks are absent in the treated samples, confirming high conversion and removal of lignin during the CDL process. Spectra acquired on CDL-treated miscanthus demonstrate that the CDL method is generally applicable to both grass and wood biomass species (**Figure 3.5**).

Figure 3.5. DNP enhanced ^{13}C CPMAS spectra of raw and CDL-treated miscanthus.[a]

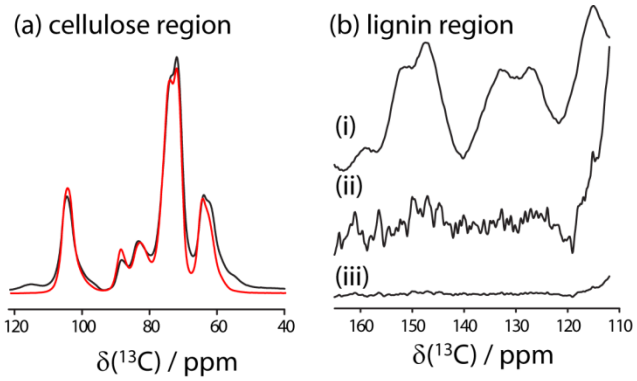

[a] In (a) the cellulose region of the ^{13}C CPMAS spectra of raw (black) and CDL-treated (red) are overlaid, thus highlighting the higher crystalline cellulose content in the treated sample. In (b) the lignin region of the spectra is shown for raw (i) and treated (iii) miscanthus. The spectrum in (ii) is identical to the one in (iii) but was scaled up by a factor of 10.

2. Comparison of lignin region in different biomass species

Remarkably, the distinctions between three types of lignin monomers in the raw samples can be provided by the DNP enabled 2D ^{13}C refocused INADEQUATE experiment (**Figure 3.6**.). Again, as can be seen in **Figure 3.6.b,i**, the 2D spectra are dominated by the resonances from cellulose and acetate, due to their relative high

abundance in the raw materials. The resonances associated with the lignin monomers, however, appear in an isolated spectral region. **Figure 3.6b** represents the 2D patterns of the lignin region, which remains in striking contrast with the almost indistinguishable 1D CPMAS spectra of the same samples shown in **Figure 3.6.a,i−iii**. It can be seen that, in agreement with the CDL data in **Table 1**, the WT biomass is composed of higher content of S lignin and has a smaller content of G and H lignin. The INADEQUATE spectrum of the high-S poplar variant is very clean and indicates exclusive amount of S lignin, while the low-S poplar mutant has a lower S lignin content and the cross-peaks from G and H lignin monomers are more easily discernible. Although the relative ratios of the three lignin monomers could be estimated based on the products of the CDL treatment, SSNMR analysis provides a noninvasive physical tool to probe the structures. The NMR spectra also clearly show that all three types of lignin are successfully depolymerized as no traces of lignin could be detected post-CDL treatment, even by DNP (**Figure 3.3**). The remaining resonances from the cellulose residue appear to be essentially unaffected in all CDL treated samples (**Figure 3.4.**). The CDL process is confirmed to be highly specific for lignin and leaves the cellulose intact without altering the atomic linkages, with the main difference in the cellulose post-CDL treatment with an increased crystallinity, vide supra.

Figure 3.6. Lignin regions of the DNP-enhanced 13C CPMAS (a) and refocused INADEQUATE (b) spectra of raw lignocellulosic poplar variants.

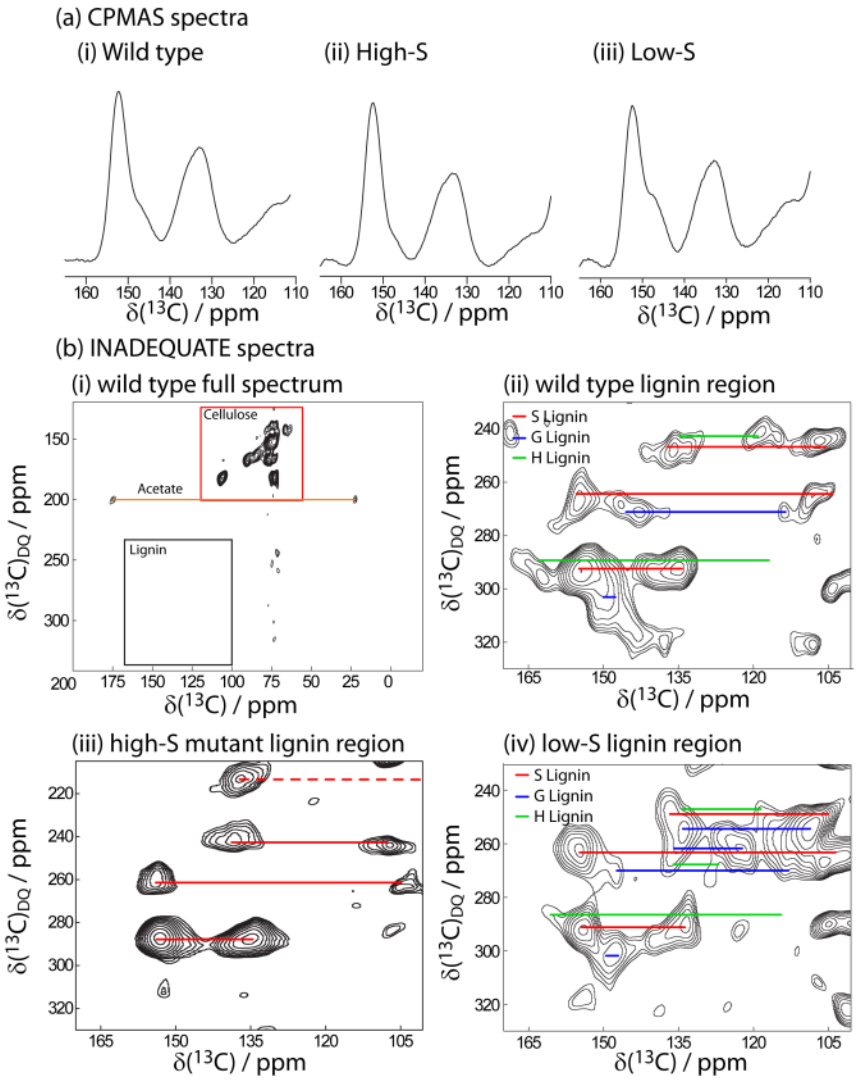

It is of great interest to be able to also determine the type of lignin interunit linkages as well as the crosslinking between lignin and hemicellulose; these are depicted in **Figure 3.7.** This information could be used to design catalysts specifically tailored for a given type of biomass. Unfortunately, the ^{13}C resonances of these dilute species arise in the 50−100 ppm range and are obscured in 1D CPMAS spectra by the strong resonances of cellulose. Again, with the use of the DNP-enabled ^{13}C refocused INADEQUATE spectra, it is possible to detect the correlations between a lignin monomer and a linkage

moiety (i.e., the ^{13}C(aromatic)–^{13}C(benzylic) cross-peak; see **Figure 3.7a**) and as such determine the types of linkages that are present in a given biomass sample. Note that, unfortunately, in many instances, only one cross-peak in an INADEQUATE pair can be observed due to the obstruction caused by the t1 noise from the larger cellulose resonances. This t1 noise is greater in a through-space post-C7 spectrum[40], and therefore, we were unable to identify long-range correlations.

Figure 3.7. Different types of lignin interunit linkages.[a]

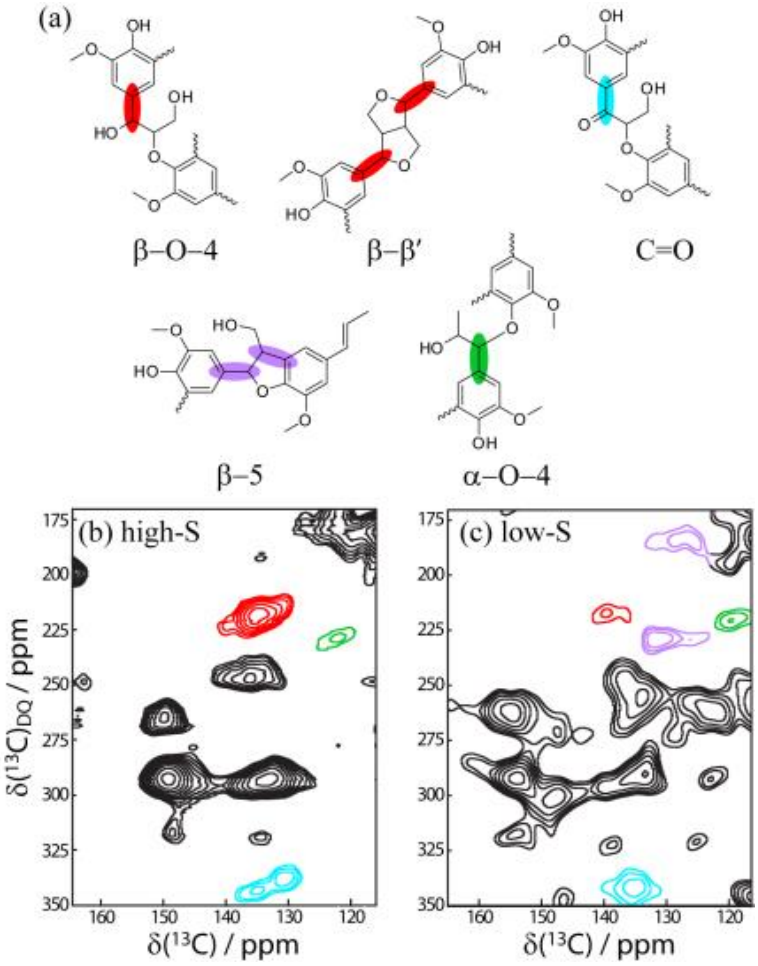

[a] Expanded ^{13}C refocused INADEQUATE spectra of high-S (b) and low-S (c) poplar genetic variants are also shown in which the additional ^{13}C–^{13}C crosspeaks corresponding to the lignin linkages are color-coded according to the carbon pairs in (a). Black cross-peaks correspond to intramonomer correlations and cellulose.

In the spectrum acquired on the high-S lignin poplar, a strong cross-peak is observed at 137/218 ppm. This resonance (shaded red in **Figure 3.7 b**) is attributed to β−O−4 linkages that connect two lignin monomers together[41]. The very high intensity of this resonance, which is comparable to the intramonomer cross-peaks, indicates that β−O−4 is by far the dominant type of lignin interunit linkage. Note that this resonance may also overlap with that from a β−β′ linkage; we cannot then comment on the relative quantities of the β−O−4 and β−β′ linkages. Lower-intensity cross-peaks are also present at 133/337 and 120/220 ppm, which can be assigned to oxidized β−O−4 (C=O) and α−O−4 linkages, respectively. Note that INADEQUATE cannot directly detect C−O−C linkages between lignin and hemicellulose. Nevertheless, the experimental ^{13}C chemical shift of 81 ppm for the β−O−4 linkage is too high for an alcohol moiety, which suggests that a majority of these linkages are connected to the carbohydrate phase via C−O−C bonds.

In the case of the low-S lignin sample, the previously dominant resonance from the β−O−4 linkage is greatly diminished, while the relative intensities of the other crosspeaks appear to be unaffected. Two new cross-peaks can also be identified at 131/229 and 128/183 ppm, which are assigned to β−5 linkages, as shown in **Figure 3.7**. The birth of these new linkages in the low-S poplar variant is not surprising given the fact that the formation of such linkages is suppressed by the methoxy moieties present in the case of S lignin. Additionally, it is known that linkages such as β−5 are more resistant to degradation, when compared to β−O−4, which has been attributed to their lessened conformational freedom[42]. β−5 linkage is a main structural difference between high S and low S biomass samples (**Figure 3.7. b,c**), which may be one of the reasons for the lower

enzymatic saccharification yields obtained when a higher proportion of G lignin is present in the parent biomass.

D. Conclusions

Clearly, DNP SSNMR provides a new and powerful nondestructive tool to study bond connectivity in biomass structures (lignin and cellulose) on the atomic scale. Notably, we have, for the first time, gained significant structural insights into the lignin portion of lignocellulose, which directly impact the CDL. In particular, we showed that the proportion of lignin's β−O−4 linkages, which are most easily removed, is increased by genetically modifying the substrate to produce more S lignin. This in turn improves the saccharification yields post CDL treatment. Our measurements also shatter the myth that cellulose crystallinity determines the rate of enzymatic saccharification of cellulose. This new approach avoids the use of invasive chemical analyses to extrapolate to the biomass structure pre- and post-treatment. DNP SSNMR promises to advance biomass utilization technologies by providing structure−function relationships in the catalytic treatment of diverse biomass species, as illustrated herein for poplar.

E. Supporting Information

1. Materials and methods

Materials.

The wild-type poplar (*P. nigra* × *P. maximowiczii*) WT-NM-6 and the genetically engineered line 717-F5H were provided by Purdue University's Department of Forestry and Natural Resources. High-S polar, or the genetically engineered line F5H-64, was provided by Dr. Clint Chapple from Purdue Univeristy's Department of Biochemistry[43].

Low-S poplar, or the genetically engineered line 1035-41, was provided by the U.S. Department of Energy (DOE) BES project (0012846) entitled: Manipulation of Lignin Biosynthesis to Maximize Ethanol Production from *Populus* Feedstocks, DOE grant # DE-FG36-04G01417. Miscanthus was obtained from Repreve Renewables. Biomass substrates were milled to pass through a 40 mesh screen using a Mini Wiley Mill (Thomas Scientific, Swedesboro, NJ) before use. The Ni/C catalyst, containing 10 wt % Ni dispersed on an activated carbon support, was synthesized and characterized based on reported literature methods[14]. Pd/C (5 wt%) was purchased from Strem Chemicals (Newburyport, MA). Solka floc was obtained from International Fiber Corporation (North Tonawanda, NY), with an extensive amount of cellulose and trace amount of hemicellulose. 4-Allyl-2,6-dimethoxyphenol (98% purity) and ferulic acid methyl ester (99% purity) were purchased from Alfa Aesar (Ward Hill, MA). Avicel PH-101 (50 μm particle size), isoeugenol, dihydro *p*-coumaric acid methyl ester, 2-methoxy-4 propylphenol (all >98% purity) and zinc acetate dehydrate (99.999% purity) were purchased from Sigma - Aldrich (St. Louis, MO). *p*-Coumaric acid methyl ester and dihydro ferulic acid methyl ester (>98% purity) were purchased from TCI America (Portland, OR). Methanol (HPLC grade) was purchased from Macron fine chemicals (Center Valley, PA). All chemicals were used without further purification.

General Heterogeneous Catalytic Reaction.

All biomass substrates were used without washing. In a typical catalytic depolymerization of lignin (CDL) reaction with poplar, 1.0 g of 40 mesh gene mutant poplar substrates, 10 wt% Pd/C catalyst, 21 mg $Zn(OAc)_2 \cdot 2H_2O$, and 45 mL methanol were added to a stainless steel Parr reactor, which was subsequently sealed. To facilitate

good separation of the catalyst and substrate, the Pd/C catalyst was first loaded into a microporous cage (325 mesh) before loading it into the Parr reactor. The catalyst cage has the functionality for allowing solvent as well as soluble solute to pass through and access the catalyst, while at the same time keeping the biomass substrate separate from the catalyst. For the CDL reaction with miscanthus, 1.0 g of 40 mesh miscanthus, 10 wt% Ni/C, and 45 mL methanol were added to Parr reactor. The Ni/C catalyst was also loaded into a microporous cage (325 mesh) prior to loading into the Parr reactor. Reaction procedures and conditions for different substrates were the same: the reaction system was sealed, followed by 5 purges with UHP grade H_2 while stirring, and then pressurized with 35 bar H_2. The mixture was then heated to 225 °C at a stirring speed of 600 rpm, and the temperature was maintained for 12 hours. The reaction was terminated by removing the heat source and cooling the reactor to room temperature. The reaction mixture was filtered to separate the liquid phase containing the aromatic products from the solid biomass residue. The residue was then washed with additional methanol to remove the remaining phenolic products from the surface, and the liquid wash was combined with the filtrate. The combined liquid phase was condensed by rotary evaporation, diluted in a volumetric flask (10 mL), and then analyzed using HPLC/UV and HPLC/MS. The solid biomass residue was left to dry thoroughly under ambient conditions.

Synthesis of 2,6-dimethoxy-4-propylphenol

2,6-Dimethoxy-4-propylphenol was synthesized through hydrogenation of 4-allyl-2,6-dimethoxyphenol[44]. 4-Allyl-2,6-dimethoxyphenol (2 g), 5 wt% Pd/C (100 mg), and 20 mL of methanol were added into a stainless steel Parr reactor. The reactor was sealed, and then purged 5 times with UHP grade H_2 while stirring. The whole system was

pressurized with 35 bar H_2, heated to 60 °C and maintained at that temperature for 3 hours at a stirring speed of 600 rpm. The catalyst was removed by filtration and methanol was removed *in vacuo* to yield 2,6 - dimethoxy-4-propylphenol as a colorless oil. The reaction product was purified on a silica-gel column with a mobile phase of 17% ethyl acetate and 83% hexanes. [$_1$H] NMR ($CDCl_3$) δ 0.94 (t, 3H, CH_3), 1.63 (m, 2H, CH_2), 2.49 (t, 2H, CH_2), 3.87 (s, 6H, OCH_3), 5.36 (s, 1H, OH), 6.40 (s, 2H, ArH).

X-Ray Diffraction (XRD)

The crystallinity of the poplar samples was evaluated by X-ray diffraction (XRD) using a LabX XRD-6000 (Shimadzu) diffractometer with a 2°/min scan speed. The samples were packed in an aluminum holder (35×50×5 mm), and X-ray intensity data were collected at room temperature over the 2θ range of 10 – 40° at intervals of 0.04°. A Cu Kα radiation source (λ = 1.54060 Å) was used with a voltage of 40 kV and current of 30 mA.

The relative crystallinity index (RCI) is based on the X-ray diffraction characteristics of two signature peaks. The RCI can be empirically determined by evaluating the relative intensity of these two reflections[45-46]. This analysis was performed on both the raw and CDL-treated biomass samples. The expression describing the RCI is:

$$RCI = ((I_{002} - I_{am})/ I_{002}) \times 100\%$$

where I_{002} is the maximum intensity of the peak at $2\theta = 22.5°$ and I_{am} is the intensity at $2\theta = 18.0°$.

Composition analysis

The total solids, ash, structural carbohydrates, and lignin of untreated and CDL-processed biomass were determined using Laboratory Analytical Procedures (LAP) established by National Renewable Energy Laboratory.

Enzymatic hydrolysis

Enzymatic hydrolysis experiments were performed in 20 mL serum bottles at a pH of 4.8 and a temperature of 50° C in a thermostatically controlled shaker operating at a frequency of 200 rpm for up to 72 h. 100 mg glucan (on a dry basis) was mixed with 5 mL of a 50 mM sodium citrate buffer to reach a glucan concentration of 2% (w/v). Cellic ™ Ctec2 (aggressive cellulose and a high level of β-glucosidase), at an enzyme loading of 20 FPU (filter paper unit) g-1 glucan, was used for the CDL-treated and untreated poplar samples. The enzyme was obtained from Novozymes North America, Inc. (Franklinton, NC). The activity of Cellic CTec2 was 90 FPU mL-1. Sodium azide (0.2%, w/v) was added to inhibit microbial growth during hydrolysis. Each experiment was performed in duplicate. During hydrolysis, samples were taken at predetermined intervals for analysis using HPLC. The hydrolysate was filtered through a 0.2 μm nominal-poresize nylon syringe filter (Pall/Gelman, Port Washington, NY) to remove the residual substrate and was then stored at -20 oC for sugar analysis.

2. Instrumentation and and chromatographic conditions

HPLC-MS analysis

All HPLC separations for mass spectrometry analysis were performed on a Surveyor Plus HPLC system from Thermo Scientific consisting of a quaternary pump, an autosampler, a photodiode array (PDA) detector, and a Zorbax SB-C18 column. A non-linear gradient of water (A) and acetonitrile (B) was used as follows: 0.00 min, 95% A

and 5% B; 10.00 min, 95% A and 5% B; 30.00 min, 40% A and 60% B; 35.00 min, 5% A and 95 %; 38.00min, 5% A and 95% B; 38.50 min, 95% A and 5% B; 45.00 min, 95% A and 5% B. Flowrate of the mobile phase was kept at 500 μL/min. PDA detector was set at the wavelength of 254 nm.

Mass spectrometric analysis (MS, MS^2 and MS^3) of HPLC eluent was performed using a Thermo Scientific linear quadrupole ion trap (LQIT) mass spectrometer equipped with an electrospray ionization (ESI) source. All mass spectrometry experiments were performed under negative ion mode. HPLC eluents were mixed via a T-connector with 1% sodium hydroxide water solution at a flow rate of 0.1 μL/min before entering the ESI source. Addition of sodium hydroxide facilitates deprotonation of the analytes. ESI source conditions were set as: 3.5 kV spray voltage; 50 (arbitrary units) sheath gas (N_2) flow and 20 (arbitrary units) auxillary gas (N_2) flow. MS^3 analysis was performed using the data dependent scan function of the Thermo Xcalibur software. The most abundant ion formed upon ESI was isolated and subjected to collision-activated dissociation (CAD). The most abundant fragment ion was further selected for isolation and fragmentation. For all MS^3 experiments, an isolation window of 2 m/z units was used along with a normalized collision energy of 30 (arbitrary units). All mass spectrometry experiments were performed under negative ion mode.

HPLC/GC analysis

The liquid phase from lignin depolymerization reactions with methanol as solvent was analyzed with Agilent 1260 Infinity Quaternary High-Performance Liquid Chromatography (HPLC) system, using Zorbax Eclipse XDB-C18 Column (250 x 74.6mm) set at 30°C. The chromatography apparatus is equipped with G1315D Diode

Array Detector (DAD). A mixture of H2O (A) and acetonitrile (B) were used as the mobile phase at a flow rate of 0.5 mL/min. Nonlinear gradient was used (80% A and 20% B from beginning to 5% A and 95 % B at 55.0 min). A fixed amount (400μL) of internal standard 3-methoxy phenol (10 mM) was added into each sample for the quantification purposes. Standard curves for all the aromatic products were made by comparison of the products to internal standard. All results were analyzed and quantified according to standard curves. Before analyzing by HPLC, the liquid samples were filtered through a 0.22μm cutoff syringe filter (2 5mm diameter).

All sugar samples as well as aqueous phase after solid carbohydrate dehydration reaction were analyzed with Agilent 1260 Infinity Quaternary High-Performance Liquid Chromatography (HPLC) system, using Aminex HPX-87H column (300 x 7.8 mm) set at 70 ˚C. The chromatography apparatus is equipped with G1362A Refractive Index Detector (RID) calibrated with external standards. A 0.005 M sulfuric acid solution was employed as the mobile phase with flow of 0.6 mL/min. A fixed amount (400μL) of internal standard tert-butyl alcohol (10 mM) was added into each sample for quantification purposes. Standard curves (glucose, xylose, and arabinose) were made by comparison of the products with internal standard. All results were analyzed and quantified according to standard curves. Before analyzing by HPLC, the aqueous solutions were filtered through a 0.22μm cutoff syringe filter (25 mm diameter).

DNP-enhanced ssNMR

All DNP-enhanced SSNMR measurements were performed using a Bruker MAS-DNP system equipped with an AVANCE III console, a 263 GHz gyrotron, and a 3.2 mm low temperature MAS probe. All samples were wet with a 10 Mm solution of AMUPol in

water, packed into 3.2 mm o.d. sapphire rotors, and sealed with a Teflon plug. These samples were then prespun using a benchtop spinning station at room temperature to equilibrate the sample and then spun at 10−13 kHz at a temperature of 105K in the probe. In all cases, cross-polarization of 13C spins from hyperpolarized ^{1}H spins was performed using a 1.5 ms contact time.

The ^{1}H excitation pulse lasted 2.75 μs. The recycle delays were set to 1.3T1 in order to maximize sensitivity and lasted between 2.7 and 6.1 s, depending on the sample. For the CPMAS measurements, 128 scans were accumulated. The refocused INADEQUATE measurements were performed using a radio frequency field strength of 88 kHz for all ^{13}C pulses and a MAS frequency of 10 kHz. The four double-quantum filtering delays were set to 3 ms, and 32 t1 increments of 33.3 μs were acquired, each being an accumulation of 640 scans. The States method was used to obtain purely absorptive phase 2D line shapes. The cross-peaks in the 2D refocused INADEQUATE spectra were assigned using ChemBioDraw-predicted chemical shifts, which are as accurate as DFT calculated ones for simple organics[47] and are sufficiently accurate to assign the broad peaks observed here.

F. References:

1. Rose, M.; Babi, M.; Moran-Mirabal, J., The study of cellulose structure and depolymerization through single-molecule methods. *Industrial Biotechnology* **2015,** *11* (1), 16-24.

2. Zhao, X.; Zhang, L.; Liu, D., Biomass recalcitrance. Part I: the chemical compositions and physical structures affecting the enzymatic hydrolysis of lignocellulose. *Biofuels, Bioproducts and Biorefining* **2012,** *6* (4), 465-482.

3. Lee, S. H.; Doherty, T. V.; Linhardt, R. J.; Dordick, J. S., Ionic liquid‐mediated selective extraction of lignin from wood leading to enhanced enzymatic cellulose hydrolysis. *Biotechnol Bioeng* **2009,** *102* (5), 1368-1376.

4. Hall, M.; Bansal, P.; Lee, J. H.; Realff, M. J.; Bommarius, A. S., Cellulose crystallinity–a key predictor of the enzymatic hydrolysis rate. *The FEBS journal* **2010,** *277* (6), 1571-1582.

5. Foston, M.; Hubbell, C. A.; Davis, M.; Ragauskas, A. J., Variations in cellulosic ultrastructure of poplar. *BioEnergy Research* **2009,** *2* (4), 193.

6. Horn, S. J.; Vaaje-Kolstad, G.; Westereng, B.; Eijsink, V., Novel enzymes for the degradation of cellulose. *Biotechnol Biofuels* **2012,** *5* (1), 45.

7. Kumar, P.; Barrett, D. M.; Delwiche, M. J.; Stroeve, P., Methods for pretreatment of lignocellulosic biomass for efficient hydrolysis and biofuel production. *Ind Eng Chem Res* **2009,** *48* (8), 3713-3729.

8. Gao, J.; Anderson, D.; Levie, B., Saccharification of recalcitrant biomass and integration options for lignocellulosic sugars from Catchlight Energy's sugar process (CLE Sugar). *Biotechnol Biofuels* **2013,** *6* (1), 10.

9. Mosier, N.; Wyman, C.; Dale, B.; Elander, R.; Lee, Y. Y.; Holtzapple, M.; Ladisch, M., Features of promising technologies for pretreatment of lignocellulosic biomass. *Bioresource Technol* **2005,** *96* (6), 673-686.

10. Chundawat, S. P. S.; Donohoe, B. S.; da Costa Sousa, L.; Elder, T.; Agarwal, U. P.; Lu, F.; Ralph, J.; Himmel, M. E.; Balan, V.; Dale, B. E., Multi-scale visualization and characterization of lignocellulosic plant cell wall deconstruction during thermochemical pretreatment. *Energ Environ Sci* **2011,** *4* (3), 973-984.

11. Pu, Y.; Ziemer, C.; Ragauskas, A. J., CP/MAS 13 C NMR analysis of cellulase treated bleached softwood kraft pulp. *Carbohydrate Research* **2006,** *341* (5), 591-597.

12. Zhang, X.; Murria, P.; Jiang, Y.; Xiao, W.; Kenttämaa, H. I.; Abu-Omar, M. M.; Mosier, N. S., Maleic acid and aluminum chloride catalyzed conversion of glucose to 5-(hydroxymethyl) furfural and levulinic acid in aqueous media. *Green Chem* **2016,** *18* (19), 5219-5229.

13. Jiang, Y.; Yang, L.; Bohn, C. M.; Li, G.; Han, D.; Mosier, N. S.; Miller, J. T.; Kenttämaa, H. I.; Abu-Omar, M. M., Speciation and kinetic study of iron promoted sugar conversion to 5-hydroxymethylfurfural (HMF) and levulinic acid (LA). *Organic Chemistry Frontiers* **2015,** *2* (10), 1388-1396.

14. Song, Q.; Wang, F.; Cai, J.; Wang, Y.; Zhang, J.; Yu, W.; Xu, J., Lignin depolymerization (LDP) in alcohol over nickel-based catalysts via a fragmentation–hydrogenolysis process. *Energ Environ Sci* **2013,** *6* (3), 994-1007.

15. Ciolacu, D.; Ciolacu, F.; Popa, V. I., Amorphous cellulose—structure and characterization. *Cellulose chemistry and technology* **2011,** *45* (1), 13.

16. Wang, T.; Phyo, P.; Hong, M., Multidimensional solid-state NMR spectroscopy of plant cell walls. *Solid state nuclear magnetic resonance* **2016,** *78*, 56-63.

17. Maly, T.; Debelouchina, G. T.; Bajaj, V. S.; Hu, K.-N.; Joo, C.-G.; Mak–Jurkauskas, M. L.; Sirigiri, J. R.; van der Wel, P. C. A.; Herzfeld, J.; Temkin, R. J., Dynamic nuclear polarization at high magnetic fields. *The Journal of chemical physics* **2008,** *128* (5), 02B611.

18. Michaelis, V. K.; Ong, T. C.; Kiesewetter, M. K.; Frantz, D. K.; Walish, J. J.; Ravera, E.; Luchinat, C.; Swager, T. M.; Griffin, R. G., Topical Developments in High -

Field Dynamic Nuclear Polarization. *Israel journal of chemistry* **2014,** *54* (1‐2), 207-221.

19. Lee, D.; Hediger, S.; De Paëpe, G., Is solid-state NMR enhanced by dynamic nuclear polarization? *Solid state nuclear magnetic resonance* **2015,** *66*, 6-20.

20. Takahashi, H.; Lee, D.; Dubois, L.; Bardet, M.; Hediger, S.; De Paëpe, G., Rapid Natural‐Abundance 2D 13C‐13C Correlation Spectroscopy Using Dynamic Nuclear Polarization Enhanced Solid‐State NMR and Matrix‐Free Sample Preparation. *Angewandte Chemie International Edition* **2012,** *51* (47), 11766-11769.

21. Rossini, A. J.; Zagdoun, A.; Hegner, F.; Schwarzwälder, M.; Gajan, D.; Copéret, C.; Lesage, A.; Emsley, L., Dynamic nuclear polarization NMR spectroscopy of microcrystalline solids. *J Am Chem Soc* **2012,** *134* (40), 16899-16908.

22. Takahashi, H.; Hediger, S.; De Paëpe, G., Matrix-free dynamic nuclear polarization enables solid-state NMR 13 C–13 C correlation spectroscopy of proteins at natural isotopic abundance. *Chemical Communications* **2013,** *49* (82), 9479-9481.

23. Mollica, G.; Dekhil, M.; Ziarelli, F.; Thureau, P.; Viel, S., Quantitative Structural Constraints for Organic Powders at Natural Isotopic Abundance Using Dynamic Nuclear Polarization Solid‐State NMR Spectroscopy. *Angewandte Chemie International Edition* **2015,** *54* (20), 6028-6031.

24. Luo, H.; Klein, I. M.; Jiang, Y.; Zhu, H.; Liu, B.; Kenttämaa, H. I.; Abu-Omar, M. M., Total utilization of Miscanthus biomass, lignin and carbohydrates, using earth abundant nickel catalyst. *Acs Sustain Chem Eng* **2016,** *4* (4), 2316-2322.

25. Vogel, J., Unique aspects of the grass cell wall. *Current opinion in plant biology* **2008,** *11* (3), 301-307.

26. Morvan, D.; Rauchfuss, T. B.; Wilson, S. R., π-Complexes of Lignols with Manganese (I) and Ruthenium (II). *Organometallics* **2009,** *28* (11), 3161-3166.

27. Hatfield, R. D.; Ralph, J.; Grabber, J. H., Cell wall cross-linking by ferulates and diferulates in grasses[1]. *Journal of the Science of Food and Agriculture* **1999,** *79*, 403-407.

28. Rouau, X.; Cheynier, V.; Surget, A.; Gloux, D.; Barron, C.; Meudec, E.; Louis-Montero, J.; Criton, M., A dehydrotrimer of ferulic acid from maize bran. *Phytochemistry* **2003,** *63* (8), 899-903.

29. Wyman, C. E.; Dale, B. E.; Elander, R. T.; Holtzapple, M.; Ladisch, M. R.; Lee, Y. Y.; Mitchinson, C.; Saddler, J. N., Comparative sugar recovery and fermentation data following pretreatment of poplar wood by leading technologies. *Biotechnology Progress* **2009,** *25* (2), 333-339.

30. Ciesielski, P. N.; Resch, M. G.; Hewetson, B.; Killgore, J. P.; Curtin, A.; Anderson, N.; Chiaramonti, A. N.; Hurley, D. C.; Sanders, A.; Himmel, M. E., Engineering plant cell walls: tuning lignin monomer composition for deconstructable biofuel feedstocks or resilient biomaterials. *Green Chem* **2014,** *16* (5), 2627-2635.

31. Kumar, R.; Mago, G.; Balan, V.; Wyman, C. E., Physical and chemical characterizations of corn stover and poplar solids resulting from leading pretreatment technologies. *Bioresource Technol* **2009,** *100* (17), 3948-3962.

32. Ko, J. K.; Ximenes, E.; Kim, Y.; Ladisch, M. R., Adsorption of enzyme onto lignins of liquid hot water pretreated hardwoods. *Biotechnol Bioeng* **2015,** *112* (3), 447-456.

33. Bax, A.; Freeman, R.; Frenkiel, T. A., An NMR technique for tracing out the carbon skeleton of an organic molecule. *J Am Chem Soc* **1981,** *103* (8), 2102-2104.

34. Lesage, A.; Bardet, M.; Emsley, L., Through-bond carbon− carbon connectivities in disordered solids by nmr. *J Am Chem Soc* **1999,** *121* (47), 10987-10993.

35. Lafon, O.; Thankamony, A. S. L.; Kobayashi, T.; Carnevale, D.; Vitzthum, V.; Slowing, I. I.; Kandel, K.; Vezin, H.; Amoureux, J.-P.; Bodenhausen, G., Mesoporous silica nanoparticles loaded with surfactant: low temperature magic angle spinning 13C and 29Si NMR enhanced by dynamic nuclear polarization. **2013**.

36. Wang, T.; Park, Y. B.; Caporini, M. A.; Rosay, M.; Zhong, L.; Cosgrove, D. J.; Hong, M., Sensitivity-enhanced solid-state NMR detection of expansin's target in plant cell walls. *Proceedings of the National Academy of Sciences* **2013,** *110* (41), 16444-16449.

37. Sauvée, C.; Rosay, M.; Casano, G.; Aussenac, F.; Weber, R. T.; Ouari, O.; Tordo, P., Highly Efficient, Water‐Soluble Polarizing Agents for Dynamic Nuclear Polarization at High Frequency. *Angewandte Chemie International Edition* **2013,** *52* (41), 10858-10861.

38. Kono, H.; Yunoki, S.; Shikano, T.; Fujiwara, M.; Erata, T.; Takai, M., CP/MAS 13C NMR study of cellulose and cellulose derivatives. 1. Complete assignment of the CP/MAS 13C NMR spectrum of the native cellulose. *J Am Chem Soc* **2002,** *124* (25), 7506-7511.

39. Mori, T.; Chikayama, E.; Tsuboi, Y.; Ishida, N.; Shisa, N.; Noritake, Y.; Moriya, S.; Kikuchi, J., Exploring the conformational space of amorphous cellulose using NMR chemical shifts. *Carbohyd Polym* **2012,** *90* (3), 1197-1203.

40. Hohwy, M.; Jakobsen, H. J.; Eden, M.; Levitt, M. H.; Nielsen, N. C., Broadband dipolar recoupling in the nuclear magnetic resonance of rotating solids: A compensated C7 pulse sequence. *The Journal of chemical physics* **1998,** *108* (7), 2686-2694.

41. Watanabe, T.; Ohnishi, J.; Yamasaki, Y.; Kaizu, S.; Koshijima, T., Binding-site analysis of the ether linkages between lignin and hemicelluloses in lignin–carbohydrate complexes by DDQ-oxidation. *Agricultural and biological chemistry* **1989,** *53* (8), 2233-2252.

42. Kobayashi, T.; Kohn, B.; Holmes, L.; Faulkner, R.; Davis, M.; Maciel, G. E., Molecular-level consequences of biomass pretreatment by dilute sulfuric acid at various temperatures. *Energy & Fuels* **2011,** *25* (4), 1790-1797.

43. Franke, R.; McMichael, C. M.; Meyer, K.; Shirley, A. M.; Cusumano, J. C.; Chapple, C., Modified lignin in tobacco and poplar plants over‐expressing the Arabidopsis gene encoding ferulate 5‐hydroxylase. *The Plant Journal* **2000,** *22* (3), 223-234.

44. Delgass, W. N.; Agrawal, R.; Ribeiro, F. H.; Saha, B.; Yohe, S. L.; Abu-Omar, M. M.; Parsell, T.; Dietrich, P. J.; Klein, I. M., Catalytic biomass conversion methods, catalysts, and methods of making the same. Google Patents: 2014.

45. Segal, L.; Creely, J. J.; Martin Jr, A. E.; Conrad, C. M., An empirical method for estimating the degree of crystallinity of native cellulose using the X-ray diffractometer. *Text Res J* **1959,** *29* (10), 786-794.

46. Harris, D.; DeBolt, S., Relative crystallinity of plant biomass: studies on assembly, adaptation and acclimation. *Plos One* **2008,** *3* (8), e2897.

47. Meiler, J.; Maier, W.; Will, M.; Meusinger, R., Using neural networks for 13C NMR chemical shift prediction–comparison with traditional methods. *Journal of Magnetic Resonance* **2002,** *157* (2), 242-252.

CHAPTER IV. Lignin Extract and Catalytic Upgrading from Genetically Modified Poplar.

A. Introduction

Non-food lignocelluosic biomass has an average energy content of 17-20 MJ/kg,[1] and the potential to provide 50-85 EJ of energy per year.[2] It has received increasing attention as a promising renewable energy source in helping decrease our reliance on fossil fuels and reducing environmental impact.[3] Major components of lignocellulosic biomass including cellulose (50%), hemicellulose (25%) and lignin (25%). Lignin as the second largest reservoir of carbon (after carbohydrate), accounts for about 30% of organic carbon in the biosphere, [4] and 40% of the energy in biomass.[5] Lignin is a three-dimensional polymer with complex structure, and it is the only natural polymer made of aromatics.

Lignin utilization is largely under-developed due to its complexity and recalcitrance. Currently, over 50 million tons of lignin is generated annually by the paper and pulp industry worldwide; however, more than 98% is treated as a waste byproduct and burned for heat.[6] With the fast development of second generation bioethanol from lignocellulosic biomass, an estimated amount of 220 million tons of lignin is expected to be produced by 2030[6-7] The isolated lignin has recalcitrant structure and is always of low purity. This has hindered the valorization of lignin into high value aromatic compounds as well as its use as a multi-functional macromolecule. Thus, development of efficient methods for lignin depolymerization is important from both scientific and economic perspectives.

One of the most prevalent strategies for lignin utilization is the direct hydrogenolysis of native lignin in biomass. In this case, heterogeneous metal catalyzed

lignin depolymerization has been shown to be among the highest in efficiency. A wide range of metal catalysts have been studied with varying success, including Pt, Ru, Rh, Pd as well as earth abundant Ni.[8-15] Another pathway is to valorize the isolated lignin derived from different pretreatment methods, which is separated from the other components in biomass (**Figure 4.1**).[16] Organosolv pretreatment affords sulfur-free lignin in high purity, which is makes it a suitable precursor for different applications.[4] Properties of organosolv lignin are largely dependent on the biomass substrate as well as the specific organosolv pretreatment method. In most cases, further depolymerization leads to low selectivity and yields of monomeric products. The reason for low yield is attributed to the re-condensation of lignin during extraction. Research to improve organosolv lignin conversion has focused on the inhibition of lignin re-condensation and achieving efficient reaction systems.[17-21]

Figure 4.1. Valorization of biomass by complementary pathways, upgrading lignin first through catalysis (top pathway) or extraction of organosolv lignin followed by catalytic upgrading (bottom pathway).

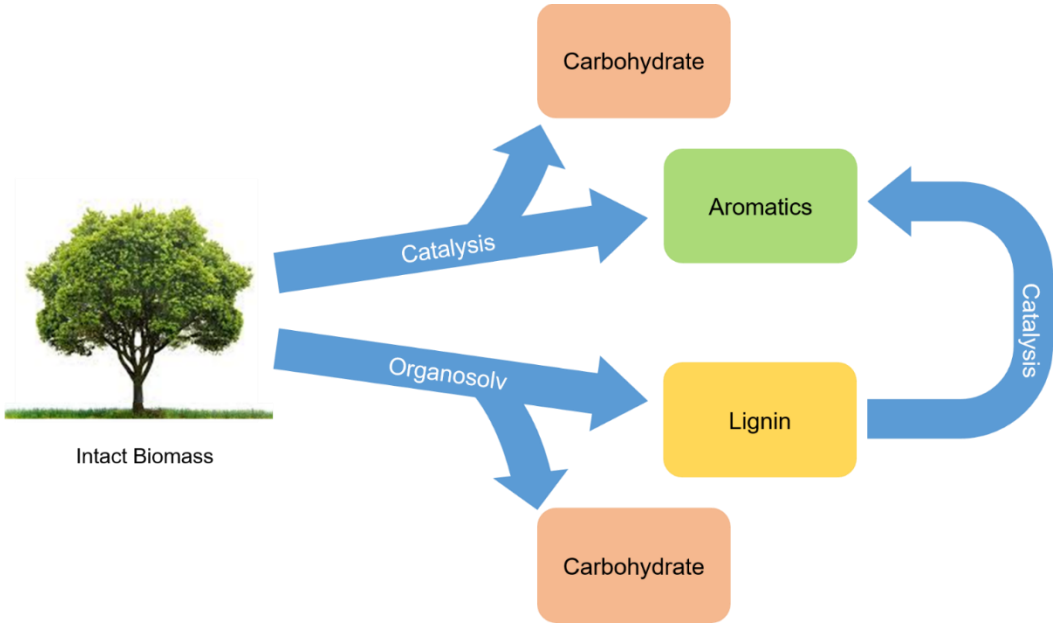

In this work, we report on organosolv extraction of wild-type and genetically modified poplars (high-S and low-S) using different solvents (acetic acid/formic acid, acetone, and methanol). High-S poplar is prepared by an over-expression of *F5H* gene, which is a cytochrome P450-dependent monooxygenase that catalyzes the hydroxylation of ferulic acid, coniferaldehyde and coniferyl alcohol to sinapic acid and syringyl lignin biosynthesis. The over-expression of this gene increases the lignin syringyl monomer content. On the other hand, low-S lignin is prepared through the suppression of the *F5H* gene by two RNAi constructs, *pCC1019* and *pCC1034*.[22] Isolated lignin samples were characterized by two-dimensional HSQC-NMR and GPC. The resulting organosolv lignin structures were imaged by SEM. They showed varying particle size and shape depending on the gene modification in poplar species and the solvent system used in extraction. Isolated organosolv lignin samples were subjected to catalytic depolymerization (CDL) over heterogeneous Ni/C. Herein, we demonstrate that nickel is highly efficient for the hydrogenolysis of organsolv lignin. Three monomeric phenolic products with alkenyl side chain were obtained. Lignin isolated from methanol extraction gave the highest yield > 60% of the three monomeric phenolic products. NMR analysis revealed the role methanol plays in minimizing undesirable re-condensation of organosolv lignin.

B. Organosolv extraction of lignin from poplar species.

Weight average (M_w) and number average (M_n) molecular weight of all isolated lignin samples were analyzed using gel permeation chromatography (GPC) (**Table 4.1.**). Among three different treatments, use of acetone as solvent resulted in the isolated lignin with smallest molecular weight, which is in accordance with a previous study.[23] γ-Valerolactone (GVL) as an aprotic solvent has been shown to increase the reaction rates

for acid catalyzed biomass hydrolysis reaction compared to protic solvents.[24-25] In our study, acetone as a polar aprotic solvent acts in a similar way to GVL, which is assumed to stabilize the carbocation intermediate formed during acid catalyzed organosolv extraction. This stabilization leads to accelerated reaction rates, and results in breaking down of lignin macromolecules into isolated lignin oligomers with relatively small molecular weight. In all cases, the polydispersity index (PDI) is indicative of a narrow range of molecular weight distribution. Genetically modified poplar substrates (High S and Low S) didn't show a discernible effect on the molecular weight of isolated organosolv lignin. Given the molar mass of lignin monomers (ca. 200 g mol^{-1}), the range of observed M_w indicates that the isolated organosolv lignin chains are 10-mers to 12-mers.

Table 4.1. Weight average molecular weight (M_w), number average molecular weight (M_n), and polydispersity index (PDI) of isolated lignin from Acetic Acid/Formic Acid (AA/FA), Acetone, and MeOH treatments.

Poplar Substrate	Organosolv Lignin Extraction[a]	Isolated Lignin (% Yield)[b]	M_w (kg mol^{-1})	M_n (kg mol^{-1})	Polydispersity Index (PDI)
Wild Type	AA/FA	54	2.5	1.9	1.27
High S	AA/FA	57	2.4	1.9	1.28
Low S	AA/FA	47	2.4	1.8	1.30
Wild Type	Acetone	62	1.8	1.3	1.34
High S	Acteone	69	1.8	1.4	1.31
Low S	Acetone	67	1.7	1.4	1.28
Wild Type	Methanol	64	2.2	1.5	1.51

High S	Methanol	68	2.0	1.4	1.40
Low S	Methanol	58	2.3	1.7	1.36

[a] Organosolv lignin extraction medium: AA/FA = acetic acid/formic acid, Acetone = Acetone/water and H_2SO_4/formaldehyde , Methanol = MeOH/water and H_2SO_4/formaldehyde.

[b] Lignin isolated yields are calculated based on the theoretical amount of lignin in raw biomass. Isolated lignin (%) = $\frac{Isolated\ Lignin\ (g)}{Theoretical\ Lignin\ (g)} \times 100$

Scanning electron microscope (SEM) images were collected on all isolated organosolv lignin samples to compare structural differences on the mesoscale. Our observations suggest that particle size and particle shape are affected by both solvent system and lignin composition of poplar substrates (**Figure 4.2**.). The comparison of lignin samples from all three poplar variants are provided in the Supporting Information. Among three treatments, acetic acid/formic acid treated organosolv lignin gives the smallest particles (2-0.5 μm), followed by acetone (5-1.5 μm). Methanol treatment results in the largest particles (10-2 μm). These sizes are well above the expected size for 10-mers, which is ca. 50-100 nm. Solid state organosolv lignin macromolecules self-assemble or aggregate into larger particle sizes in the solid-state. The effect on the shape of organosolv lignin particles is most evident for methanol treated samples. In specific, organosolv lignin from methanol treated wild type poplar shows highly regular three dimensional spherical particles (**Figure 4.2. g**); methanol treated low-S poplar shows a combination of both spherical and plate-like particles (**Figure 4.2.i**) while lignin from high-S poplar gives random shapes (**Figure 4.2.h**). The other two treatments (acetic acid and acetone), on the other hand, result in a less defined or irregular particle shapes. This observation illustrates the effect of genetic modification, specifically degree of methoxylation of the phenyl group, on the structure of isolated organosolv lignin

assembly of macromolecules. The difference in isolated lignin structure on the meso-scale may impact its utility in further upgrading reactions as well as in making materials.

Figure 4.2. Scanning electron microscope (SEM) images of isolated organosolv lignin from poplar species using different solvent extraction methods.

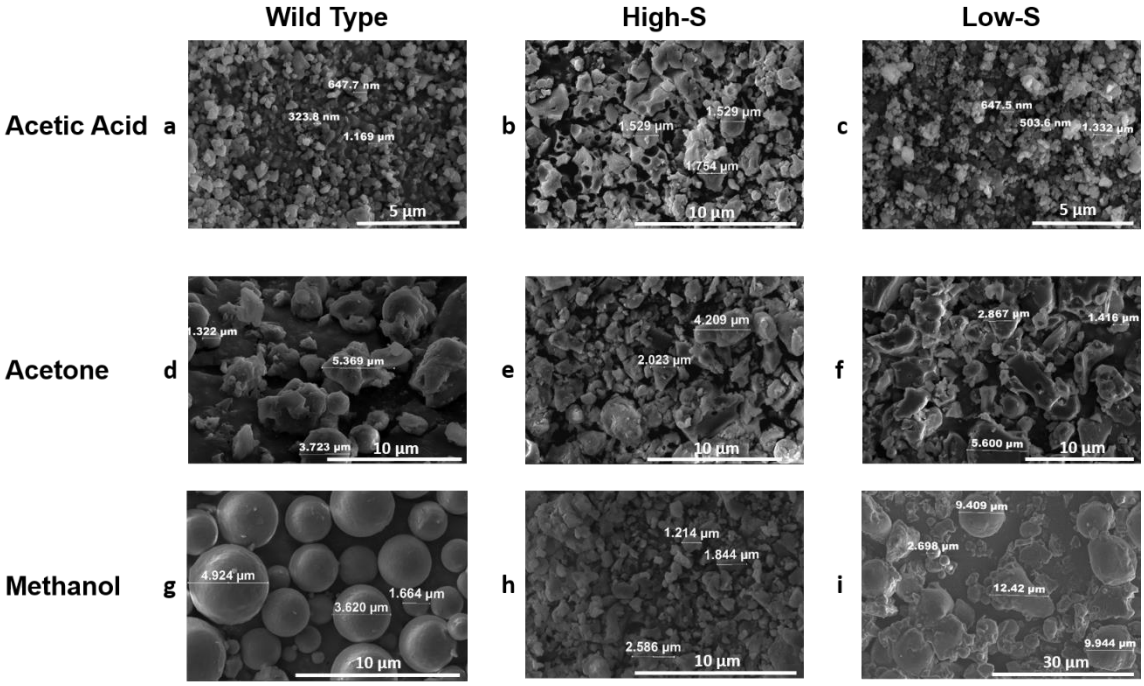

C. Two dimensional HSQC-NMR analysis of organosolv lignin.

For molecular scale structure information of the isolated organosolv lignin samples, two-dimensional HSQC NMR experiments were conducted. Assignments of common carbon-proton correlations are based on previous studies (**Table 4.2.**).[26,27-28] Organosolv lignin samples from wild type poplar are presented here in **Figures 4.3 and 4.4**. Comparison of lignin samples from genetically modified poplar species are provided in **Figures 4.5 and 4.6**. Lignin side chain region (δ_C/δ_H 45-100/2.5-5.5 ppm) provides information on interunit linkages (**Figure 4.3-I**). For all organosolv lignin samples, β-O-4 is the most abundant linkage, followed by β-β and β-5 linkages. Organosolv lignin

derived from high-S poplar shows higher content of β-β linkages, while organosolv lignin derived from low-S poplar contains more β-5 linkage. Methanol treated organosolv lignin samples show a unique signal (not observed for lignin from the other treatments) at δ_C/δ_H 57.5/3.15, which is indicative of methoxy functional group on the α position of β-O-4 linkage. The explanation is methanol acts as a nucleophile protecting benzylic carbocations formed at the α position of β-O-4 during acid catalyzed organosolv extraction (**Figure 4.3-II**). Consistent with this hypothesis is the observation of 1,3-dioxane type structure at the β-O-4 linkage for acetone treated organosolv lignin; this dioxane structure results from the addition of formaldehyde to the α and γ positions (**Figure 4.3-III**). This dioxane structure is absent from acetic acid and methanol treated organosolv lignin as formaldehyde was not used in that treatment. For the methanol treatment, the methoxy group at the α position of β-O-4 linkage blocks addition of formaldehyde and protects against C-C bond forming re-condensation of lignin. As a result the addition of formaldehyde as a potential protecting group in the methanol treatment was not necessary.

Table 4.2. Assignments on the common carbon-proton correlations of organosolv lignin in HSQC-NMR spectra (a) side chain region and (b) aromatic region.

(a)

Carbon-proton correlations	**Assignments[I]**
71.0-72.0/4.9-5.1	A_α
83.0-84.0/4.3-4.5	A_β (H,G)[II]
86.0-87.0/4.1-4.3	A_β (S)[III]
60.0-61.0/3.4-3.7	A_γ
84.0-85.0/4.6-4.7	B_α

53.0-54.0/3.0-3.1	B_β
71.0-72.0/3.8; 71.0-72.0/4.2	B_γ
86.8-87.1/5.5-5.6	C_α
53.0-54.0/3.5-3.6	C_β
61.6-62.5/3.7-3.8	C_γ

[I] For the assignments on carbon-proton correlations for the side chain region, A is used to represent β-O-4 linkage, B is used to represent β-β linkage, C is used to represent β-5 linkage. A_α is for the α position of β-O-4 linkage, B_α for the α position of β-β linkage, C_α for the α position of β-5 linkage, etc.

[II] β position of β-O-4 linkage in H and G type lignin.

[III] β position of β-O-4 linkage in S type lignin.

(b).

Carbon-proton correlations	**Assignments[I]**
128.0-129.0/7.2-7.3	$H_{2,6}$
114.0-115.0/6.7-6.9	$H_{3,5}$
110.0-111.0/7.0-7.1	G_2
114.0-115.0/6.7-6.9	G_5
118.0-119.0/6.8-6.9	G_6
103.0-104.0/6.6-6.8	$S_{2,6}$
130.0-131.0/7.7-7.8	$H'_{2,6}$[II]
105.0-106.0/7.3-7.4	$S'_{2,6}$[III]

[I] For the assignments on carbon-proton correlations for the aromatic region, H is used to represent H type lignin, G is used to represent G type lignin, S is used to represent S type lignin. $H_{2,6}$ for the 2 and 6 positions of H lignin, G_2 for the 2 position of G lignin, $S_{2,6}$ for the 2 and 6 positions of S lignin, etc.

[II] Oxidized H unit (p-Hydroxybenzoic Acid).

[III] Oxidized S unit (Syringic Acid)

Figure 4.3. Two dimensional HSQC-NMR spectra of the side chain region (δ_C/δ_H 45-100/2.5-5.5) of organosolv lignin from wild type poplar using three different treatment media (**I**). Illustration of methoxy substituted benzylic carbocation in methanol extracted

lignin (**II**). Illustration of dioxane ring structure at the β-O-4 linkage of acetone extracted lignin (**III**).

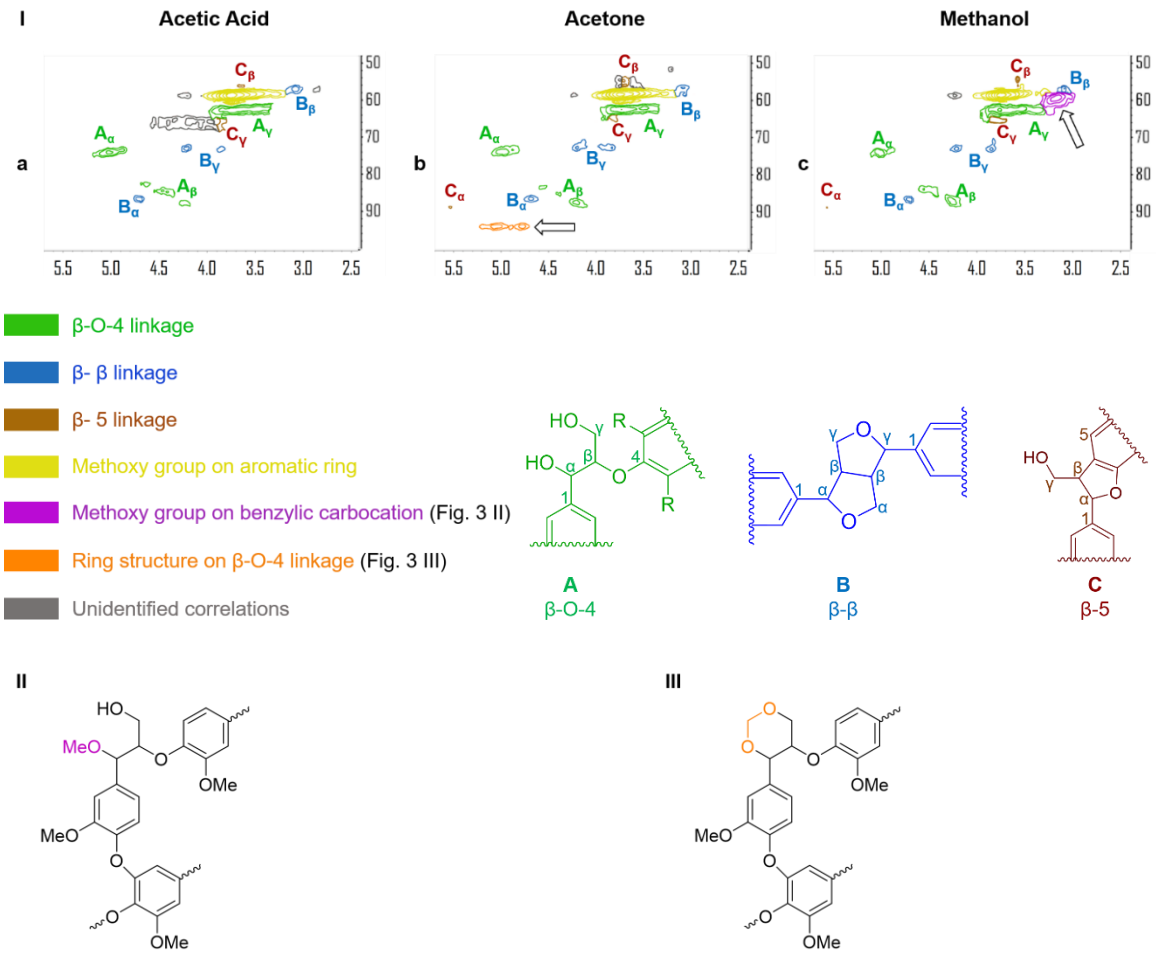

Figure 4.4. Two dimensional HSQC-NMR spectra of the aromatic region (δ_C/δ_H 95-140/6.0-8.0) of organosolv lignin from wild type (**a, b, c**) and high-S poplar (**d, e, f**) in three different media.

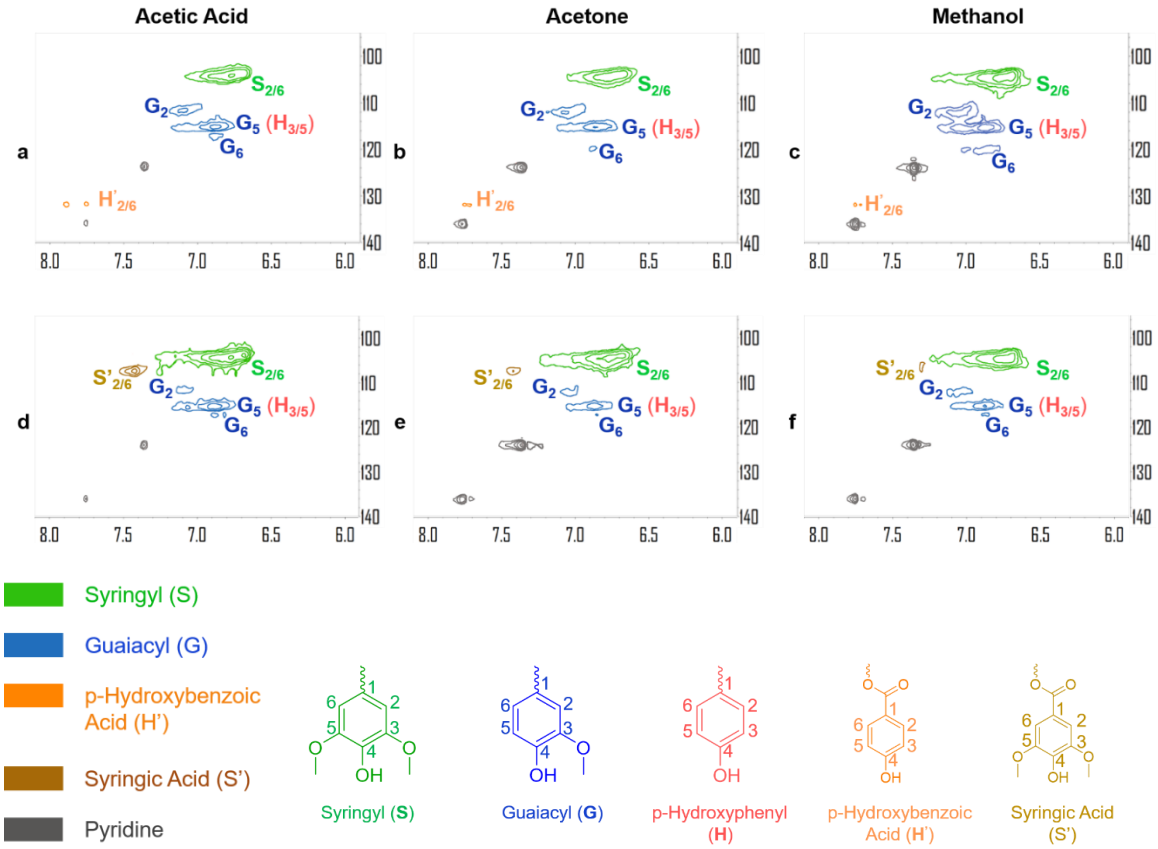

The aromatic region (δ_C/δ_H 95-140/6.0-8.0 ppm) provides information on the extent of methoxy substitution, **H**, **G**, and **S** units (**Figure 4.4**). Organosolv lignin derived from high-S and low-S poplar samples show higher content of S and G units, respectively, which confirms the success of gene manipulation and dominance of one monomer in making up lignin in the biomass (**Table 4.3.**)[22]. Choice of solvent in orgnaosolv lignin preparation has no bearing on the aromatic region of isolated lignin.

Figure 4.5. Two dimensional HSQC-NMR spectra of the side chain region (δ_C/δ_H 45-100/2.5-5.5 ppm) of organosolv lignin from different treatments.

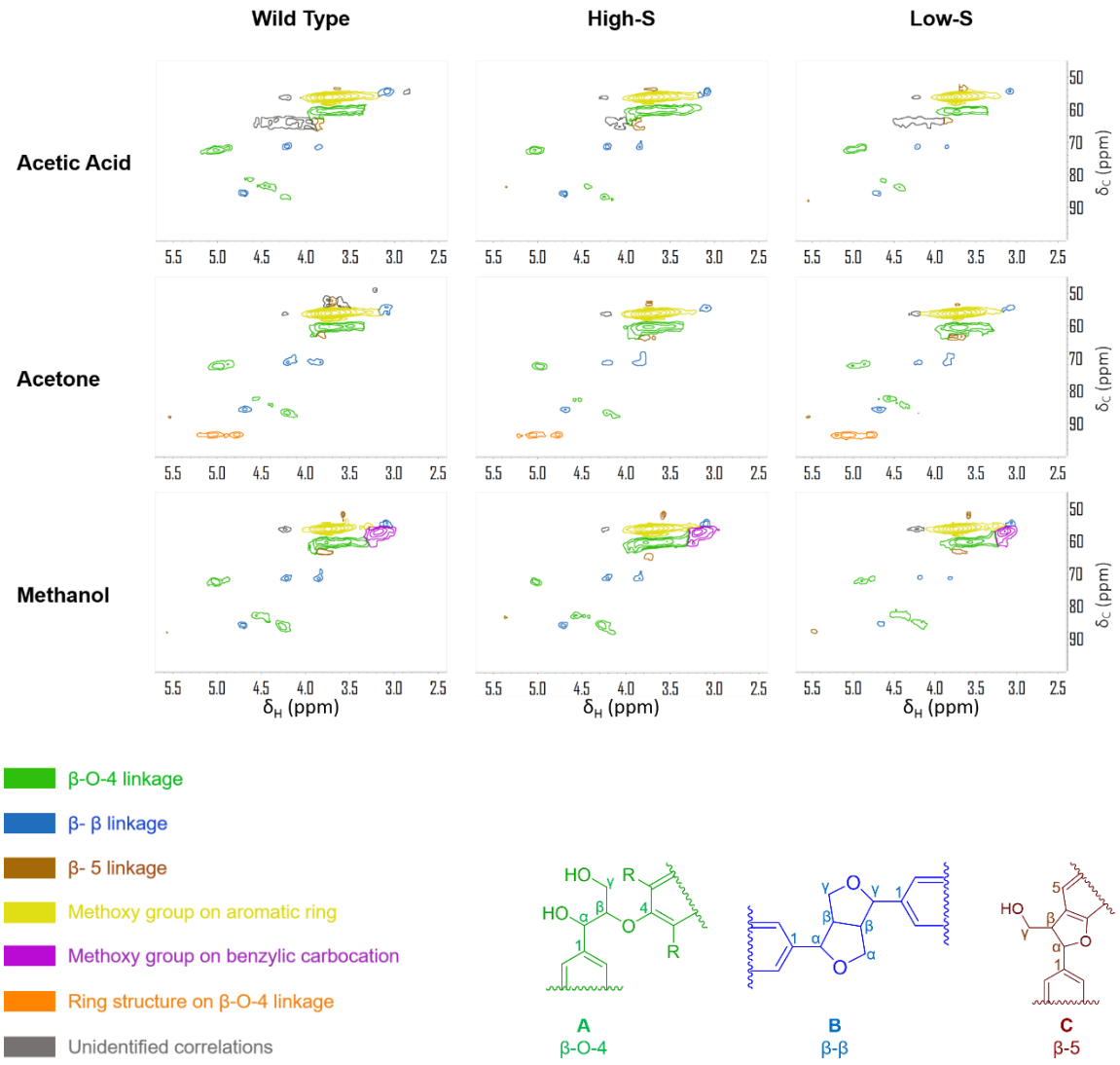

Figure 4.6. Two dimensional HSQC-NMR spectra of the aromatic region (δ_C/δ_H 95-140/6.0-8.0 ppm) of organosolv lignin from different treatments.

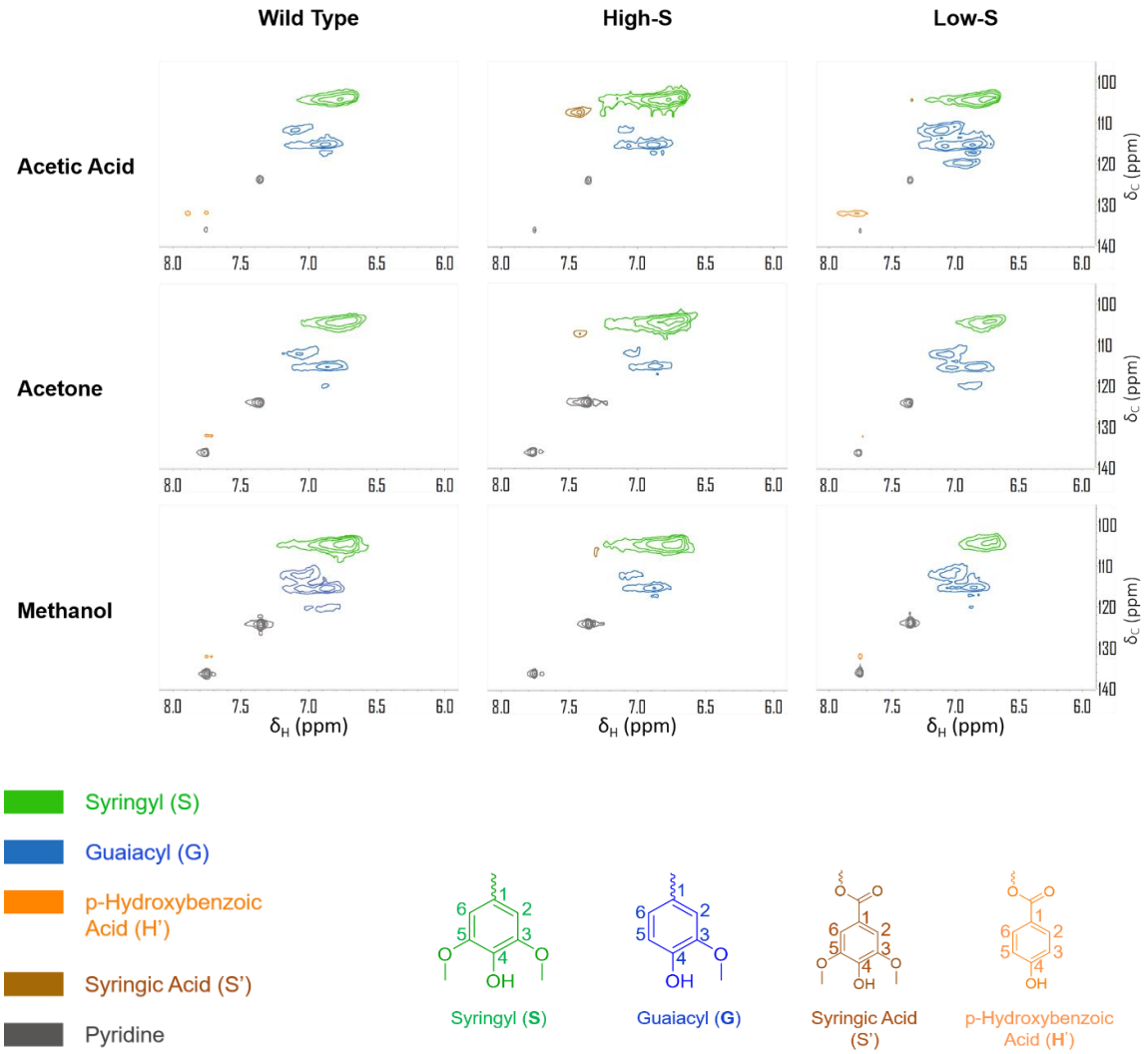

Table 4.3. Relative ratio of S-lignin in poplar substrates.

Substrate	% S-lignin[a]
Wild-Type	64
High-S	82
Low-S	34

[a] Lignin composition as determined by DFRC (derivatization followed by reductive cleavage) analysis.

D. Catalytic depolymerization of organosolv lignin.

Catalytic depolymerization of isolated organosolv lignin samples gave three major phenolic products with alkenyl side chains (**Table 4.4. and Figure 4.7.**). Our results show high selectivity of Ni/C catalyst towards depolymerization of organosolv lignin macromolecules, compared to a wide variety of other metal catalysts which form a mixture of aromatic and cyclohexyl compounds.[21, 29,30,31,32,33] Mass balance based on the formed three aromatic products and residual unconverted organosolv lignin, which can be recovered by precipitation upon water addition, has been achieved from 85% and up to 96% mass recovery (see **Table 4.5.**).

Table 4.4. Catalytic depolymerization of organosolv lignin from different treatment with 10 wt% Ni/C catalyst.[a]

Organosolv Treatment Medium[b]	Poplar Variant	% Yield of Isoeugenol 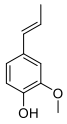	% Yield of 4-Propenyl syringol 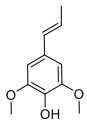	% Yield of Guaiacol 	% Total Yield[c]
Methanol	WT	8	43	9	60
	High S	2	54	7	63
	Low S	14	34	8	56
Acetone	WT	4	29	2	35
	High S	1	27	3	31
	Low S	7	13	8	28
Acetic Acid	WT	3	12	5	20
	High S	2	15	4	21
	Low S	6	17	2	25

[a] Organosolv lingin (50 mg) with 10wt% Ni/C catalyst in 20 mL of MeOH, at 225 °C and 35 bar H_2 for 12 h.

[b] Organosolv lignin samples were named as the solvent used for extraction followed by the specific poplar species.

[c] Yields are calculated based on initial organosolv lignin substrate.

Figure 4.7. Aromatic products (HPLC-UV) after catalytic depolymerization of (a) organosolv lignin and (b) native lignin.

a

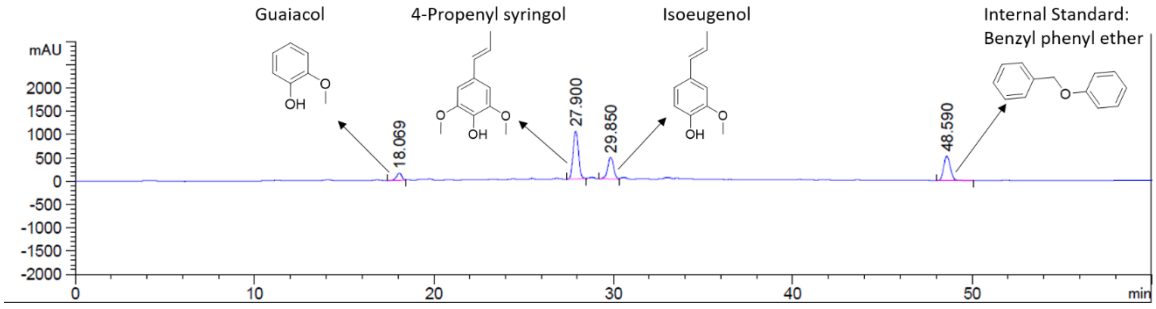

b

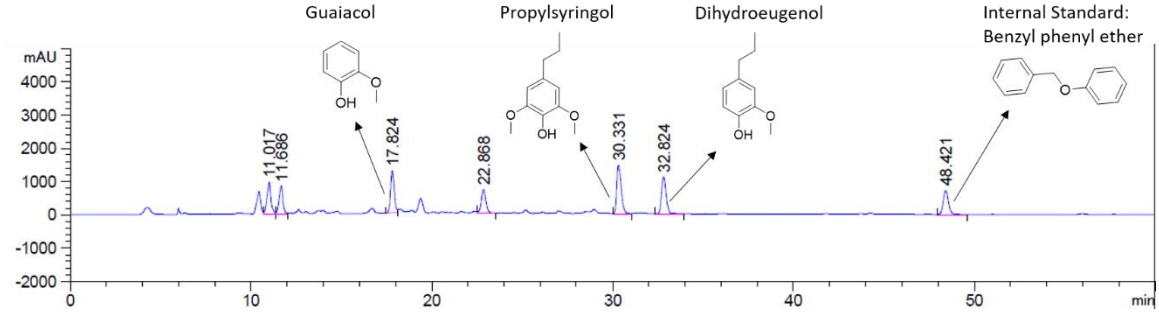

Table 4.5. Mass balance calculation after catalytic depolymerization of organosolv lignin.[a]

Substrates[b]	Toluene soluble aromatics%	Water precipitated oligomer & unconverted organosolv lignin%	Total%[c]
AA-Wild type	20	72	92
AA-High-S	21	67	88
AA-Low-S	25	52	87
Acetone-Wild type	35	57	92
Acetone-High-S	31	65	96
Acetone-Low-S	28	64	92
Methanol-Wild type	60	36	96
Methanol-High-S	63	28	91
Methanol-Low-S	56	29	85

[a] Organosolv lingin (50 mg) with 10wt% Ni/C catalyst in 20 mL of MeOH, at 225 °C and 35 bar H_2 for 12 h.

[b] Organosolv lignin samples were named as the solvent used for extraction followed by the specific poplar species. For example, AA-Wild type means wild type poplar being extracted by acetic acid/formic acid solvent, Methanol-Wild type means wild type poplar being extracted by methanol, etc.

[c] Total mass balance is calculated based on initial organosolv lignin substrate.

As can be seen from **Table 4.4.**, products yield for organosolv lignin made from the methanol treatment is significantly higher than those from the other two treatments. This is attributed to the degree of lignin re-condensation during the organosolv process. When methanol is used it acts as a protecting group on the C_α position (**Figure 4.3-Ic and II**) minimizing C-C bond formation. The use of acid during organosolv extraction leads to irreversible condensation of extracted lignin. In specific, the protonated hydroxyl group on C_α becomes a good leaving group, resulting in the formation of carbocation. This carbocation can attack another electron rich aromatic ring in lignin to form stable

carbon-carbon bond (**Scheme 4.1**). The resulting structure is highly recalcitrant towards further upgrading because carbon-carbon bonds are quite inert towards hydrogenolysis catalysts.[17, 34] Methanol prevents the formation of carbon-carbon bonds by reacting with the carbocation to form C-OMe. MeO- Cα is observed in 2D-HSQC NMR spectra (**Figure 4.3-Ic**). This phenomenon is similar to reported interactions of ethanol and 2-napthanol with lignin linkages, which hinder re-condensation of lignin.[18, 32] Organosolv lignin from acetone is second best because formaldehyde provides some protection (**Figures 3b & III**), but not as effective as methanol.

Scheme 4.1. Illustration of acid catalyzed cleavage of α-aryl ether linkage in lignin macromolecules.

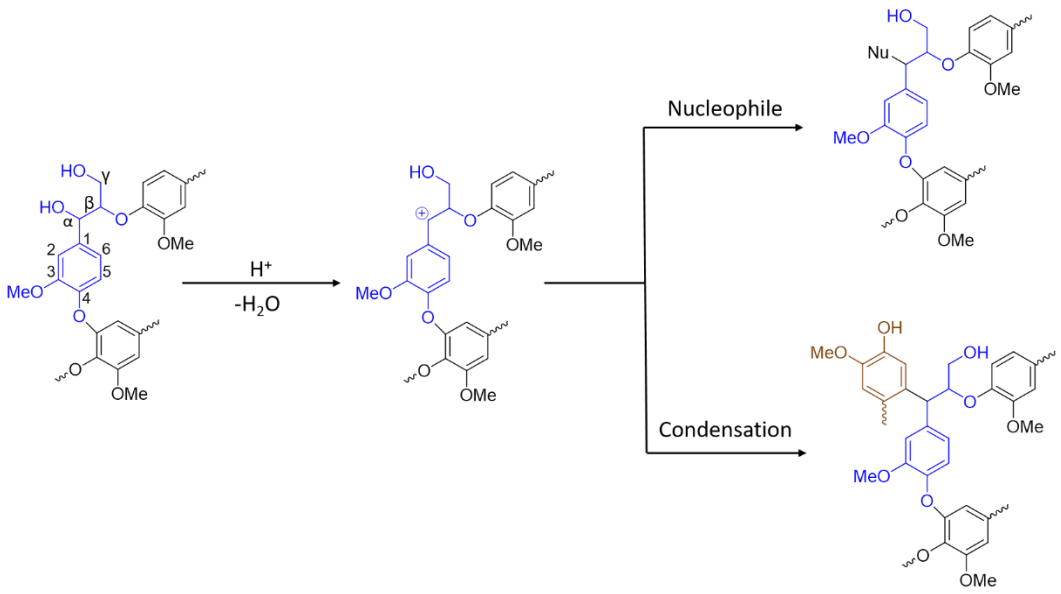

Unconverted lignin residue after the catalytic depolymerization reaction was analyzed by HSQC NMR (**Figure 4.8**). The residue from MeOH-Wild type poplar organosolv lignin is used as an example. Compared with **Figure 4.3**, ether bonds in the

three major interunit linkages had disappeared after CDL, which suggest that cleavage of aryl alkyl ether bonds is the major pathway in the depolymerization of lignin. The unconverted residue is then precipitated with H_2O and used for the mass balance calculation (**Table 4.5**). The aromatic region (δ_C/δ_H 95-140/6.0-8.0 ppm) after CDL shows a simplified spectrum compared to untreated organosolv lignin (**Figure 4.4**). In this case, G_2/H_2 and G_6/H_6 signals of G type lignin are absent. G type lignin has been reported to be the most reactive towards re-condensation, because of the electron-rich positions ortho and para to the methoxy group (G_2 and G_6 positions).[18, 34] The absence of the corresponding signals in G lignin indicate that re-condensation has occurred between nearby lignin units. The re-condensed structure is highly recalcitrant and survives in the residue lignin. This observation is also consistent with the observed low yield of monomer products from G type lignin (isoeugenol) after CDL (**Table 4.4**).

Figure 4.8. Two dimensional HSQC-NMR spectra of unconverted lignin[a] after catalytic depolymerization of lignin (CDL) reaction, (a) side chain region and (b) aromatic region.

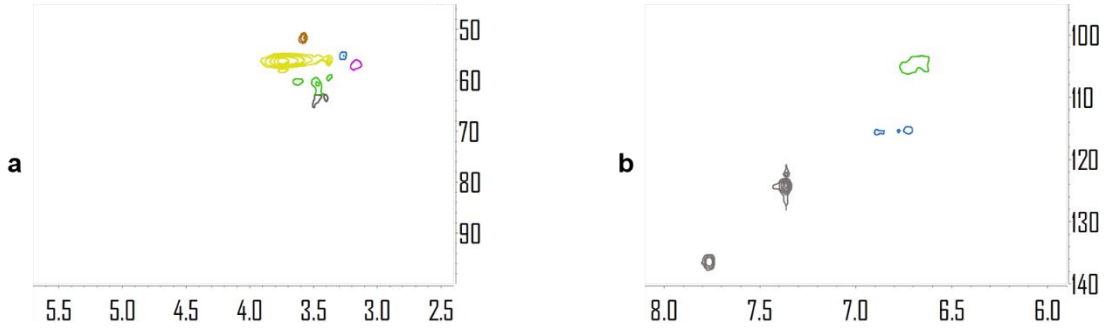

[a] Unconverted lignin from MeOH - wild type poplar organosolv lignin is used as an example.

Based on our study, catalytic depolymerization of organosolv lignin into monomeric phenolic products is feasible if lignin re-condensation is prevented or minimized. In case of organosolv lignin depolymerization, only three products were

formed. Catalyst and product separation is straightforward. As all the monomers together with unconverted organosolv lignin are soluble, simple filtration can efficiently separate the liquid phase from solid catalyst. Finally, residual unconverted lignin can be precipitated subsequently and separated from the three phenolic products. Mass basis comparison between organosolv upgrading using methanol treatment versus direct catalytic conversion of lignin from biomass is presented in **Figure 4.9**.

Figure 4.9. Mass basis comparison between the CDL (Catalytic Depolymerization of Lignin) reaction of (a) intact raw biomass and (b) organosolv lignin. Reaction conditions for CDL: 225 °C, 35 bar H_2, 12 hours, 10 wt% Ni/C catalyst, methanol solvent.

(a)

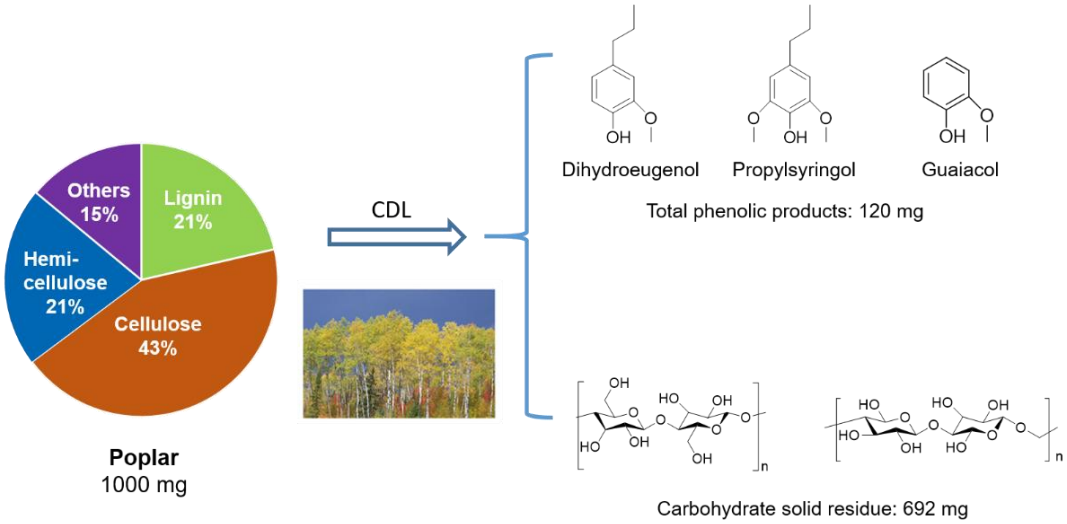

(b)

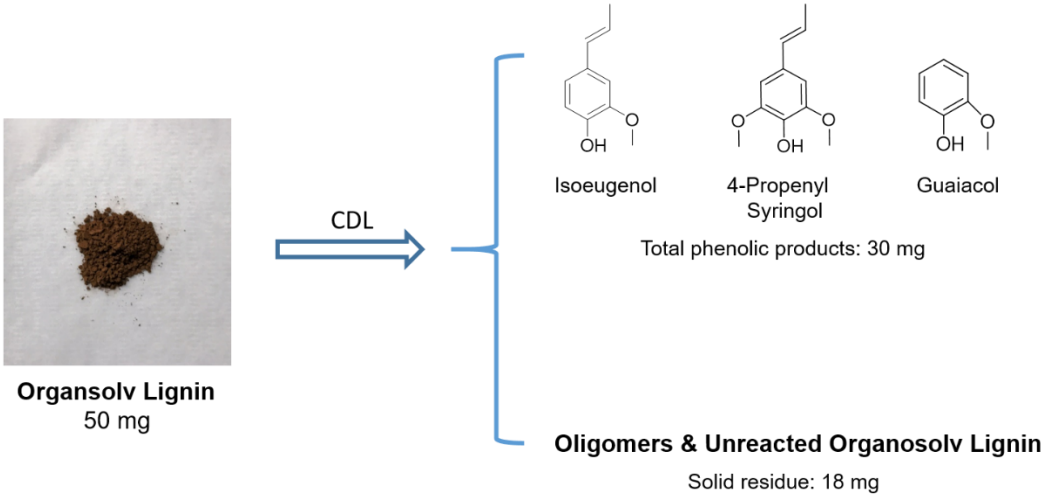

E. Conclusions

Organosolv extraction of poplar species indicated that both gene manipulation and extractive solvent influence the structure and subsequent reactivity of isolated lignin. GPC analysis showed that acetone treated organosolv gave the smallest molecular weight. Isolated organosolv lignin were composed on average of 10-mers. SEM images revealed that using methanol as an extraction solvent gave the most uniform particle shape but largest particle size. Despite particle size, methanol treatment gave organosolv lignin that performed best under CDL (Catalytic Depolymerization of Lignin). Methanol formed methoxy group on benzylic positions (C_α), which limits lignin re-condensation, C-C bond formation, and recalcitrance. Nickel catalyst was proved to be effective in catalyzing the depolymerization of methanol extracted organosolv lignin, which was attributed to the methoxy group at α position of typical β-O-4 linkages. Under optimized conditions, > 60% conversion of organosolv lignin into three major phenolic products was achieved. Aryl alkyl ether bond cleavage was proposed to be the major pathway for the depolymerization of lignin.

F. Supporting Information

1. Materials and methods

Materials.

Wild-type poplar (*P. nigra* × *P. maximowiczii*) was provided by Purdue University's Department of Forestry and Natural Resources. High-S polar, or the genetically engineered line F5H-64, was provided by Drs. Clint Chapple and Richard Meilan from Purdue University.[22] Low-S poplar, the genetically engineered line 1035-41, was provided by the U.S. Department of Energy (DOE) BES project (0012846) entitled: Manipulation of Lignin Biosynthesis to Maximize Ethanol Production from *Populus* Feedstocks, DOE grant # DE-FG36-04G01417. All biomass substrates were milled to pass through a 40 mesh screen using a Mini Wiley Mill (Thomas Scientific, Swedesboro, NJ) before use. Detailed composition analysis of poplar biomass was performed according to the standard NREL procedures (**Tables 4.6**).[35] Ni/C catalyst, containing 11 wt% Ni dispersed on activated carbon support, was synthesized and characterized based on previously reported methods.[36] Sulfuric acid (98 wt%) and acetic acid were purchased from EMD Millipore Corporation. Acetone, methanol, formic acid (88 wt%) and formaldehyde (37 wt%) were purchased from Fisher Chemical. All chemicals were used as received.

Table 4.6. Composition analysis of gene modified poplar species.[1,2]

Substrates	Glucan[a] %	Xylan[a] %	Lignin[b] %	Others[c] %	Mass Balance%
Wild Type Poplar	43.4	21.2	21.4	12.1	98.1
High-S Poplar	44.5	21.6	22.3	6.5	94.9
Low-S Poplar	44.5	22.0	21.4	10.3	98.2

[a] Cellulose content was reported as glucan, hemicellulose content was reported as xylan.

[b] Lignin content determined by ABSL (acetyl bromide-soluble lignin) lignin analysis.

[c] Including acetyl, ash and other water and ethanol extractives.

Isolation of organosolv lignin from poplar.

Extraction of organosolv lignin from wild-type and genetically modified poplar species (wild type, high-S, and low-S) was conducted in three different solvents, acetic acid/formic acid/water, acetone/water and methanol/water, with modified procedures according to previous reports.[26, 37-39] For treatment with acetic acid/formic acid/water, 30 g of 40 mesh raw biomass substrate was combined with 300 mL solvent in a 1 L round bottom flask. Acetic acid, formic acid and water were used in a 50:30:20 v/v/v ratio. The mixture was first heated to 60 ˚C and the temperature held for 1 hour, followed by increased heating to 110 ˚C and held for 3 hours. After reaction, the mixture wa allowed to cool to room temperature, and the liquid phase containing extracted lignin was separated from the solid fraction by filtration. 3 portions of 200 mL 0.5 N acetic acid solution were used to wash the solid fraction at 60 ˚C with 0.5 hour incubation time for each wash. The filtrate and washing solutions were combined and concentrated by rotary evaporation to a volume less than 10 mL. 300 mL Milli-Q Academic A10 grade water was added to the condensed liquid phase in order to precipitate lignin. Lignin precipitate was then filtered using Whatman filter paper, washed with small portion of water during filtration and dried under vacuum overnight before further use. Isolated lignin samples (47-54% yield) were analyzed by NMR, GPC and SEM.

For treatment with acetone and methanol, 2 g of 40 mesh raw biomass was combined with solvent solid:liquid ratio 1:20 in a 75 mL stainless steel Parr reactor. The reaction was catalyzed by 0.045 N H_2SO_4. Liquid phase was composed of 20 mL organic solvent,

20 mL 0.045 N H_2SO_4 aqueous solution and 4 mL 37 wt% aqueous formaldehyde. The reaction vessel was sealed, and purged with UHP grade N_2 5 times while stirring. The reaction was performed at 160 ˚C for 0.5 hour, under 12 bar N_2 atmosphere with a stirring speed 700 rpm. The reaction was terminated by cooling down the system to room temperature. The liquid phase containing extracted lignin was separated from the solid fraction by filtration. 3 portions of 20 mL organic solvent were used to wash the solid residue to remove any remaining lignin on the surface. The filtrate was combined with washing solution and concentrated by rotary evaporation to a volume < 10 mL. 200 mL Milli-Q Academic A10 grade water was added to the concentrated liquid phase in order to precipitate lignin. Lignin precipitate was filtered using Whatman filter paper, washed with small portion of water during filtration and dried under vacuum overnight before further use. Isolated lignin samples (58-69% yield) were analyzed by NMR, GPC and SEM.

Catalytic depolymerization of organosolv lignin.

Catalytic depolymerization of organosolv lignin was performed in a 75 mL stainless steel pressure reactor (Parr Instrument Company). In a typical reaction, 50 mg of dry organosolv lignin, 10 wt% of Ni/C catalyst (5 mg), and 20 mL methanol were added to the reactor. The reactor was sealed, and purged with UHP grade H_2 for 5 times while stirring. The reaction system was then pressurized with 35 bar H_2, heated to 225 ˚C at stirring speed 700 rpm, and the temperature maintained for 12 hours. The reaction was terminated by cooling down the reactor to room temperature. The reaction mixture was then filtered to separate the liquid phase containing monomeric aromatic products from the solid catalyst, which was subsequently washed with additional methanol, and the

liquid wash was combined with filtrate. The combined liquid phase was concentrated by rotary evaporation, diluted in a volumetric flask (10 mL), and analyzed by HPLC/UV as well as by HPLC/MS.

2. Instrumentation and Characterization Conditions

HPLC-MS analysis

All HPLC separations for mass spectrometry analysis were performed on a Surveyor Plus HPLC system from Thermo Scientific consisting of a quaternary pump, an autosampler, a photodiode array (PDA) detector, and a Zorbax SB-C18 column. A non-linear gradient of water (A) and acetonitrile (B) was used as follows: 0.00 min, 95% A and 5% B; 10.00 min, 95% A and 5% B; 30.00 min, 40% A and 60% B; 35.00 min, 5% A and 95 %; 38.00min, 5% A and 95% B; 38.50 min, 95% A and 5% B; 45.00 min, 95% A and 5% B. Flowrate of the mobile phase was kept at 500 μL/min. PDA detector was set at the wavelength of 254 nm.

Mass spectrometric analysis (MS, MS^2 and MS^3) of HPLC eluent was performed using a Thermo Scientific linear quadrupole ion trap (LQIT) mass spectrometer equipped with an electrospray ionization (ESI) source. All mass spectrometry experiments were performed under negative ion mode. HPLC eluents were mixed via a T-connector with 1% sodium hydroxide water solution at a flow rate of 0.1 μL/min before entering the ESI source. Addition of sodium hydroxide facilitates deprotonation of the analytes. ESI source conditions were set as: 3.5 kV spray voltage; 50 (arbitrary units) sheath gas (N_2) flow and 20 (arbitrary units) auxillary gas (N_2) flow.

MS^3 analysis was performed using the data dependent scan function of the Thermo Xcalibur software. The most abundant ion formed upon ESI was isolated and subjected to collision-activated dissociation (CAD). The most abundant fragment ion was further selected for isolation and fragmentation. For all MS^3 experiments, an isolation window of 2 m/z units was used along with a normalized collision energy of 30 (arbitrary units).

HPLC-UV analysis

The liquid phase from lignin depolymerization reactions with methanol as solvent was analyzed with Agilent 1260 Infinity Quaternary High-Performance Liquid Chromatography (HPLC) system, using Zorbax Eclipse XDB-C18 Column (250 x 74.6mm) set at 30˚C. The chromatography apparatus is equipped with G1315D Diode Array Detector (DAD). A mixture of H_2O (A) and acetonitrile (B) were used as the mobile phase at a flow rate of 0.5 mL/min. Nonlinear gradient was used (80% A and 20% B from beginning to 5% A and 95 % B at 55.0 min). A fixed amount (400μL) of internal standard benzyl phenyl ether (10 mM) was added into each sample for the quantification purposes. Standard curves for all the aromatic products were made by comparison of the products to internal standard. All results were analyzed and quantified according to standard curves. Before analyzing by HPLC, the liquid samples were filtered through a 0.22μm cutoff syringe filter (2 5mm diameter).

Nuclear Magnetic Resonance (NMR)

All NMR spectra were collected on a Bruker Avance DMX500 spectrometer with a 11.74 Tesla standard-bore superconducting magnet operating at 500.13 and 125.77 MHz for ^1H and ^{13}C nuclei, respectively. C-H correlation spectra were recorded through a

phase sensitive gradient enhanced 2D HSQC using echo-antiecho experiment (HSQCETGP experiment). Isolated lignin sample (20mg) was dissolved in 700μL mixture of 5:1 v/v DMSO-d_6/pyridine-d_5 solvent for each experiment.

Scanning Electron Microscopy (SEM)

SEM images were taken on an FEI Nova NanoSEM 650 high resolution instrument, equipped with a high stability Schottky field emission gun and a large specimen chamber. Oxford Inca x-ray EDX system was used as detector, back scattering detector for Z-imaging. Lignin samples were first coated with palladium metal at plasma discharge current 10mA for 100s under argon atmosphere. The instrument was vented to pressure less than 9×10^{-5} torr before use. Electron beam used for image taking was set to voltage at 7 keV.

Gel Permeation Chromatography (GPC)

Gel permeation chromatography (GPC) was carried out on a Waters (Millford, MA) chromatograph equipped with a Waters Alliance high performance liquid chromatography (HPLC) system pump (2695 Separation Module) and two Tosoh TSKgel Super HM-M columns. Detection was provided by a Waters 2414 differential refractometer, and N,N-dimethyl formamide with 0.1% LiBr was used as the mobile phase. Number average molecular weights (Mn) and weight average molecular weights (Mw) were calculated relative to linear polystyrene standard.

G. References:

1. Agrawal, R.; Singh, N. R.; Ribeiro, F. H.; Delgass, W. N., Sustainable fuel for the transportation sector. *P Natl Acad Sci USA* **2007,** *104* (12), 4828-4833.

2. Singh, N. R.; Delgass, W. N.; Ribeiro, F. H.; Agrawal, R., Estimation of Liquid Fuel Yields from Biomass. *Environ. Sci. Technol.* **2010,** *44* (13), 5298-5305.

3. Scown, C. D.; Gokhale, A. A.; Willems, P. A.; Horvath, A.; McKone, T. E., Role of Lignin in Reducing Life-Cycle Carbon Emissions, Water Use, and Cost for United States Cellulosic Biofuels. *Environ Sci Technol* **2014,** *48* (15), 8446-8455.

4. Upton, B. M.; Kasko, A. M., Strategies for the Conversion of Lignin to High-Value Polymeric Materials: Review and Perspective. *Chem Rev* **2016,** *116* (4), 2275-2306.

5. Li, C. Z.; Zhao, X. C.; Wang, A. Q.; Huber, G. W.; Zhang, T., Catalytic Transformation of Lignin for the Production of Chemicals and Fuels. *Chem. Rev.* **2015,** *115* (21), 11559-11624.

6. Cotana, F.; Cavalaglio, G.; Nicolini, A.; Gelosia, M.; Coccia, V.; Petrozzi, A.; Brinchi, L., Lignin as co-product of second generation bioethanol production from ligno-cellulosic biomass. *Ati 2013 - 68th Conference of the Italian Thermal Machines Engineering Association* **2014,** *45*, 52-60.

7. Abu-Omar, H. L. M. M., Chemicals from Lignin. In *Encyclopedia of Sustainable Technologies*, 2017; pp 573-585.

8. Parsell, T.; Yohe, S.; Degenstein, J.; Jarrell, T.; Klein, I.; Gencer, E.; Hewetson, B.; Hurt, M.; Kim, J. I.; Choudhari, H.; Saha, B.; Meilan, R.; Mosier, N.; Ribeiro, F.; Delgass, W. N.; Chapple, C.; Kenttamaa, H. I.; Agrawal, R.; Abu-Omar, M. M., A

synergistic biorefinery based on catalytic conversion of lignin prior to cellulose starting from lignocellulosic biomass. *Green Chem.* **2015,** *17* (3), 1492-1499.

9. Luo, H.; Klein, I. M.; Jiang, Y.; Zhu, H. Y.; Liu, B. Y.; Kenttamaa, H. I.; Abu-Omar, M. M., Total Utilization of Miscanthus Biomass, Lignin and Carbohydrates, Using Earth Abundant Nickel Catalyst. *ACS Sustain. Chem. Eng.* **2016,** *4* (4), 2316-2322.

10. Yan, N.; Zhao, C.; Dyson, P. J.; Wang, C.; Liu, L. T.; Kou, Y., Selective Degradation of Wood Lignin over Noble-Metal Catalysts in a Two-Step Process. *Chemsuschem* **2008,** *1* (7), 626-629.

11. Xu, C. P.; Arancon, R. A. D.; Labidi, J.; Luque, R., Lignin depolymerisation strategies: towards valuable chemicals and fuels. *Chem. Soc. Rev.* **2014,** *43* (22), 7485-7500.

12. Li, C. Z.; Zheng, M. Y.; Wang, A. Q.; Zhang, T., One-pot catalytic hydrocracking of raw woody biomass into chemicals over supported carbide catalysts: simultaneous conversion of cellulose, hemicellulose and lignin. *Energy Environ. Sci.* **2012,** *5* (4), 6383-6390.

13. Stark, K.; Taccardi, N.; Bosmann, A.; Wasserscheid, P., Oxidative Depolymerization of Lignin in Ionic Liquids. *Chemsuschem* **2010,** *3* (6), 719-723.

14. Patil, P. T.; Armbruster, U.; Richter, M.; Martin, A., Heterogeneously Catalyzed Hydroprocessing of Organosolv Lignin in Sub-and Supercritical Solvents. *Energy Fuel* **2011,** *25* (10), 4713-4722.

15. Perras, F. A.; Luo, H.; Zhang, X. M.; Mosier, N. S.; Pruski, M.; Abu-Omar, M. M., Atomic-Level Structure Characterization of Biomass Pre- and Post-Lignin Treatment

by Dynamic Nuclear Polarization-Enhanced Solid-State NMR. *J Phys Chem A* **2017,** *121* (3), 623-630.

16. Mosier, N.; Wyman, C.; Dale, B.; Elander, R.; Lee, Y. Y.; Holtzapple, M.; Ladisch, M., Features of promising technologies for pretreatment of lignocellulosic biomass. *Bioresour Technol* **2005,** *96* (6), 673-86.

17. Luterbacher, J. S.; Azarpira, A.; Motagamwala, A. H.; Lu, F. C.; Ralph, J.; Dumesic, J. A., Lignin monomer production integrated into the gamma-valerolactone sugar platform. *Energ Environ Sci* **2015,** *8* (9), 2657-2663.

18. Li, J.; Gellerstedt, G., Improved lignin properties and reactivity by modifications in the autohydrolysis process of aspen wood. *Ind. Crop. Prod.* **2008,** *27* (2), 175-181.

19. Cai, Z. P.; Li, Y. W.; He, H. Y.; Zeng, Q.; Long, J. X.; Wang, L. F.; Li, X. H., Catalytic Depolymerization of Organosolv Lignin in a Novel Water/Oil Emulsion Reactor: Lignin as the Self-Surfactant. *Ind Eng Chem Res* **2015,** *54* (46), 11501-11510.

20. Ye, Y. Y.; Zhang, Y.; Fan, J.; Chang, J., Novel Method for Production of Phenolics by Combining Lignin Extraction with Lignin Depolymerization in Aqueous Ethanol. *Ind. Eng. Chem. Res.* **2012,** *51* (1), 103-110.

21. Barta, K.; Warner, G. R.; Beach, E. S.; Anastas, P. T., Depolymerization of organosolv lignin to aromatic compounds over Cu-doped porous metal oxides. *Green Chem* **2014,** *16* (1), 191-196.

22. Franke, R.; McMichael, C. M.; Meyer, K.; Shirley, A. M.; Cusumano, J. C.; Chapple, C., Modified lignin in tobacco and poplar plants over-expressing the Arabidopsis gene encoding ferulate 5-hydroxylase. *Plant J* **2000,** *22* (3), 223-234.

23. Balogh, D. T.; Curvelo, A. A. S.; Degroote, R. A. M. C., Solvent Effects on Organosolv Lignin from Pinus-Caribaea-Hondurensis. *Holzforschung* **1992,** *46* (4), 343-348.

24. Mellmer, M. A.; Alonso, D. M.; Luterbacher, J. S.; Gallo, J. M. R.; Dumesic, J. A., Effects of gamma-valerolactone in hydrolysis of lignocellulosic biomass to monosaccharides. *Green Chem.* **2014,** *16* (11), 4659-4662.

25. Mellmer, M. A.; Sener, C.; Gallo, J. M. R.; Luterbacher, J. S.; Alonso, D. M.; Dumesic, J. A., Solvent Effects in Acid-Catalyzed Biomass Conversion Reactions. *Angew. Chem. Int. Ed.* **2014,** *53* (44), 11872-11875.

26. Abdelkafi, F.; Ammar, H.; Rousseau, B.; Tessier, M.; El Gharbi, R.; Fradet, A., Structural Analysis of Alfa Grass (Stipa tenacissima L.) Lignin Obtained by Acetic Acid/Formic Acid Delignification. *Biomacromolecules* **2011,** *12* (11), 3895-3902.

27. Martinez, A. T.; Rencoret, J.; Marques, G.; Gutierrez, A.; Ibarra, D.; Jimenez-Barbero, J.; del Rio, J. C., Monolignol acylation and lignin structure in some nonwoody plants: A 2D NMR study. *Phytochemistry* **2008,** *69* (16), 2831-2843.

28. Kim, H.; Ralph, J., Solution-state 2D NMR of ball-milled plant cell wall gels in DMSO-d(6)/pyridine-d(5). *Org Biomol Chem* **2010,** *8* (3), 576-591.

29. Chan, J. M. W.; Bauer, S.; Sorek, H.; Sreekumar, S.; Wang, K.; Toste, F. D., Studies on the Vanadium-Catalyzed Nonoxidative Depolymerization of Miscanthus giganteus-Derived Lignin. *ACS Catal.* **2013,** *3* (6), 1369-1377.

30. Konnerth, H.; Zhang, J. G.; Ma, D.; Prechtl, M. H. G.; Yan, N., Base promoted hydrogenolysis of lignin model compounds and organosolv lignin over metal catalysts in water. *Chem. Eng. Sci.* **2015,** *123*, 155-163.

31. Kim, M.; Son, D.; Choi, J.-W.; Jae, J.; Suh, D. J.; Ha, J.-M.; Lee, K.-Y., Production of phenolic hydrocarbons using catalytic depolymerization of empty fruit bunch (EFB)-derived organosolv lignin on Hβ-supported Ru. *Chem. Eng. J.* **2017,** *309,* 187-196.

32. Zakzeski, J.; Jongerius, A. L.; Bruijnincx, P. C. A.; Weckhuysen, B. M., Catalytic Lignin Valorization Process for the Production of Aromatic Chemicals and Hydrogen. *Chemsuschem* **2012,** *5* (8), 1602-1609.

33. Klamrassamee, T.; Laosiripojana, N.; Faungnawakij, K.; Moghaddam, L.; Zhang, Z. Y.; Doherty, W. O. S., Co- and Ca-phosphate-based catalysts for the depolymerization of organosolv eucalyptus lignin. *RSC Adv.* **2015,** *5* (57), 45618-45621.

34. Shuai, L.; Amiri, M. T.; Questell-Santiago, Y. M.; Heroguel, F.; Li, Y. D.; Kim, H.; Meilan, R.; Chapple, C.; Ralph, J.; Luterbacher, J. S., Formaldehyde stabilization facilitates lignin monomer production during biomass depolymerization. *Science* **2016,** *354* (6310), 329-333.

35. Sluiter, A.; Hames, B.; Ruiz, R.; Scarlata, C.; Sluiter, J.; Templeton, D.; Crocker, D. *Determination of Structural Carbohydrates and Lignin in Biomass*; National Renewable Energy Laboratory: Golden, CO, 08/03/2013, 2012.

36. Klein, I.; Saha, B.; Abu-Omar, M. M., Lignin depolymerization over Ni/C catalyst in methanol, a continuation: effect of substrate and catalyst loading. *Catal. Sci. Technol.* **2015,** *5* (6), 3242-3245.

37. Gilarranz, M. A.; Oliet, M.; Rodriguez, F.; Tijero, J., Methanol-based pulping of Eucalyptus globulus. *Can. J. Chem. Eng.* **1999,** *77* (3), 515-521.

38. Huijgen, W. J. J.; Reith, J. H.; den Uil, H., Pretreatment and Fractionation of Wheat Straw by an Acetone-Based Organosolv Process. *Ind. Eng. Chem. Res.* **2010,** *49* (20), 10132-10140.

39. Sidiras, D. K. S., I. S In *Organosolv pretreatment as a major step of lignocellulosic biomass refining*, Biorefinery I: Chemicals and Materials From Thermo-Chemical Biomass Conversion and Related Processes, 2015.

CHAPTER V. Bio-based Epoxy Resin through the Curing of Surface Modified Cellulose with Epoxy Monomer Derived from Biomass.

A. Introduction

The previous research has focused on the valorization of biomass through two pathways, direct catalysis into value-added chemicals (**Chapter 2**) as well as organosolv extraction followed by catalytic upgrading (**Chapter 4**). In both the two cases, research has been focused on the generation of monomeric compounds from lignocellulosic biomass. In addition, the production of polymeric materials based on major biomass components is now attracting increasing attention in both industrial application and academic research. One of the currently ongoing research projects focuses on the synthesis of novel bio-based epoxy resin through the curing of surface modified cellulose from the organosolv extraction of biomass with epoxide monomers derived from lignin depolymerization products (**Scheme 5.1.**).

Scheme 5.1. Bio-based epoxy resin generated from cellulose and lignin derived epoxide components.

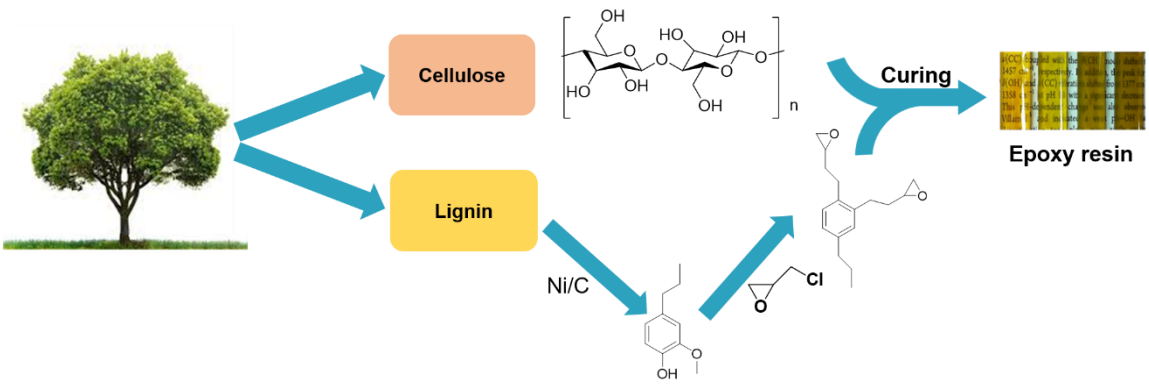

Epoxy resin is among one of the most versatile thermosetting polymers with a wide range of applications.[1] Its superior chemical, electrical, heat resistance and mechanical properties make it the suitable material applied in composites, coatings, adhesives, etc.[2]

Currently, most of the epoxy resins are derived from petroleum based materials, which may result in a series of environmental issues as well as the potential effects on human health. Thus, the application of renewable and nontoxic materials in the synthesis of epoxy resins is a highly active area of research. Several examples have illustrated the replacement of fossil fuel derived precursors by sustainable components in the synthesis of epoxy resins. Incorporation of vegetable oils into epoxy resins has attracted much attention in the past few years.[3-4] The vegetable oil incorporated material exhibited increased fracture toughness and impact strength.[5] Glucose derived isosorbide, furan and its derivates as well as other plant-sourced molecules have also been used for the synthesis of epoxy resin components.[6-8]

Cellulose as the most abundant component in lignocellulosic biomass has the great potential to be used as a renewable fuel source as well as for the generation of high value chemicals.[9] In addition, the low density and outstanding mechanical properties of cellulose also makes it a promising candidate for the production of polymer products.[10] Cellulose contains three hydroxyl groups in each of its anhydroglucose unit (AGU). The presence these hydroxyl groups are therefore mainly responsible for the reactions of cellulose. Currently, the applications of cellulose in epoxy composites mainly focused on its use as filler.[10-16] It has been proved that the incorporation of a small amount of cellulose can significantly improve the mechanical properties of the epoxy composites, due to their high specific strength, modulus and aspect ratio.[17] Besides, the presence of hydroxyl groups in cellulose allows it to be applied as curing agent for the cross-linking with epoxides. The success in doing this is thus highly promising as it stresses on reducing our reliance on petroleum based chemicals such as amines, and at the meantime

improves the mechanical property of the epoxy resin. However, there are currently two major difficulties in making cellulose - epoxy resins. The first difficulty comes from the large network of intermolecular hydrogen bonding of cellulose. This strong hydrogen bond makes cellulose insoluble in most of the common solvents, leading to its combination with epoxide compounds a heterogeneous mixture.[18] Second difficulty comes from the low reactivity of hydroxide groups on the surface of cellulose towards the cross-linking with epoxide rings. In order to improve the efficiency of cross-linking between cellulose and epoxide rings, a chemical modification process is promising to convert the less reactive hydroxide groups into one of the moieties with higher reactivity, such as carboxyl groups. Surface modification of cellulose is an active area of research that has been extensively studied during the past few decades. Among a wide variety of techniques, TEMPO catalyzed oxidation of cellulose, as well as the succinoylation of cellulose using succinic anhydride are two of the pathways that receive particular interests for the introduction of carboxyl functional group to the surface of cellulose.[19-20]

In this work, organosolv extraction was first performed on wild type poplar using methanol as solvent. Three major components in biomass (cellulose, hemicellulose and lignin) will be separated following the organosolv extraction. After separation, isolated cellulose was subjected to a surface modification process to convert the hydroxide groups to carboxyl groups. Two different methods were applied for the modification purpose: (1) Succinylation of cellulose by reaction with succinic anhydride in TBAA/DMSO mixed solvent, and (2) Selective oxidation of primary hydroxyl group in cellulose into carboxyl group through TEMPO (2,2,6,6-tetramethylpyperidine-1-oxyl) catalyzed oxidation reaction. Modified cellulose was characterized by DNP enhanced NMR and FTIR. The

resulting structures of modified and unmodified cellulose were imaged by scanning electron microscopy (SEM). Thermal properties were analyzed by thermogravimetric analysis (TGA). Our previous studies have illustrated the high efficient conversion of lignin into major methoxyphenol products using Zn/Pd/C and Ni/C catalyst systems[21-22]. In this study, the epoxy monomer was synthesized from one of these lignin depolymerized compounds, 2-methoxy-4-propylphenol (DHE). In specific, DHE was first converted to the corresponding catechol (DHEO), and followed by the reaction with epichlorohydrin for the formation of lignin-based epoxy monomer[23]. Surface modified cellulose and lignin derived epoxides were cured for fabricating bio-based epoxy polymers.

B. Surface modification of cellulose derived from organosolv extraction of poplar biomass.

Cellulose samples used in this study were obtained from the organosolv extraction of poplar biomass, using methanol as solvent. Detailed procedures for the orgransolv extraction of biomass can be found in Chapter 4. In this project, the modification of cellulose was performed by (1) reaction of native cellulose with succinic anhydride and (2) TEMPO mediated oxidation of native cellulose. Structure of unmodified cellulose (UC), succinylated cellulose (C-SA) and TEMPO oxidized cellulose (C-TEMPO) are illustrated in **Figure 5.1**.

Succinoylation of cellulose was carried out through the reaction of cellulose with succinic anhydride, using tetrabutylammonium acetate (TBAA)/ dimethyl sulfoxide (DMSO) mixed solvent. Combination of TBAA and DMSO has been proved to be an

efficient system for the dissolution of cellulose.[24] After the modification process, isopropanol was added to quench the reaction and to precipitate solid cellulose.

Another method for cellulose modification is TEMPO mediated oxidation of cellulose. This reaction was carried out in aqueous media under basic condition with catalytic amount of TEMPO and an excess amount of NaClO as the primary oxidant. NaBr is applied to regenerate TEMPO catalyst. A simplified reaction mechanism of TEMPO mediated oxidation of cellulose has been reported by Vignon et al. and illustrated in **Scheme 5.2**.[25] TEMPO mediated oxidation reaction has been proved to be highly efficient in selective oxidization of primary hydroxyl groups in polysaccharides to carboxyl groups, leaving the secondary hydroxyl groups unaffected.[19, 26]

Figure 5.1. Structure illustration of **(a)** unmodified cellulose (UC), **(b)**, succinylated cellulose (C-SA), **(c)**, TEMPO oxidized cellulose (C-TEMPO).

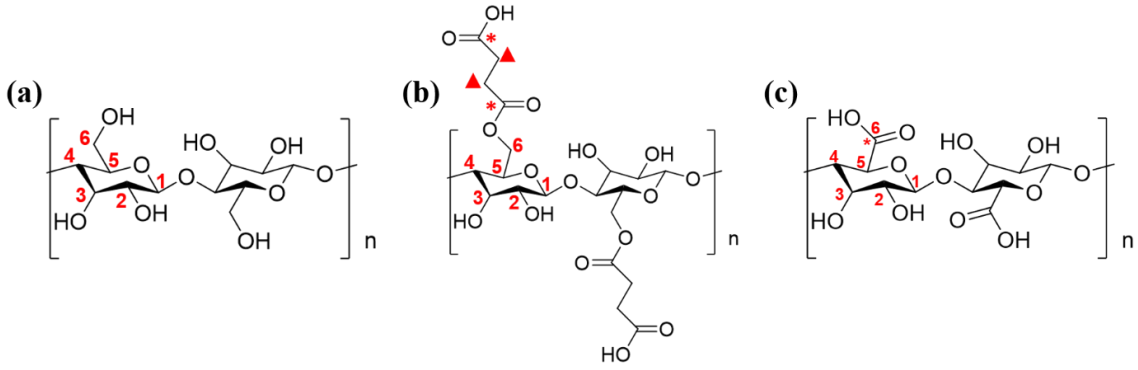

Scheme 5.2. Mechanistic illustration of TEMPO catalyzed oxidation of cellulose.[25]

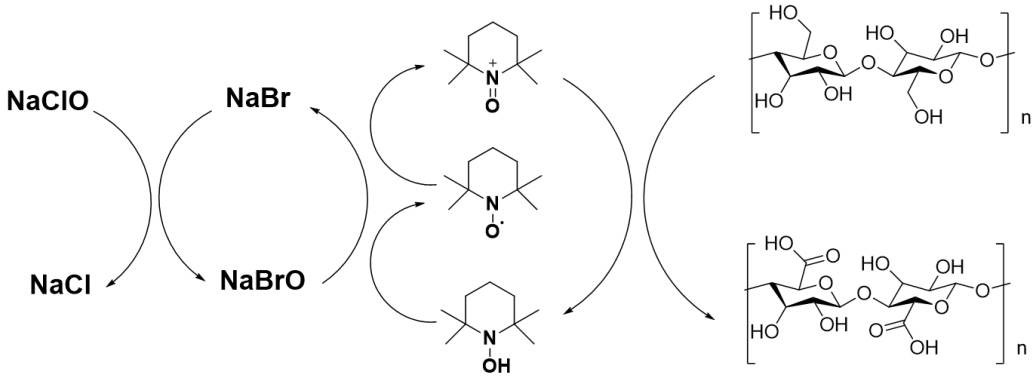

1. DNP-Enhanced ssNMR Analysis

Molecular structure of native cellulose, succinylated cellulose and TEMPO oxidized cellulose were characterized by DNP (Dynamic Nuclear Polarization) enhanced NMR (**Figure 5.1 and Figure 5.2)**. DNP utilizes the much larger Boltzmann polarization of the electrons in order to enhance nuclear polarization. The electron paramagnetic resonance (EPR) of biradical dopants impregnated in the samples are transferred to the nuclei via an irradiation by high-power microwaves. Compared to normal ssNMR, DNP leads to maximum enhancement in the signal sensitivity about 660 for ^{1}H and 2600 for ^{13}C, and it has been proved to be a powerful noninvasive tool to probe the complex structure of biomass.[9]

Compared with native cellulose, the spectrum of succinylated cellulose shows two additional peaks (**Figure 5.2 a,b**). The peak at 174 ppm is attributed to the carbonyl carbon, while the peak at 28.4 ppm is attributed to the methylene group on a cellulose succinoyl ester. The appearance of these additional peaks indicates the success in succinoylation of cellulose. It is known that the main reactive sites of cellulose are hydroxyl groups on C2, C3 and C6. After succinoylation reaction, the C6 signal displays a decrease in intensity compared with the unmodified cellulose. This indicates

that the reaction between succinic anhydride and the primary hydroxyl group on C6 has higher preference over the secondary hydroxyl groups on C2 and C3.

NMR spectrum of TEMPO oxidized cellulose (**Figure 5.2c**) also shows the appearance of an additional peak at 175 ppm, which is attributed to the carbonyl carbon in a carboxyl group. It can be noticed that compared with unmodified cellulose (**Figure 5.2a**), the relative intensity of C6 decreases in TEMPO-oxidized cellulose, and the signals of the other five carbons are only weakly affected (**Figure 5.2c**). This further confirmed the high selectivity for the oxidation of primary hydroxyl groups in TEMPO catalyzed reactions[19].

Figure 5.2. DNP-NMR of **(a)** unmodified cellulose (UC), **(b)**, succinylated cellulose (C-SA)[a], **(c)**, TEMPO oxidized cellulose (C-TEMPO)[b].

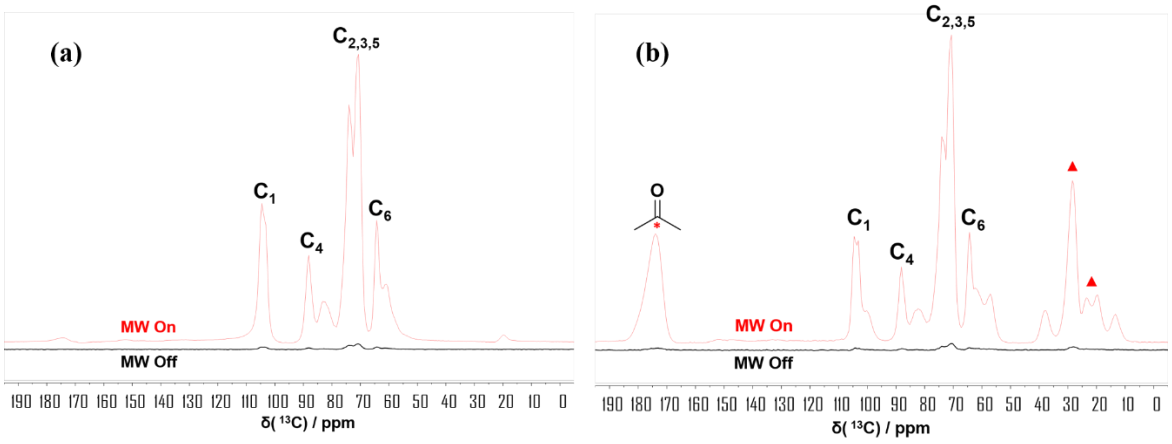

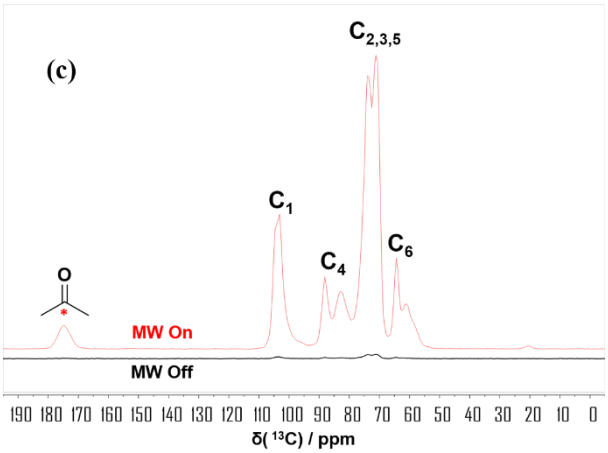

[a] Triangle and asterisk labels match with the corresponding carbons in **Figure 5.1 (b)**.

[b] Asterisk label matches with the corresponding carbon in **Figure 5.1 (c)**.

2. FTIR Analysis

FTIR spectrum of succinylated cellulose (**Figure 5.3, yellow**) shows the appearance of one additional peak at 1722 cm^{-1} compared with unmodified cellulose (**Figure 5.3, red**). This band is assigned to the carbonyl groups in carboxylic acids or esters. In addition, the intensity of the peak at 1160 cm^{-1} has increased after the succinolyation reaction, which can be attributed to the C-O antisymmetric bridge stretching in esters[24]. Presence of the above characteristic peaks indicate the success in succinoylation of cellulose. FTIR spectrum for TEMPO-oxidized cellulose sample indicates the presence of one peak around 1600 cm^{-1}, which is the C=O stretching band for carboxylate[27] (**Figure 5.3, blue**).

Figure 5.3. FT-IT spectra of unmodified cellulose (**red**), succinylated cellulose (**yellow**) and TEMPO oxidized cellulose (**blue**).

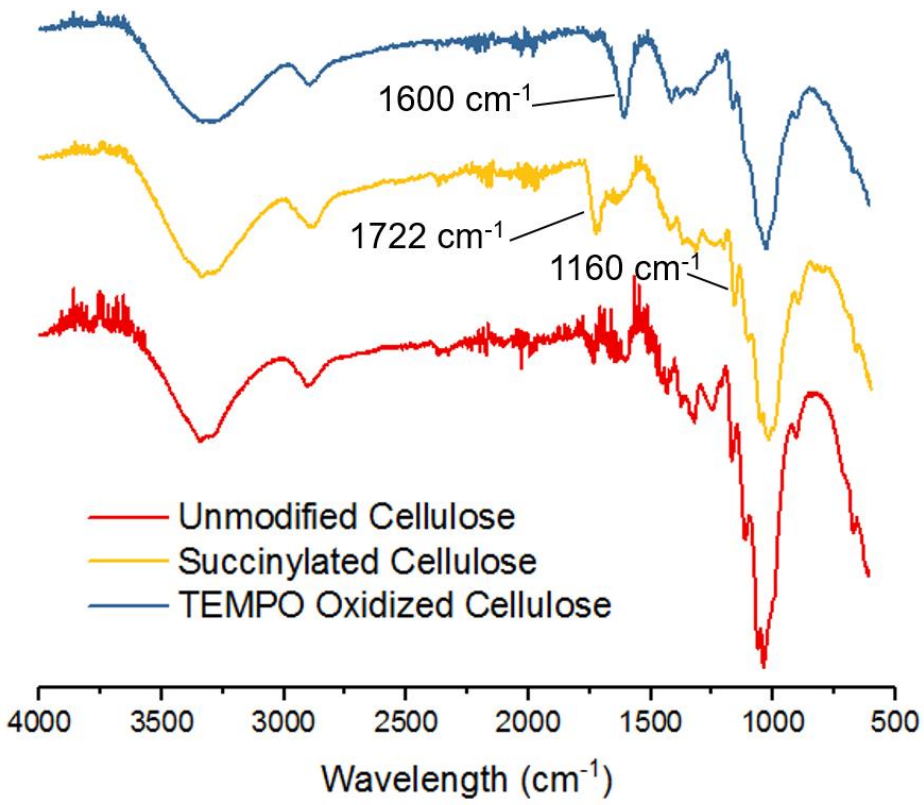

3. Scanning Electron Microscope (SEM) Images

Scanning electron microscope (SEM) images were collected on unmodified cellulose, succinylated cellulose and TEMPO oxidized cellulose samples to compare structure difference on mesoscale (**Figure 5.4.**). Our observations suggest that particle size is significantly affected by different modification methods. Unmodified cellulose derived from the organosolv extraction of poplar has particles as large as 100 μm, and the particles show random shapes. TEMPO catalyzed oxidation of cellulose results in the particle size around 50 μm, and in this case, the particles have a more regular plate shape. Succinic anhydride modification leads to the aggregation of cellulose, with the final particles as small as 2 μm. The aggregated particles also show less regulated shapes. The difference in cellulose structure on the meso-scale may impact the property of epoxy resin generated from the curing of epoxy monomer with modified cellulose.

Figure 5.4. Scanning electron microscope (SEM) images of (a) unmodified cellulose (UC), (b) succinylated cellulose (C-SA) and (c) TEMPO oxidized cellulose (C-TEMPO).

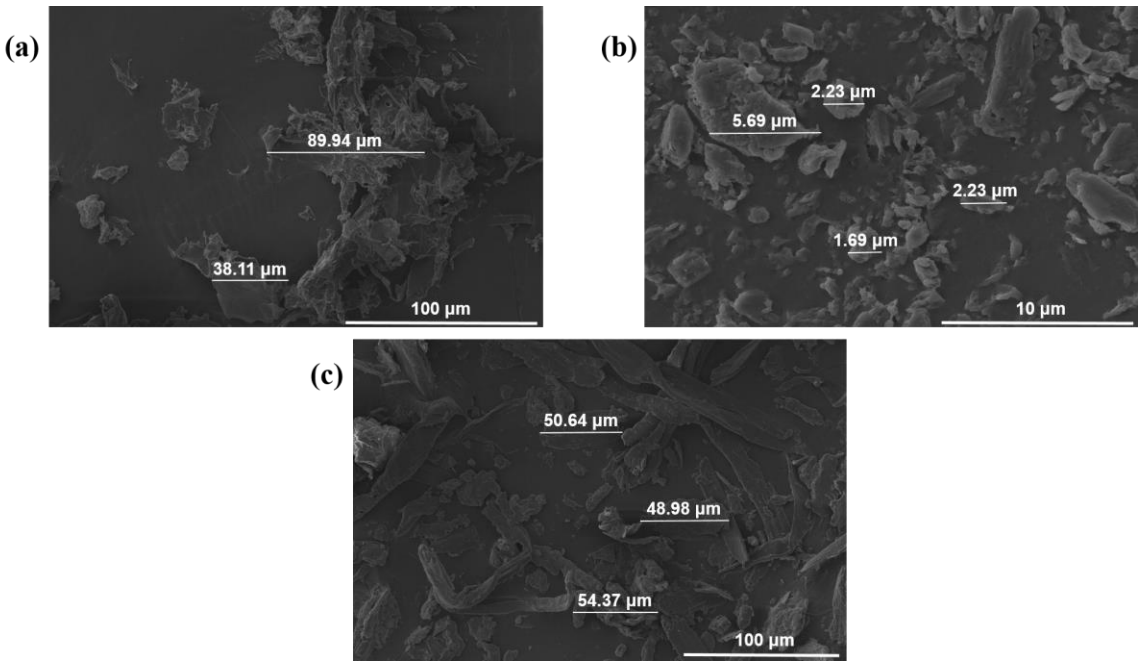

4. Thermogravimetric Analysis (TGA)

Thermal properties of unmodified cellulose (UC), succinylated cellulose (C-SA) and TEMO oxidized cellulose (C-TEMPO) were investigated by thermogravimetric analysis (TGA) (**Figure 5.5**.). UC shows rapid decomposition in a narrow temperature range of 330- 390˚C, possibly through the formation of levoglucosan and other volatile compounds[28]. Both C-SA and C-TEMPO show significantly lowered decomposition temperature compared to UC. Onsite decomposing temperature (T_{d5}, 5% weight loss) for UC is around 288˚C, while for C-SA and C-TEMPO are only around 174˚C and 83˚C, respectively. At 50% weight loss (T_{d50}), the decomposition of UC occurs at 365˚C, while for C-TEMPO occurs at 314˚C and for C-SA occurs at 273˚C. This trend of decreasing decomposition temperature implied that the thermal stability of modified cellulose

samples is lower than that of the native cellulose. Among the three, C-SA has the lowest thermal stability at high temperature. This behavior is due to the formation of cellulose esters in the succniylated cellulose, which is believed to lower its thermal stability[29-31]. Char formation at 600˚C of TEMPO oxidized cellulose is observed to be about twice as much as the other two cellulose samples.

Figure 5.5. Thermogravimetric analysis (TGA) of unmodified cellulose (red), succinylated cellulose (blue) and TEMPO oxidized cellulose (yellow).

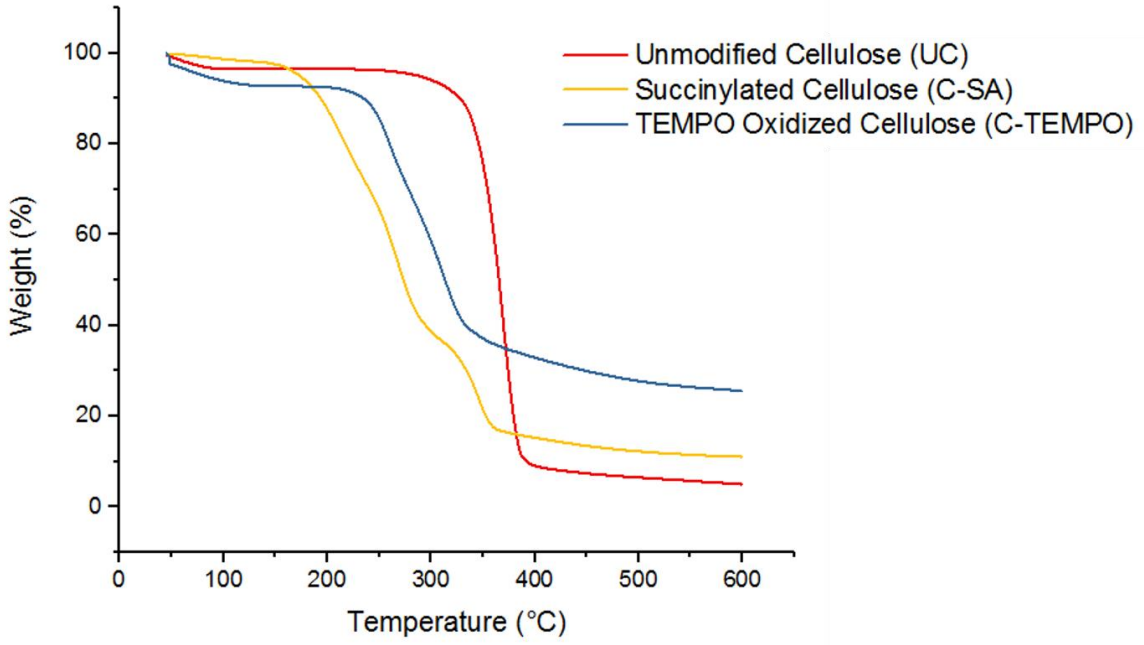

C. Curing of surface modified cellulose with epoxide monomer

The epoxy monomer used in this study was synthesized and characterized according to a previous publication by Zhao et al.[23] In a typical curing process, the mixture of epoxy monomer and cellulose component was first heated at 60 ˚C *in vacuo* for 30 minutes, in order to remove entrapped air in the system. The epoxy composite was

then cured at 150 ˚C for 2 hours, followed by 180 ˚C for additional 72 hours. In this study, composites prepared contain cellulose to epoxy monomer with the weight ratio ranging from 2:3 to 1:4. Curing of unmodified cellulose with epoxy monomer was performed as a control experiment. In this case, a dark color rubber-like solid was obtained after 7 days under 180 ˚C, which indicated that a fully curing of the composite was not achieved. This behavior revealed the low reactivity of cellulose hydroxyl groups towards cross-linking with epoxy rings.

Thermogravimetric analysis (TGA) of the unmodified cellulose – epoxy composite (UC-E), succinylated cellulose - epoxy composite (C-SA-E) and TEMPO oxidized cellulose – epoxy composite (C-TEMPO-E) were illustrated in **Figure 5.6**. Weight ratio of cellulose component to epoxy monomer were kept at 1:2 for all three samples. As can be noticed, SA-E shows a two-step degradation profile. The first degradation is likely associated with the breaking of strong cross-linking between succinic motif and epoxy ring, while the second mass loss is possibly the rupture of weak hydroxyl – epoxy linking. It is noteworthy that the polymer network generated from curing of succinylated cellulose and epoxy monomer (C-SA-E) shows significant improvement on the thermal property. This is reflected in the change of onset decomposition temperature ($T_{d5,}$ 5% weight loss) from 191˚C of the UC-E composite to 192˚C and 234˚C of C-TEMPO-E and C-SA-E composites, respectively. Decomposition temperature at 50% mass loss (T_{d50}) for C-SA-E composite is 392˚C, considerably higher than the value of 310˚C for UC-E composite and 318˚C for C-TEMPO-E composite. This improved thermal property can be attributed to a strong crossing-linking effect between the succinic acid motif on the surface of succinylated cellulose and epoxy monomer[20, 32]. The fact that C-TEMPO-E

composite shows less significant improvement on the thermal property is likely due to the steric hindrance arising from the hexose unit, which weakens the cross-linking effect between the carboxyl group and epoxy ring. The statistic heat-resistant index temperature (T_s)[33], which is calculated based on T_{d5} (temperature at 5% weight loss) and T_{d30} (temperature at 30% weight loss), is characteristic for the thermal stability of cured resins (**Equation 5.1.**). As can be noticed in **Table 5.1**, C-SA-E has the highest T_s value (144 ˚C) among all three samples, further supported the positive role of cellulose succinoylation on the thermal stability of epoxy composite.

Equation 5.1. Calculation of statistic heat-resistant index temperature (T_s)

$$T_s = 0.49[T_{d5} + 0.6(T_{d30} - T_{d5})]$$

Figure 5.6. Thermogravimetric analysis (TGA) of unmodified cellulose – epoxy composite (UC-E, red), succinylated cellulose - epoxy composite (C-SA-E, yellow) and TEMPO oxidized cellulose – epoxy composite (C-TEMPO-E, blue). Mass ratio of cellulose component to epoxy monomer = 1:2.

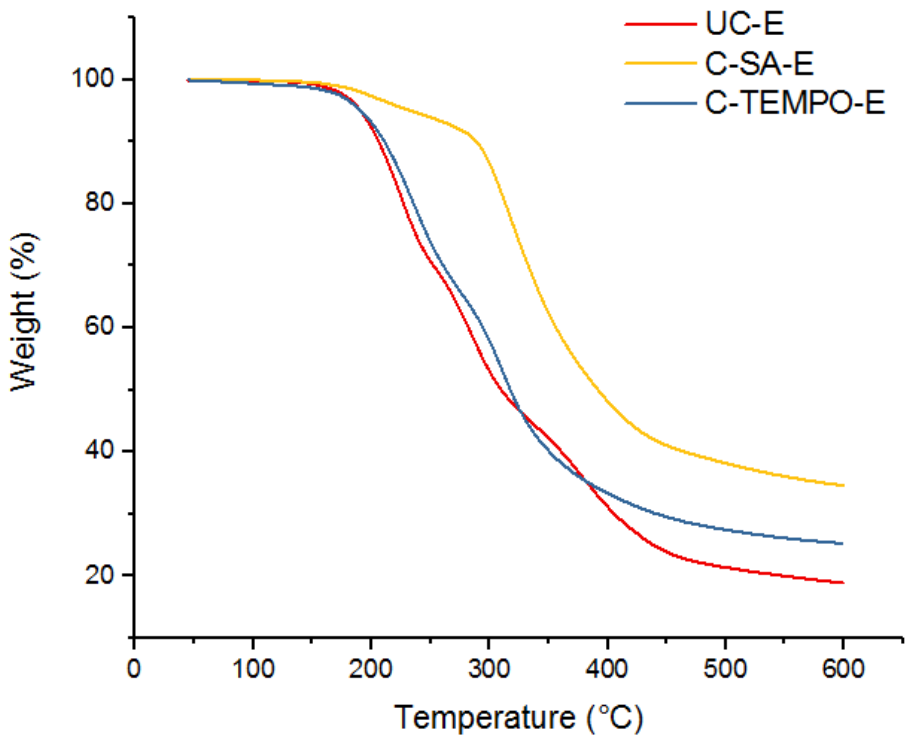

Table 5.1. Thermogravimetric Data of T_{d5}, T_{d30}, T_{d50} (Temperature at 5%, 30% and 50% weight loss), T_s (Statistic heat-resistant index temperature) and $Char_{600}$ (Char residue at 600 ˚C) of surface modified cellulose samples (Entries 1-3) and cellulose based epoxy composites (Entries 4-6).

Entries	Samples	T_{d5} (˚C)	T_{d30} (˚C)	T_{d50} (˚C)	T_s (˚C)	$Char_{600}$ (%)
1	UC	288	354	365	-	5
2	C-SA	174	240	273	-	11
3	C-TEMPO	83	279	314	-	25
4	UC-E	191	253	310	112	18
5	C-SA-E	234	333	392	144	34

6	C-TEMPO-E	192	261	318	114	25

Thermogravimetric analysis (TGA) were also performed on epoxy composites containing different cellulose amounts to study the effect of cellulose content on the thermal stability of epoxy resin (**Figure 5.7.**). As can be observed, changing the weight ratio of succinylated cellulose to epoxy monomer from 2:3 to 1:3 only changes T_{d5} from 226 ˚C to 234 ˚C and T_{d50} from 383 ˚C to 392 ˚C (**Figure 5.7a**). Variation of TEMPO oxidized cellulose content also has less significant effect on the decomposition temperatures of epoxy composites (**Figure 5.7b**). In this case, T_{d5} changes from 192 ˚C to 197 ˚C and T_{d50} changes from 318 ˚C to 329 ˚C. The above results indicated that the modification of cellulose has major effect on the thermal stability of the epoxy composite, due to the introduction of new functional groups. On the other hand, variation of cellulose content in a relatively narrow range has only neglectable effects.

Figure 5.7. Thermogravimetric analysis (TGA) of (**a**) C-SA-E, (**b**) C-TEMPO-E at different cellulose to epoxy monomer weight ratio.

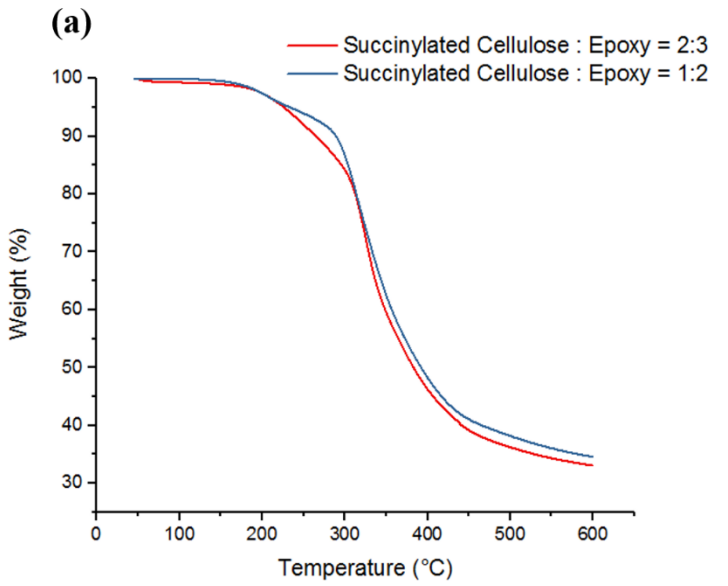

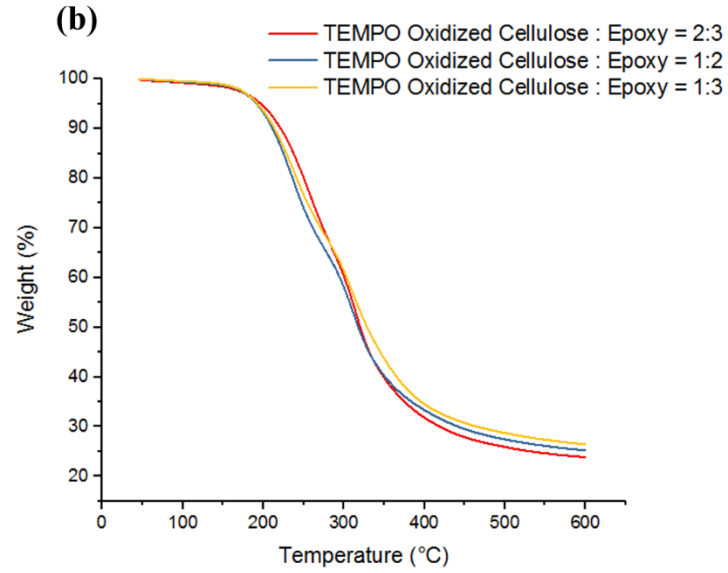

D. Conclusion and Future Work:

The synthesis of a renewable based epoxy nanocomposite has been demonstrated using components derived from biomass. The abundant hydroxyl groups in cellulose allows surface modification to introduce different functional groups to the polysaccharide. Succinic anhydride modification as well as TEMPO catalyzed oxidation

of cellulose served as two pathways for the introduction of carboxyl groups, which was illustrated to further improve the efficiency towards cross-linking between modified cellulose with epoxy monomers. SEM images revealed that the succinic anhydride modification in TBAA/DMSO solvent resulted in the particles remarkably alerted from unmodified cellulose. DNP ssNMR as a powerful noninvasive tool indicated the success in partial replacing hydroxyl groups by carboxyl groups. TGA analysis indicated that curing of succinylated cellulose with epoxide compounds has significant improvement on the thermal property of epoxy composite.

The insolubility of cellulose in the epoxy monomer resulted in the combination of the two components a heterogeneous mixture. Meanwhile, high viscosity of epoxy monomer restricted a well dispersion of cellulose in the mixture. Due to the above limitations, one of our future plans for this currently ongoing project aims at improving the dispersion of cellulose by applying an extra solvent before mixing with epoxy monomers. Dimethylformamide (DMF) and TBAA/DMSO mixture are among the top candidacies for the purpose of cellulose dispersion. The applied solvent will be removed during the curing process by heating. Ionic liquid, on the other hand, has been proved to be capable to dissolve cellulose[34]. Dissolution of cellulose in ionic liquid followed by curing with epoxy monomer is thus another attracting area to be studied. However, in this case, the removal of ionic liquid from the epoxy resin mixture is challenging due to its high boiling point. The effect on the properties (thermal and mechanical properties) of epoxy resin with the presence of ionic liquid needs to be investigated. Further analyses need to be performed including DMA and stress-strain tests, in order to reveal the mechanical properties of the synthesized cellulose-epoxy composite.

E. Supporting Information

1. Materials and methods

Materials.

Dihydroeugenol (DHE), epichlorohydrin, 48% aquesous hydrobromic acid, tetrabutylammonium bromide, 2,2,6,6-tetramethylpyperidine-1-oxyl (TEMPO), succinic anhydride, 1,8-Diazabicyclo [5.4.0] undec-7-ene, sodium bromide were purchased from Aldrich Chemical Co. Sulfuric acid (98 wt%) was purchased from EMD Millipore Corporation. 5% w/v Sodium hypochlorite was purchased from Lab Chem. Dimethyl sulfoxide was purchased from EMD Millipore Corporation. Methanol and formaldehyde (37 wt%) were purchased from Fisher Chemical. All chemicals were used as received. Wild-type poplar (*P. nigra* × *P. maximowiczii*) was provided by Purdue University's Department of Forestry and Natural Resources. Biomass substrate was milled to pass through a 40 mesh screen using a Mini Wiley Mill (Thomas Scientific, Swedesboro, NJ) before use.

Organosolv extraction of biomass

Cellulose samples used in this study were obtained from the organosolv extraction of poplar biomass, using methanol as solvent. In a typical experiment, 2 g of 40 mesh raw biomass was combined with methanol solvent, and solid:liquid ratio 1:20 in a 75 mL stainless steel Parr reactor. The reaction was catalyzed by 0.045 N H_2SO_4. Liquid phase was composed of 20 mL organic solvent, 20 mL 0.045 N H_2SO_4 aqueous solution and 4 mL 37 wt% aqueous formaldehyde. The reaction vessel was sealed, and purged with UHP grade N_2 5 times while stirring. The reaction was performed at 160 ˚C for 0.5 hour, under 12 bar N_2 atmosphere with a stirring speed 700 rpm. The reaction was terminated

by cooling down the system to room temperature. The solid phase containing cellulose was separated from the liquid phase containing lignin and hemicellulose by filtration. 3 portions of 20 mL organic solvent followed by 50 mL Milli-Q Academic A10 grade water were used to wash the solid residue to remove any remaining lignin and hemicellulose on the surface. The cellulose sample was dried under vacuum overnight before further use.

Succinoylation of cellulose

The succinoylation of cellulose was carried out under optimized conditions that has been modified according to previous literature[20]. In this study, 10wt% of tetrabutylammonium acetate (TBAA) in dimethyl sulfoxide (DMSO) was applied as mixed solvent. In a general modification process, 2 g of dried cellulose sample was first added to 10 mL of homogeneously mixed solvent in a 100 mL round bottom flask, and the mixture was stirred at 60 °C for 30 minutes. Succinic anhydride was then added to the mixture and purged with N_2 to ensure that air in the system was fully removed. Molar ratio of succinic anhydride and cellulose was determined to be 4:1. The mixture was further heated at 60 °C for another 60 minutes. The reaction was terminated by slowly adding 50 mL isopropanol into the mixture with continuous stirring at room temperature. Solid precipitate was filtered and thoroughly washed with extra amount of isopropanol to remove TBAA/DMSO solvent, unreacted succinic anhydride and side products. The solid was first dried overnight under vacuum and then in a 45 °C oven for another 24 hours before further use.

TEMPO catalyzed oxidation of cellulose

TEMPO catalyzed oxidation of cellulose was carried out under optimized conditions that has been modified according to previous literature[19]. In a general reaction, 2 g of cellulose samples were suspended in 150 mL of H_2O containing 50 mg of 2,2,6,6-2,2,6,6-tetramethylpyperidine-1-oxyl (TEMPO) and 600 mg of sodium bromide (NaBr), the mixture was first stirred under room temperature for 30 minutes. 30 mL of 5 % NaClO was then added slowly at room temperature in a 40 minutes period under gentle agitation. The reaction pH was monitored using a pH meter and maintained between 10 and 10.5 by incrementally adding 0.5 M NaOH solution. Reaction was considered complete when no decrease in pH was observed. 15 mL of MeOH was then added to quench the extra oxidant. The system was finally adjusted to pH = 7 by adding 0.5 M HCl. TEMPO oxidized cellulose was washed with Milli-Q Academic A10 grade water by centrifugation and further purified by dialysis against water for three days. The recovered solid was freeze dried before further use.

o-Demethylation of dihydroeugenol (DHE)

Demethylation of DHE was carried out under optimized conditions that has been modified according to a previous publication[23]. In a typical reaction, 19 g DHE was added to 85 g of 48% aqueous hydrobromic acid. The reaction mixture was magnetically stirred at 115 °C for 19 h, followed by cooling to ambient temperature, saturated with NaCl (concentrated brine, 15 mL), and extracted with 15 mL diethyl ether for three times. The organic layer was dried over $MgSO_4$ and concentrated using rotary evaporation. The obtained DHE demethylated product was used as a dihydroxyl starting compound for epoxy monomer synthesis.

Synthesis of glycidyl ether of propylcatechol (GEDHEO)

The synthesis of GEDHEO was performed by reaction of 10 g DHEO with 100 g epichlorohydrin. 1 g tetrabutylammonium bromide (TBAB) was used as a phase transfer catalyst. The mixture was stirred at 60 °C for 3 h, followed by a dropwise addition of 50% w/w NaOH solution. Amount of NaOH solution (10 g) and DHEO was optimized to a 1:1 ratio. The mixture was stirred for another three hours under same temperature, washed with acetone, followed by filtration to remove salts and finally concentrated by rotary evaporation.

Preparation of cellulose-epoxy composites

Synthesis of cellulose-epoxy composite was carried through the curing of cellulose component with epoxy monomer (GEDHEO). In a typical reaction, 0.1g of cellulose sample (unmodified cellulose, succinylated cellulose or TEMPO oxidized cellulose) was mixed with appropriate amount of epoxy monomer (GEDHEO). 3 wt% of 1,8-diazabicyclo [5.4.0] undec-7-ene was added as catalyst. The mixture was stirred vigorously for 30 minutes to improve the dispersion of cellulose, followed by heating at 60 °C for 30 minutes under vacuum to remove any entrapped air. Curing was performed according to the profile: 150 °C for 2 hours and 180 °C for additional 72 hours. Composites containing cellulose to epoxy monomer weight ratio between 2:3 and 1:4 were prepared.

2. Instrumentation and Characterization Conditions

Dynamic nuclear polarization (DNP) enhanced solid-state nuclear magnetic resonance (NMR)

All DNP-enhanced SSNMR measurements were performed using a Bruker 400MHz (9.6T) ASCEND DNP-NMR spectrometer MAS-DNP system equipped with a 263 GHz gyrotron, and a 3.2mm MAS DNP-NMR triple resonance broadband X/Y/H probe. All samples were wet with a 10 mM solution of AMUPol in water, packed into 3.2 mm o.d. Sapphire rotors, and sealed with a Zirconia cap. These samples were then prespun using a benchtop spinning station at room temperature to equilibrate the sample and then spun at 8 kHz at operating temperature of 90K in the probe. In all cases, cross-polarization of 13C spins from hyperpolarized ^{1}H spins was performed using a 1.5 ms contact time. The ^{1}H excitation pulse lasted 2.75 μs. The recycle delays were set to 1.3T1 in order to maximize sensitivity and lasted between 2.7 and 6.1 s, depending on the sample. For the measurements, 16 scans were accumulated.

Scanning electron microscope (SEM)

SEM images were taken on an FEI Nova NanoSEM 650 high resolution instrument, equipped with a high stability Schottky field emission gun and a large specimen chamber. Oxford Inca x-ray EDX system was used as detector, back scattering detector for Z-imaging. Cellulose samples were first coated with palladium metal at plasma discharge current 10mA for 100s under argon atmosphere. The instrument was vented to pressure less than 9×10^{-5} torr before use. Electron beam used for image taking was set to voltage at 7 keV.

TGA

Thermal stability studies were carried out on a TGA Q500 (TA Instruments) under a nitrogen flow of 40 mL/min. Samples (10-15mg) were placed in a platinum pan and

scanned from 25 to 600 ˚C at a ramp rate of 20 ˚C/min.

FTIR

FTIR analyses were conducted using a Thermo-Nicolet Nexus 470 FTIR spectrometer equipped with an ultrahigh-performance, versatile attenuated total reflectance (ATR) sampling accessory. The spectra were scanned over a wavenumber range of 500 to 4000 cm^{-1} with a resolution of 4 cm^{-1}. 16 scans were collected for each spectrum.

F. References

1. Liu, W. S.; Zhou, R.; Goh, H. L. S.; Huang, S.; Lu, X. H., From Waste to Functional Additive: Toughening Epoxy Resin with Lignin. *Acs Appl Mater Inter* **2014,** *6* (8), 5810-5817.

2. Yang, G. Z.; Rohde, B. J.; Tesefay, H.; Robertson, M. L., Biorenewable Epoxy Resins Derived from Plant-Based Phenolic Acids. *Acs Sustain Chem Eng* **2016,** *4* (12), 6524-6533.

3. Raquez, J. M.; Deleglise, M.; Lacrampe, M. F.; Krawczak, P., Thermosetting (bio)materials derived from renewable resources: A critical review. *Prog Polym Sci* **2010,** *35* (4), 487-509.

4. Tan, S. G.; Chow, W. S., Biobased Epoxidized Vegetable Oils and Its Greener Epoxy Blends: A Review. *Polym-Plast Technol* **2010,** *49* (15), 1581-1590.

5. Miyagawa, H.; Misra, M.; Drzal, L. T.; Mohanty, A. K., Fracture toughness and impact strength of anhydride-cured biobased epoxy. *Polym Eng Sci* **2005,** *45* (4), 487-495.

6. Chrysanthos, M.; Galy, J.; Pascault, J. P., Preparation and properties of bio-based epoxy networks derived from isosorbide diglycidyl ether. *Polymer* **2011,** *52* (16), 3611-3620.

7. van Beilen, J. B.; Poirier, Y., Production of renewable polymers from crop plants. *Plant J* **2008,** *54* (4), 684-701.

8. Kristufek, S. L.; Yang, G. Z.; Link, L. A.; Rohde, B. J.; Robertson, M. L.; Wooley, K. L., Synthesis, Characterization, and Cross-Linking Strategy of a Quercetin-Based Epoxidized Monomer as a Naturally-Derived Replacement for BPA in Epoxy Resins. *Chemsuschem* **2016,** *9* (16), 2135-2142.

9. Perras, F. A.; Luo, H.; Zhang, X.; Mosier, N. S.; Pruski, M.; Abu-Omar, M. M., Atomic-level structure characterization of biomass pre-and post-lignin treatment by dynamic nuclear polarization-enhanced solid-state NMR. *The Journal of Physical Chemistry A* **2017,** *121* (3), 623-630.

10. Khelifa, F.; Habibi, Y.; Benard, F.; Dubois, P., Effect of cellulosic nanowhiskers on the performances of epoxidized acrylic copolymers. *Journal of Materials Chemistry* **2012,** *22* (38), 20520-20528.

11. Varma, A. J.; Chavan, V. B., Cellulosic Diamines as Reaction-Incorporated Fillers in Epoxy Composites. *Cellulose* **1994,** *1* (3), 215-219.

12. Xiao, X. E.; Lu, S. R.; Qi, B.; Zeng, C.; Yuan, Z. K.; Yu, J. H., Enhancing the thermal and mechanical properties of epoxy resins by addition of a hyperbranched aromatic polyamide grown on microcrystalline cellulose fibers. *Rsc Adv* **2014,** *4* (29), 14928-14935.

13. Tang, L. M.; Weder, C., Cellulose Whisker/Epoxy Resin Nanocomposites (vol 2, pg 1073, 2010). *Acs Appl Mater Inter* **2010,** *2* (11), 3396-3396.

14. Abraham, E.; Kam, D.; Nevo, Y.; Slattegard, R.; Rivkin, A.; Lapidot, S.; Shoseyov, O., Highly Modified Cellulose Nanocrystals and Formation of Epoxy-Nanocrystalline Cellulose (CNC) Nanocomposites. *Acs Appl Mater Inter* **2016,** *8* (41), 28086-28095.

15. Pan, H.; Song, L.; Ma, L.; Hu, Y., Transparent epoxy acrylate resin nanocomposites reinforced with cellulose nanocrystals. *Ind Eng Chem Res* **2012,** *51* (50), 16326-16332.

16. Wu, G.-m.; Liu, D.; Liu, G.-f.; Chen, J.; Huo, S.-p.; Kong, Z.-w., Thermoset nanocomposites from waterborne bio-based epoxy resin and cellulose nanowhiskers. *Carbohyd Polym* **2015,** *127*, 229-235.

17. Wu, G. M.; Liu, D.; Liu, G. F.; Chen, J.; Huo, S. P.; Kong, Z. W., Thermoset nanocomposites from waterborne bio-based epoxy resin and cellulose nanowhiskers. *Carbohyd Polym* **2015,** *127*, 229-235.

18. Swatloski, R. P.; Spear, S. K.; Holbrey, J. D.; Rogers, R. D., Dissolution of cellose with ionic liquids. *J Am Chem Soc* **2002,** *124* (18), 4974-4975.

19. Filpponen, I.; Argyropoulos, D. S., Regular linking of cellulose nanocrystals via click chemistry: synthesis and formation of cellulose nanoplatelet gels. *Biomacromolecules* **2010,** *11* (4), 1060-1066.

20. Xin, P.-P.; Huang, Y.-B.; Hse, C.-Y.; Cheng, H. N.; Huang, C.; Pan, H., Modification of Cellulose with Succinic Anhydride in TBAA/DMSO Mixed Solvent under Catalyst-Free Conditions. *Materials* **2017,** *10* (5), 526.

21. Luo, H.; Klein, I. M.; Jiang, Y.; Zhu, H.; Liu, B.; Kenttämaa, H. I.; Abu-Omar, M. M., Total utilization of Miscanthus biomass, lignin and carbohydrates, using earth abundant nickel catalyst. *Acs Sustain Chem Eng* **2016,** *4* (4), 2316-2322.

22. Parsell, T.; Yohe, S.; Degenstein, J.; Jarrell, T.; Klein, I.; Gencer, E.; Hewetson, B.; Hurt, M.; Im Kim, J.; Choudhari, H., A synergistic biorefinery based on catalytic conversion of lignin prior to cellulose starting from lignocellulosic biomass. *Green Chem* **2015,** *17* (3), 1492-1499.

23. Zhao, S.; Abu-Omar, M. M., Biobased epoxy nanocomposites derived from lignin-based monomers. *Biomacromolecules* **2015,** *16* (7), 2025-2031.

24. Xin, P. P.; Huang, Y. B.; Hse, C. Y.; Cheng, H. N.; Huang, C. B.; Pan, H., Modification of Cellulose with Succinic Anhydride in TBAA/DMSO Mixed Solvent under Catalyst-Free Conditions. *Materials* **2017,** *10* (5).

25. Perez, D. D.; Montanari, S.; Vignon, M. R., TEMPO-mediated oxidation of cellulose III. *Biomacromolecules* **2003,** *4* (5), 1417-1425.

26. Bragd, P. L.; Van Bekkum, H.; Besemer, A. C., TEMPO-mediated oxidation of polysaccharides: survey of methods and applications. *Topics in Catalysis* **2004,** *27* (1), 49-66.

27. da Silva Perez, D.; Montanari, S.; Vignon, M. R., TEMPO-mediated oxidation of cellulose III. *Biomacromolecules* **2003,** *4* (5), 1417-1425.

28. Kim, D. Y.; Nishiyama, Y.; Wada, M.; Kuga, S., Influence of Dehydrating Agents on Carbonization of Cellulose and Wood. *A Better World through Environmental Discovery. www. esf. edu/outreach/pd/2000/cellulose* **2000**.

29. Vaidya, A. A.; Gaugler, M.; Smith, D. A., Green route to modification of wood waste, cellulose and hemicellulose using reactive extrusion. *Carbohyd Polym* **2016,** *136*, 1238-1250.

30. Huang, Y.-B.; Xin, P.-P.; Li, J.-X.; Shao, Y.-Y.; Huang, C.-B.; Pan, H., Room-temperature dissolution and mechanistic investigation of cellulose in a tetra-butylammonium acetate/dimethyl sulfoxide system. *Acs Sustain Chem Eng* **2016,** *4* (4), 2286-2294.

31. Liu, C. F.; Zhang, A. P.; Li, W. Y.; Yue, F. X.; Sun, R. C., Succinoylation of cellulose catalyzed with iodine in ionic liquid. *Industrial Crops and Products* **2010,** *31* (2), 363-369.

32. Anand, A.; Kulkarni, R. D.; Patil, C. K.; Gite, V. V., Utilization of renewable bio-based resources, viz. sorbitol, diol, and diacid, in the preparation of two pack PU anticorrosive coatings. *Rsc Adv* **2016,** *6* (12), 9843-9850.

33. Benyahya, S.; Aouf, C.; Caillol, S.; Boutevin, B.; Pascault, J. P.; Fulcrand, H., Functionalized green tea tannins as phenolic prepolymers for bio-based epoxy resins. *Industrial Crops and Products* **2014,** *53*, 296-307.

34. Zhu, S.; Wu, Y.; Chen, Q.; Yu, Z.; Wang, C.; Jin, S.; Ding, Y.; Wu, G., Dissolution of cellulose with ionic liquids and its application: a mini-review. *Green Chem* **2006,** *8* (4), 325-327.